Université de Montréal

Caractérisation fonctionnelle des gènes *NOTCHLESS* et *MIDASIN* lors du développement végétal

par

Sier-Ching Chantha

Département de sciences biologiques

Faculté des arts et des sciences

Thèse présentée à la Faculté des études supérieures

en vu de l'obtention du grade de Philosophiæ Doctor (Ph. D.)

en Sciences biologiques

Octobre, 2006

Université de Montréal

Faculté des études supérieures

Cette thèse intitulée:

Caractérisation fonctionnelle des gènes *NOTCHLESS* et *MIDASIN* lors du développement végétal

présentée par:

Sier-Ching Chantha

a été évaluée par un jury composé des personnes suivantes:

Anja Geitmann

président-rapporteur

Daniel Philippe Matton

directeur de recherche

David Morse

membre du jury

Jean-Philippe Vielle-Calzada

examinateur externe

Normand Brisson

représentant du doyen de la FES

RÉSUMÉ

Les protéines à WD-repeat (WDR) servent à l'assemblage de complexes multiprotéiques et participent à la régulation de multiples processus cellulaires chez les eucaryotes. Parmi les 237 membres de la famille des protéines à WDR répertoriés chez *Arabidopsis thaliana*, très peu ont été testés pour une possible fonction lors du développement végétal. Le gène *NOTCHLESS* (*NLE*) code pour une protéine à WDR conservée chez les eucaryotes. Chez les métazoaires, NLE a été impliquée dans la régulation de la voie de signalisation Notch. Alors que les principales composantes de cette voie sont inexistantes chez la levure et les végétaux, NLE a été identifiée chez la levure en tant que protéine non-ribosomale participant à la biogenèse de la sous-unité 60S, un processus cellulaire qui serait conservé chez les eucaryotes.

La voie Notch est utilisée dans plusieurs processus de différenciation cellulaire lors du développement animal, justifiant ainsi cette première étude sur la fonction possible de *NLE* lors du développement des angiospermes. Une caractérisation fonctionnelle du gène a été menée de façon complémentaire chez *Solanum chacoense* (*Sc*) et *Arabidopsis thaliana* (*At*). L'utilisation du système de double-hybride de la levure a permis de définir que ScNLE interagit avec les homologues MDN1 et NSA2 de la levure, tous deux des composantes non-ribosomales des complexes d'assemblage de la sous-unité 60S du ribosome. Les gènes *NLE* et *MDN1* présentent par ailleurs des profils d'expression très similaires dans les divers organes de *S. chacoense* et d'*Arabidopsis*. Une sous-expression du gène *ScNLE* induite par interférence d'ARN dans des lignées transformées de *S. chacoense* résulte en la production d'un phénotype pléiotropique. Principalement, les lignées sous-exprimant *ScNLE* produisent des organes aériens de taille réduite résultant d'une réduction en nombre et en taille des cellules qui les composent. En accord avec un rôle dans la prolifération et l'expansion cellulaires, les niveaux d'expression de *ScNLE* et *AtNLE* sont plus élevés dans les organes comprenant des

cellules en division active. Chez *S. chacoense*, une augmentation transitoire des niveaux d'expression de *ScNLE* est de plus associée aux ovules et ovaires au moment de la fécondation et de l'initiation du développement des graines et des fruits, qui représente une période de division cellulaire intense. L'interférence d'ARN ciblant l'activité du gène *NLE* chez *S. chacoense* et *Arabidopsis* mène de plus à des taux plus élevés d'avortement d'ovules. Tel que déterminé dans les lignées d'interférence d'*Arabidopsis*, le développement de gamétophytes femelles, en proportions correspondant aux taux d'ovules avortés, est arrêté à divers stades précoces de leur développement. Chez *Arabidopsis*, la mutation insertionnelle *mdn1* mène également à des défectuosités dans le développement des gamétophytes femelles, ce développement étant retardé comparativement à celui des gamétophytes de type sauvage. Les gènes *AtNLE* et *AtMDN1* sont exprimés de façon constitutive dans tous les organes de la plante. En somme, les résultats obtenus dans cette étude montrent que NLE et MDN1 sont requis pour la croissance cellulaire lors du développement sporophytique et gamétophytique des angiospermes. Leur fonction cellulaire serait associée à la biogenèse de la sous-unité 60S du ribosome.

Mots clés: biogenèse du ribosome, croissance cellulaire, fécondation, gamétophyte femelle, Notchless, Midasin, ovule, ovaire, protéine à WD-repeat, sous-unité ribosomale 60S.

ABSTRACT

WD-repeat (WDR) proteins serve in assembling multiprotein complexes and are involved in the regulation of diverse cellular processes in eukaryotes. Among the 237 members of the WDR protein family identified in *Arabidopsis thaliana*, only a few have been characterized for a possible function during plant growth and development. The *NOTCHLESS* (*NLE*) gene encodes a highly conserved WDR protein. In metazoans, NLE has been involved in the regulation of the animal-specific Notch signaling pathway. While most components of this pathway do not exist in yeast and plants, NLE has been identified in yeast as a trans-acting factor involved in 60S ribosomal subunit biogenesis, a well conserved cellular process in eukaryotes.

The Notch pathway is used in multiple differentiation processes of animal development, justifying this first study on the possible role played by the *NLE* gene in angiosperm development. A functional characterization of the gene was carried out in this study in *Solanum chacoense* (*Sc*) and *Arabidopsis thaliana* (*At*). Yeast two-hybrid screens with ScNLE identified the yeast homologs MDN1 and NSA2 as binding partners. Both candidates represent trans-acting factors in 60S ribosomal subunit assembly complexes in yeast. In *S. chacoense* and *Arabidopsis* organs, both *NLE* and *MDN1* show very similar expression patterns. Underexpression of the *ScNLE* gene by RNA interference in *S. chacoense* transformed lines leads to a pleitropic phenotype. Mainly, *ScNLE* underexpressing lines produce smaller aerial organs resulting from reduced cell number and cell size composition. In agreement with a role in cell proliferation and cell growth, expression levels of *ScNLE* and *AtNLE* are higher in plant organs comprising actively dividing cells. In *S. chacoense*, a transitory increase in *ScNLE* expression levels is moreover observed in ovules and ovaries during fertilization and initiation of seed and fruit development time, which represents a period of intense cell division. RNA interference targeting *NLE* gene activity in *S. chacoense* and *Arabidopsis* leads to high levels of ovule abortion. As

determined in *Arabidopsis* RNA interference lines, female gametophytes in proportions corresponding to ovule abortion levels are arrested at different precocious developmental stages. In *Arabidopsis*, an insertional mutation in the *MDN1* gene also leads to defects in female gametophyte development, being delayed compared to their wild-type female gametophyte siblings. Both *AtNLE* and *AtMDN1* are constitutively expressed in all the plant organs examined. Taking together, the results obtained in this study show that NLE and MDN1 are both required for cell growth and proliferation during sporophytic and gametophytic development. As in yeast, the cellular function of NLE and MDN1 is likely to be associated with 60S ribosomal subunit biogenesis.

Keywords: ribosome biogenesis, cell growth, fertilization, female gametophyte, Notchless, Midasin, ovule, ovary, WD-repeat protein, 60S ribosomal subunit.

TABLE DES MATIÈRES

LISTE DES FIGURES

LISTE DES TABLEAUX

LISTE DES SIGLES ET ABRÉVIATIONS

Sauf si mentionné, le nom d'un gène et son abréviation proviennent de l'espèce *Arabidopsis thaliana*.

+	symbole parfois utilisé pour désigner un allèle de type sauvage
°C	degré Celcius
%	pourcentage
18S	*ARN ribosomal 18S* de *Solanum chacoense* ou d'*Arabidopsis thaliana*
3AT	3-amino-1',2'3'-triazole
3'	extrémité 3' hydroxyl
5'	extrémité 5' phosphate
a/A	adénine
A	alanine
aa	amino acid/acide aminé
ABI	Applied Biosystems
AD	GAL4 activation domain
Ade	adénine
ADN	acide déoxyribonucléique
ADNc	ADN complémentaire
AGB1	gène *Arabidopsis G-beta 1*
AGP18	gène *ARABINOGALACTAN PROTEIN 18*
AN	antipodal nucleus
ANT	gène *AINTEGUMENTA*
ap	gène *apterous* de *Drosophila melanogaster*
AP	arbitrary primer
APC2	gène *ANAPHASE PROMOTING COMPLEX 2*
APC/C	anaphase promoting complex/cyclosome
ARN	acide ribonucléique
ARNm	ARN messager
ARNr	ARN ribosomal
as	lignée transgénique antisens
AscI	endonucléase I des *Arthrobacter*
Asp	acide aspartique
AtMDN1	gène *MIDASIN1* d'*Arabidopsis thaliana*
AtNLE	gène *NOTCHLESS* d'*Arabidopsis thaliana*
ATP	adénosine triphosphate
BamHI	endonucléase I de *Bacillus amyloliquefaciens* H
B	bundle sheath
BD	GAL4 binding domain

BEL1	gène *BELL1*
bp	base pair
bZIP	basic leucine zipper motif transcription factor
C	cytosine
C	cystéine
C	compatible
C	témoin (control)
CA	California
CaMV 35S	cauliflower mosaic virus 35S promoter
cap	mutant *capulet*
CCS52	gène *CELL CYCLE SWITCH 52* de *Medicago*
cdc25H	souche de levure
cDNA	complementary DNA
CHR11	gène *CHROMATIN-REMODELING PROTEIN 11*
CKI1	gène *CYTOKININE HISTIDINE KINASE 1*
cm	centimètre
CN	chalazal nucleus
COP1	gène *CONSTITUTIVELY MORPHOGENETIC 1*
CPN	chalazal polar nucleus
CSL	CBF-1, Su(H), Lag-1
C-terminal	domaine carboxyl terminal d'une protéine
C-terminus	extrémité carboxy-terminale d'une protéine
CTR1	gène *CONSTITUTIVE TRIPLE RESPONSE 1*
D	acide aspartique
DAG1	gène *DOF AFFECTING GERMINATION 1*
DAP	days after pollination
dATP	déoxyadénosine triphosphate
DIC	differential interference contrast
DME	gène *DEMETER*
DmNLE	gène *NOTCHLESS* de *Drosophila melanogaster*
DNA	deoxyribonucleic acid
dNTP	deoxyribonucleotide triphosphate/désoxyribonucléotide triphosphate
Dof	DNA-binding with one finger motif transcription factor
Dr.	docteur
DraI	endonucléase I de *Deinococcus radiophilus*
DSL	Delta, Serrate, Lag-2
E	acide glutamique
EcoRI	endonucléase RI d'*Escherichia coli*
EcoRV	endonucléase RV d'*Escherichia coli*
eda	mutant gamétophytique avec noyaux polaires non-fusionnés
eGFP	enhanced GFP
email	electronic mail
EN	egg cell nucleus
EST	expressed sequence tag

F	phénylalanine
F1	première génération filiale
FAX	facimile
FBP	gène *FLORAL BINDING PROTEIN* de *Petunia hybrida*
fem	mutant *female gametophyte*
FER	gène *FERONIA*
FG	female gametophyte
FIE	gène *FERTILIZATION-INDEPENDENT ENDOSPERM*
FIS	gène *FERTILIZATION-INDEPENDENT SEED*
Fig.	figure
FQRNT	Fonds Québécois de la Recherche sur la Nature et les Technologies
g	gramme
Gα	sous-unité alpha de la protéine G hétérotrimérique
Gβ	sous-unité beta de la protéine G hétérotrimérique
G	guanine
G	glycine
G4	lignée G4 de *Solanum chacoense*
GABA	acide gamma-amino butyrique
GAL4	activateur de la transcription GAL4
GE	General Electric
gfa	mutant *gametophytic factor*
GFP	Green Fluorescent Protein
GMC	guard mother cell
GPA1	gène *G-PROTEIN ALPHA SUBUNIT*
GPCRs	G Protein-Coupled Receptors
GCR1	gène *G-PROTEIN COUPLED RECEPTOR*
GST	Glutathione-S-transferase
GUS	gène marqueur β-*GLUCURONIDASE*
h	hour/heure
h	hydrophobic amino acid
H	histidine
HAF	hours after flowering
HAP	hours after pollination
hdd	mutant *hadad*
HindIII	endonucléase III d'*Haemophilus influenzar* RD
H_2O	eau
i	lignée transgénique à interférence d'ARN
I	isoleucine
ig	mutant *inderteminate gametophyte1* de *Zea mays*
Int.	intron
IRBV	Institut de Recherche en Biologie Végétale
K	lysine
kb	kilobase

kDa	kiloDalton
KpnI	endonucléase I de *Klebsiella pneumoniae* OK8
$K_3Fe(CN)_6$	Potassium ferricyanide
$K_4Fe(CN)_6$	Potassium ferrocyanide
L/l	litre
L	leucine
LB	Luria-Bertani
LB	T-DNA left border
LBA4404	souche d'*Agrobacterium tumefaciens*
Leu	leucine
LiAc	acétate de lithium
LGC1	gène *LILY GENERATIVE CELL SPECIFIC 1* de *Lilium longiflorum*
LPAT	gène *LYSOPHOSPHATIDYL ACYLTRANSFERASE*
LRR	leucine-rich repeat
LUG	gène *LEUNIG*
M	molaire
M	méthionine
M	MIDAS
M	nucléotides adénine ou cytosine
maa	mutant *magatama*
MADS	MCM1, AGAMOUS, DEFICIENS, SRF
MDN1	gène *MIDASIN1* de *Saccharomyces cerevisiae*
MEA	gène *MEDEA*
mee	mutant gamétophytique arrêté au stade zygotique
mel1	mutant *maternal effect lethal 1* de *Zea mays*
MIDAS	metal ion-dependent adhesion site
min	minute
MN	micropylar nucleus
mg	miligramme
$Mg(OAc)_2$	acétate de magnésium
mm	milimètre
mM	milimolaire
MMC	meristemoid mother cell
ml	millilitre
MPN	micropylar polar nucleus
mRNA	messenger RNA
MS	mass spectrometry
MS	Murashige and Skoog
MSI1	gène *Multiple Copy Supressor of IRA*
MYR	myristoylation signal
MW	molecular weight
n	nombre d'échantillon
N	asparagine
nb	number

NaeI	endonucléase I de *Nocardia aerocolonigenes*
NcoI	endonucléase I de *Nocardia corallina*
ND	not determined (non déterminé)
ng	nanogramme
NLE	gène *NOTCHLESS*
NLS	nuclear localization signal
nm	nanomètre
nmol	nanomole
no.	number/numéro
Nos	gène *Nopaline synthase*
NSA2	gène *Nop seven associated 2* de *Saccharomyces cerevisiae*
NSERC	Natural Sciences and Engineering Research Council of Canada
nt	nucléotide
N-terminal	domaine amino-terminal d'une protéine
N-terminus	extrémité amino-terminale d'une protéine
ON	Ontario
ORF	open reading frame
p	plasmide
p	probability/probabilité
P	proline
P	palisade parenchyma
P	pavement cell
PCR	polymerase chain reaction
pH	potentiel hydrogène
Ph D	Philosophiæ doctor
PHE1	gène *PHERES1*
PE	Perkin Elmer
pI	point isoélectrique
PJ69-4A	souche de levure
PLACE	plant cis-acting regulatory DNA element database
poly(A)	polyadénine
Pro.	promoter/ promoteur
PRL	gène *PROLIFERA*
PvuII	endonucléase II de *Proteus vulgaris*
Pwo	ADN polymérase de *Pyrococcus woesei*
Q	glutamine
QC	Québec
R	arginine
R	nucléotides adénine ou guanine
RB	T-DNA right border
RBR1	gène *RETINOBLASTOMA RELATED 1*
RLK	receptor-like kinase
RNA	ribonucleic acid
RNAi	RNA interference

RSA4	gène *Ribosome assembly 4* de *Saccharomyces cerevisiae*
RT-PCR	reverse transcription polymerase chain reaction
r*Tth*	recombinant *Thermus thermophilus* DNA polymerase
S	sérine
S	nucléotides cytosine ou guanine
S	stomata
S	unité de sédimentation d'une ou d'un ensemble de molécules
S_{11}	allèle *S-RNase 11* d'incompatibilité de *Solanum chacoense*
S_{12}	allèle *S-RNase 12* d'incompatibilité de *Solanum chacoense*
S_{13}	allèle *S-RNase 13* d'incompatibilité de *Solanum chacoense*
S_{14}	allèle *S-RNase 14* d'incompatibilité de *Solanum chacoense*
S	spongy parenchyma
SalI	endonucléase I de *Streptomyces albus* G
SAM	shoot apical meristem
SC	self-compatible
SC	synthetic complete
ScMDN1	gène *MIDASIN1* de *Solanum chacoense*
ScNLE	gène *NOTCHLESS* de *Solanum chacoense*
ScNSA2	gène *Nop seven associated 2* de *Solanum chacoense*
SD	standard deviation
sec	secondes
SEM	scanning electron microscopy
SEN	secondary endosperm nucleus
Ser	serine
si	stomatal index
SI	self-incompatibility
SIN1	gène *SHORT INTEGUMENT 1*
SmaI	endonucléase I de *Serratia marcescens*
Sos	gène *Son of sevenless* de l'humain
StuI	endonucléase I de *Streptomyces tubercidicus*
SRN	gène *SIRÈNE*
SWA1	gène *SLOW WALKER 1*
SYN	synergid nucleus
T	thymine
T	thréonine
T	transformed line/lignée transformée
T-DNA	transfer DNA
TE	transmission efficiency
tel	téléphone
Ter.	terminator/terminateur
Thr	thréonine
TP	tube pollinique
Trp	tryptophane
u/U	uracile
U	unité d'activité d'une enzyme

UAS	upstream activating sequence
uidA	gène codant la β-GLUCURONIDASE
une	mutant gamétophytique affecté dans la fécondation
Ura	uracile
UTP	uridine triphosphate
UTR	untranslated region
v	small vacuole
V	central vacuole
V	valine
V	volt
var.	variety/variété
vol	volume
W	tryptophane
WD	tryptophane-acide aspartique
WDR	tryptophane-acide aspartique repeat
WI	Wisconsin
WT	wild type (témoin, type sauvage)
x/X	n'importe quel acide aminé
X	unité de concentration d'une solution
XbaI	endonucléase I de *Xanthomonas badrii*
X-Gluc	beta-D-glucuronide cyclohexylamine salt
XhoI	endonucléase I de *Xanthomonas holcicola*
Y	tyrosine
Y	nucléotides cytosine ou thymine
ZmEA1	gène *Zea mays EGG APPARATUS 1* de *Zea mays*
α-^{32}P-dATP	dATP radioactif sur le phosphate α
µF	microfarad
µg	microgramme
µl	microlitre
µm	micromètre
µM	micromolaire

CHAPITRE I :

INTRODUCTION GÉNÉRALE

Le cycle de vie des plantes est caractérisé par une alternance entre deux générations multicellulaires: la génération diploïde, représentée par le sporophyte, et la génération haploïde, représenté par les gamétophytes. La méiose établie ainsi la séparation entre les générations sporophytique et gamétophytique. À la différence des animaux, chez qui les produits de la méiose se différencient directement en gamètes, chez les végétaux, les produits de la méiose, les spores, se divisent et se différencient en gamétophytes multicellulaires haploïdes. Ces gamétophytes produisent des gamètes par un processus nommé gamétogénèse. La fusion d'un gamète mâle et d'un gamète femelle génère un zygote qui est à l'origine d'un sporophyte multicellulaire diploïde. Le sporophyte a pour fonction principale de produire des spores haploïdes par un processus nommé sporogénèse, complétant ainsi le cycle de vie de la plante (Drews and Yadegari 2002; Yadegari and Drews 2004).

Le cycle reproductif des angiospermes possède quelques caractéristiques distinctives d'un ou de plusieurs des autres groupes de végétaux (bryophytes, ptéridophytes, gymnospermes) (Drews and Yadegari 2002; Brukhin et al. 2005). D'abord, la génération gamétophytique des angiospermes est fortement réduite comparativement à une génération sporophytique nettement dominante. Les gamétophytes ne sont en effet composés que d'un très petit nombre de cellules. Ensuite, le développement des gamétophytes dépend physiologiquement du sporophyte, puisqu'il se produit à l'intérieur des organes sexués de la fleur. De plus, le sporophyte produit deux types de spores sexuellement différenciées, les microspores et les mégaspores, qui sont à l'origine respectivement des gamétophytes mâles et des gamétophytes femelles. Le gamétophyte mâle, aussi nommé grain de

pollen ou microgamétophyte, se développe dans l'anthère de l'étamine et est composé de trois cellules: une cellule végétative qui englobe deux cellules spermatiques (McCormick 2004). Le gamétophyte femelle, aussi nommé sac embryonnaire ou mégagamétophyte, se développe à l'intérieur de l'ovule, qui est lui-même logé dans l'ovaire du pistil. La forme la plus commune du gamétophyte femelle présente un arrangement typique de sept cellules: une cellule-œuf, deux synergides, une cellule centrale diploïde et trois cellules antipodales (Maheshwari 1950; Willemse and van Went 1984; Huang and Russell 1992).

Lors de la reproduction sexuée, le gamétophyte mâle va à la rencontre du gamétophyte femelle, qui est enfoui dans les tissus sporophytiques de l'ovule. Les gamètes mâles, étant non-motiles, sont transportés à travers les tissus sporophytiques du pistil jusqu'aux ovules par le tube pollinique, qui est une excroissance polaire du grain de pollen. Les gamètes mâles sont ensuite libérés à l'intérieur du gamétophyte femelle pour effectuer la fécondation des deux gamètes femelles: la cellule-œuf et la cellule centrale. La double fécondation est un processus reproductif unique aux angiospermes et initie le développement de la graine porteuse de la génération sporophytique suivante. La fusion de la cellule-œuf et d'une cellule spermatique génère un embryon diploïde alors que la fusion de la cellule centrale et de la seconde cellule spermatique génère un albumen nourricier triploïde. En simultannée, les téguments de l'ovule et les tissus de l'ovaire se développent respectivement en enveloppe de la graine et structures du fruit (Russell 1992; Russell 1996).

Bien que de nos connaissances sur les aspects morphologiques et cytologiques de la biologie reproductive aient été acquises depuis plus d'un siècle, l'étude de ses aspects génétiques et moléculaires fait partie quant à elle de développements récents (Raghavan 2003; Brukhin et al. 2005). L'ensemble de ces études a par ailleurs révélé la place centrale qu'occupe le gamétophyte femelle lors de la reproduction sexuée. Non seulement représente-t-il le lieu où s'effectue la double fécondation et l'établissement d'une nouvelle génération sporophytique, mais l'expression du

génome haploïde du gamétophyte femelle participe également au contrôle de son propre développement et de plusieurs processus reproductifs (Drews et al. 1998; Drews and Yadegari 2002; Yadegari and Drews 2004; Brukhin et al. 2005). De plus, le développement du gamétophyte est intimement lié aux tissus sporophytiques qui l'enveloppent. L'identification de plusieurs mutants sporophytiques et gamétophytiques affectant le développement du gamétophyte femelle ou l'initiation du développement de la graine montrent que ces processus requièrent l'action concertée de gènes d'origine sporophytique et gamétophytique.

Cette introduction générale présente tout d'abord un survol de la structure et du développement du gamétophyte femelle d'un point de vue descriptif. Seront ensuite abordés les aspects génétiques et moléculaires associés au développement et aux fonctions reproductives du gamétophyte femelle, ainsi que les approches utilisées pour leur étude. Une emphase particulière est mise sur la plante modèle *Arabidopsis thaliana*, chez qui les analyses génétiques ont été principalement menées.

1.1. Structure et développement du gamétophyte femelle des angiospermes

Chez les angiospermes, le développement du gamétophyte femelle résulte de deux processus successifs qui sont la mégasporogénèse et la mégagamétogénèse (Maheshwari 1950; Willemse and van Went 1984; Christensen et al. 1997). La forme de développement observée chez plus de 70% des angiospermes, dont *Arabidopsis*, les Solanacées et plusieurs espèces d'importance économique (Yadegari and Drews 2004), suit une mégasporogénèse de type monosporique combinée à une mégagamétogénèse de type *Polygonum*, ainsi nommé car originellement décrit chez l'espèce *Polygonum divaricatum* (Maheshwari 1950; Willemse and van Went 1984; Huang and Russell 1992). Les aspects morphologiques du développement du gamétophyte femelle de type monosporique *Polygonum* ont été décrits de façon détaillée chez *Arabidopsis* (Webb and Gunning 1990; Mansfield et al. 1991; Murgia et al. 1993; Webb and Gunning 1994; Schneitz et al. 1995; Christensen et al. 1997) et

seront ici résumés. La mégagamétogénèse a été divisée en sept stades morphologiques distincts (stades FG) à des fins de référence pour l'analyse de mutants (Christensen et al. 1997) et est illustrée à la figure 1-1.

1.1.1. La mégasporogénèse

La mégasporogénèse (stade FG0) débute avec la différenciation d'une seule cellule archésporiale par ovule en cellule-mère diploïde des mégaspores. La cellule-mère des mégaspores entre en méiose et génère quatre mégaspores uninucléés haploïdes. Les trois mégaspores les plus micropylaires dégénèrent alors que la mégaspore la plus chalazale survit (Schneitz et al. 1995; Christensen et al. 1997). Cette mégaspore fonctionnelle s'élargit et représente le début de la mégagamétogénèse (stade FG1) (fig. 1-1).

1.1.2. La mégagamétogénèse

Lors de la mégagamétogénèse (fig. 1-1), le noyau de la mégaspore fonctionnelle entreprend d'abord trois rondes successives de mitose sans cytocinèse pour produire un syncytium de huit noyaux haploïdes. La première mitose génère un sac embryonnaire à deux noyaux dans lequel se trouvent plusieurs petites vacuoles dispersées (stade FG2). Une rapide coalescence de ces vacuoles résulte en la formation d'une grosse vacuole centrale qui sépare les deux noyaux aux pôles micropylaire (de l'orifice de l'ovule) et chalazal (du lieu d'attachement de l'ovule au placenta) et une plus petite vacuole additionnelle se forme au pôle chalazal (stade FG3). Les deuxième et troisième mitoses génèrent successivement des sacs embryonnaires à quatre noyaux (stade FG4) et à huit noyaux (stade FG5). La vacuole principale centrale est conservée lors de ces mitoses. Immédiatement après la troisième division mitotique, deux évènements importants modifient

considérablement la morphologie du sac embryonnaire (stade FG5). D'abord, les noyaux polaires,un provenant de chaque pôle, migrent l'un vers l'autre pour se rejoindre et se positionner côte à côte dans la moitié micropylaire du gamétophyte femelle. En concomitance à cette migration nucléaire, le sac embryonnaire se cellularise. Ces évènements résultent en la formation d'une structure à sept cellules présentant un arrangement caractéristique qui défini la forme mature des sacs embryonnaires de type *Polygonum* (Maheshwari 1950; Willemse and van Went 1984; Mansfield et al. 1991; Schneitz et al. 1995; Christensen et al. 1997). À l'extrémité micropylaire, une cellule-oeuf et les deux synergides qui la flanquent forment l'appareil ovulaire (*egg apparatus*). L'extrémité opposée chalazale est occupée par trois cellules antipodales. La grosse cellule centrale occupe quant à elle la majeure partie du sac embryonnaire. Chez *Arabidopsis*, les deux noyaux polaires haploïdes de la cellule centrale fusionnent pour créer un noyau homodiploïde nommé noyau secondaire de l'albumen (*secondary endosperm nucleus*) (stade FG6) (Webb and Gunning 1994; Schneitz et al. 1995; Christensen et al. 1997), alors que chez d'autres espèces, les noyaux polaires ne fusionnent que partiellement avant la fécondation (Drews et al. 1998). Le sac embryonnaire à sept cellules peut également subir des modifications subséquentes. Par exemple, chez *Arabidopsis*, les cellules antipodales dégénèrent (Schneitz et al. 1995; Christensen et al. 1997), alors que chez le maïs, les cellules antipodales prolifèrent (Drews et al. 1998). En somme, le sac embryonnaire mature d'*Arabidopsis* est composé de quatre cellules (cellule centrale, cellule-œuf, deux synergides) qui constituent l'unité germinale femelle (*female germ unit*) (stade FG7) (Christensen et al. 1997).

Le développement du gamétophyte femelle et celui des tissus sporophytiques de l'ovule semblent intimement liés. Par exemple, des plasmodesmes relient la mégaspore fonctionnelle aux cellules nucellaires (cellules sporophytiques au centre de l'ovule qui entourent la mégasore fonctionnelle et au milieu desquelles le sac embryonnaire se développe), formant une voie potentielle d'échange entre ces deux structures (Bajon et al. 1999). De plus, au cours de son développement, le

gamétophyte femelle acquiert une polarité et des caractéristiques structurales qui facilitent le processus de fécondation (Drews and Yadegari 2002; Yadegari and Drews 2004). Lors de la mégagamétogénèse, les noyaux positionnés à l'extrémité micropylaire se différencient en cellule-œuf et en synergides alors que les noyaux à l'extrémité chalazale se différencient en cellules antipodales. Toutes les cellules de l'unité germinale femelle sont fortement polarisées (Schneitz et al. 1995; Christensen et al. 1997). Dans la cellule-œuf, le noyau est localisé vers le pôle chalazale et sa vacuole occupe l'extrémité micropylaire, alors que les synergides et la cellule centrale possèdent une polarité inverse (Willemse and van Went 1984; Christensen et al. 1997). Dans cet arrangement, les noyaux de la cellule-œuf et de la cellule centrale sont situés très près l'un de l'autre (Christensen et al. 1997). Il y a également absence de parois cellulaires à l'interface de l'appareil ovulaire et de la cellule centrale, permettant ainsi un contact direct entre les membranes plasmiques de ces cellules (Mansfield et al. 1991). Ces caractéristiques structurales sont importantes pour le processus de fécondation puisque le pôle micropylaire représente le point d'entrée du tube pollinique dans le sac embryonnaire et que les noyaux des cellule-œuf et centrale représentent les cibles des noyaux des cellules spermatiques. La correspondance entre la polarité acquise par le gamétophyte femelle et le développement asymétrique des tissus sporophytiques de l'ovule suggère que la mégagamétogénèse serait régulée, au moins en partie, par les tissus sporophytiques de l'ovule (Yadegari and Drews 2004).

1.2. Aspects génétiques et moléculaires du développement et des fonctions reproductives du gamétophyte femelle

L'ovule étant composé de tissus de deux générations différentes, les cellules gamétophytiques enveloppées par des tissus sporophytiques (nucelle et/ou téguments), les gènes requis pour le développement et les fonctions reproductives du gamétophyte femelle peuvent être exprimés par le gamétophyte femelle lui-même et par les tissus sporophytiques de l'ovule. Ainsi, le gamétophyte femelle peut être

affecté par deux classes de mutations dont les modes de transmission sont différents: les mutations sporophytiques et les mutations gamétophytiques.

1.2.1. Identification de mutations sporophytiques qui affectent le gamétophyte femelle

Les mutations sporophytiques affectent la génération sporophytique diploïde et, relativement au gamétophyte femelle, perturbent des processus tels que le développement de la cellule-mère des mégaspores, la méiose, et le contrôle de la mégagamétogénèse par les tissus sporophytiques environnants – nucelle et/ou téguments (Yadegari and Drews 2004). Sous forme hétérozygote récessive, ces mutations sporophytiques ne causent pas de phénotype et sont transmises à la génération sporophytique suivante dans un rapport de ségrégation mendélienne de 1:2:1. Cependant, sous forme homozygote, ces mutations causent la stérilité femelle, un critère utilisé dans l'identification de mutations sporophytiques qui affectent le développement de l'ovule (Grossniklaus and Schneitz 1998; Schneitz 1999).

Tel que mentionné précédemment, les tissus sporophytiques de l'ovule ont le potentiel d'influencer la mégagamétogénèse. De ce fait, plusieurs mutants sporophytiques du développement de l'ovule montrent également une mégagamétogénèse anormale (Grossniklaus and Schneitz 1998; Schneitz 1999). Cependant, la nature de cette interaction, qui peut être purement physique ou bien moléculaire, reste indéterminée dans la majorité de ces mutations puisqu'elles causent un développement anormal des tissus sporophytiques. Par exemple, les mutants *aintegumenta* (*ant*), chez qui les téguments sont absents (Klucher et al. 1996), et *bell1*, chez qui les téguments sont anormaux (Reiser et al. 1995), montrent également un arrêt de la mégasporogénèse. Les mutations sporophytiques qui contrôlent spécifiquement la mégagamétogénèse devraient affecter la mégagamétogénèse sans toutefois affecter le développement des tissus sporophytiques de l'ovule (Yadegari

and Drews 2004). Bien que l'existence de ce genre de mutants ait été rapportée (Schneitz et al. 1997), les gènes correspondants n'ont toujours pas été identifiés. Ainsi, les aspects moléculaires du contrôle sporophytique de la mégagamétogénèse sont indéterminés.

1.2.2. Identification de mutations gamétophytiques qui affectent le gamétophyte femelle

Les mutations gamétophytiques femelle-spécifiques affectent quant à elles la génération gamétophytique haploïde femelle de la plante et perturbent les processus qui se produisent après la méiose, tels que la mégagamétogénèse et les fonctions reproductives reliées au gamétophyte femelle mature (Yadegari and Drews 2004). Chez une plante hétérozygote pour une mutation, la moitié des gamétophytes mâles et des gamétophytes femelles sont porteurs de l'allèle mutant. Dans le cas d'une mutation gamétophytique femelle-spécifique, la moitié des ovules portant un gamétophyte femelle dysfonctionnel, ne peuvent se développer en graines et avortent éventuellement, résultant en une semistérilité. De plus, cette mutation est transmise à la génération sporophytique suivante exclusivement par la moitié des gamètes mâles porteur de l'allèle mutant. Par conséquent, cette mutation est transmise à la génération sporophytique suivante sous forme hétérozygote seulement et suit un rapport de ségrégation non-mendélienne de 1:1. Cependant, plusieurs des mutations gamétophytiques sont de type général, c'est-à-dire qu'elles touchent les gamétophytes femelles et les gamétophytes mâles. Les mutations gamétophytiques générales ont souvent une pénétrance incomplète, c'est-à-dire que la mutation ne cause pas de dommage au gamétophyte qui le porte dans 100% des cas, et sont ainsi transmises aux générations sporophytiques suivantes dans des rapports de ségrégation plus sévères que 1:1. Pour déterminer l'efficacité de transmission de la mutation par l'entremise de chaque type de gamétophyte, des croisements réciproques avec des plantes de type sauvage doivent être effectués. En somme, les mutations

gamétophytiques qui affectent le gamétophyte femelle sont typiquement identifiées sur la base des deux critères suivants: une réduction du taux de graines produite par la plante et une ségrégation non-mendélienne de l'allèle mutant dans la progéniture (Feldmann et al. 1997; Moore et al. 1997; Howden et al. 1998).

Au cours de la dernière décennie, quelques centaines de mutants gamétophytiques affectés dans le développement et les fonctions reproductives du gamétophyte femelle ont été identifiés, chez *Arabidopsis* principalement et de façon secondaire chez le maïs (tableau 1-1) (Drews and Yadegari 2002; Brukhin et al. 2005). Notamment, la majorité de ces mutants ont été identifiés lors de criblages de lignées insertionnelles de T-DNA ou de transposon (Feldmann et al. 1997; Christensen et al. 1998; Howden et al. 1998; Shimizu and Okada 2000; Christensen et al. 2002; Pagnussat et al. 2005). Les analyses phénotypiques et moléculaires de plusieurs de ces mutants ont mis en évidence que des gènes d'une grande diversité fonctionnelle et exprimés à partir du génome haploïde du gamétophyte femelle participent à la mégagamétogénèse et au contrôle de plusieurs processus reproductifs. Les sections suivantes rapportent la caractérisation de quelques-uns de ces mutants, et parfois des gènes correspondants, ainsi que des données complémentaires qui ont permis de mieux comprendre le développement et les fonctions reproductives du gamétophyte femelle.

1.2.3. Les gènes gamétophytiques impliqués dans la mégagamétogénèse

Plusieurs mutants gamétophytiques ne peuvent compléter la formation d'un sac embryonnaire mature et sont ainsi affectés dans la mégagamétogénèse. Les mutations gamétophytiques identifiés affectent essentiellement tous les stades du développement du gamétophyte femelle. Ces mutants manifestent une grande variété de phénotypes qui ont été classés en catégories phénotypiques correspondant à plusieurs des processus cellulaires impliqués dans la mégagamétogénèse, tels que la

mitose, la formation des vacuoles, la fusion nucléaire et la cellularisation (table 1-1) (Schneitz et al. 1995; Christensen et al. 1997; Christensen et al. 2002; Drews and Yadegari 2002; Brukhin et al. 2005; Pagnussat et al. 2005).

Une première catégorie phénotypique est formée par les nombreux mutants qui sont affectés dans l'initiation ou la progression des divisions mitotiques (stades FG1 à FG5). Ces mutants sont caractérisés par un nombre anormal et/ou une distribution anormale des noyaux dans le sac embryonnaire. Un arrêt du développement au stade aussi précoce que l'initiation de la mégagamétogénèse (stade FG1) observé chez certains de ces mutants montre que l'expression du génome haploïde est requise très tôt lors de la mégagamétogénèse (Drews and Yadegari 2002). Par exemple, une sous-expression par interférence d'ARN du gène *AGP18*, qui code pour une arabinogalactane classique, empêche la transition de la mégaspore fonctionnelle en mode de développement mégagamétophytique (Acosta-Garcia and Vielle-Calzada 2004). Plusieurs mutants de cette catégorie phénotypique peuvent progresser au-delà du stade à un noyau (FG1) mais montrent un arrêt ou un retard dans la phase de division nucléaire. Par exemple, des mutations dans les gènes *NOMEGA* (Kwee and Sundaresan 2003) et *APC2* (Capron et al. 2003), qui codent pour des composantes de l'*anaphase-promoting complex/cyclosome* (APC/C), un complexe ubiquitine ligase qui régule la progression de la mitose, causent un arrêt des divisions au stade à deux noyaux (FG2). D'autres composantes de voies de dégradation des protéines par l'ubiquitine ont également été identifiées dans cette classe de mutants (Pagnussat et al. 2005). Une mutation dans le gène *SLOW WALKER 1* (*SWA1*), qui code pour une composante du complexe snoRNP U3 qui participe à la maturation de l'ARN ribosomale 18S, cause un retard ainsi qu'une désynchronisation de la division des noyaux (Shi et al. 2005). Alors que les phénotypes de ces mutants montrent que plusieurs gènes sont requis pour la progression de la division cellulaire lors de la mégagamétogénèse, d'autres mutants montrent également la nécessité de restreindre ces divisions. Notamment, une mutation dans le gène *RBR*, qui code pour un homologue de rétinoblastoma, un

régulateur négatif de la prolifération cellulaire, entraîne une prolifération nucléaire excessive résultant en la formation d'un amas de cellules au pôle micropylaire du sac embryonnaire (Ebel et al. 2004).

Une seconde catégorie phénotypique comprend les mutants qui montrent une absence de fusion des noyaux polaires. Chez ces mutants, les noyaux polaires migrent normalement et se positionnent côte-à-côte mais ne fusionnent pas. Un exemple d'un tel mutant est *gfa2*, dont le gène correspondant code pour un membre de la famille des protéines DnaJ qui est localisé dans la mitochondrie et qui possède une fonction de chaperonne (Christensen et al. 2002).

Une autre catégorie phénotypique est formée par les mutants qui manifestent des problèmes de cellularisation, entraînant des anormalités dans leur morphologie cellulaire, dans la position des noyaux à l'intérieur des cellules ou d'autres caractéristiques cellulaires inhabituelles. Chez le mutant *myb98*, par exemple, l'appareil filiforme, qui est une élaboration de la paroi cellulaire micropylaire des synergides par où le tube pollinique pénètre dans le sac embryonnaire, ne développe pas d'invaginations (Kasahara et al. 2005). Le gène *MYB98* code pour un facteur transcriptionnel qui serait impliqué dans la différentiation cellulaire des synergides.

L'identification de ces mutants permet d'ordonner jusqu'à un certain point les processus cellulaires et les gènes gamétophytiques requis tout au long de la mégagamétogénèse. Plusieurs mutations affectant ces processus ne pourraient être identifiées dans des criblages sporophytiques typiques parce qu'elles ne peuvent survivre à l'état homozygote lors de la génération sporophytique. Par sa nature haploïde, le gamétophyte femelle représente ainsi un bon système d'étude pour l'analyse de gènes requis dans des fonctions cellulaires fondamentales qui ne pourraient être analysées autrement qu'à travers le stade gamétophytique (Schneitz et al. 1995; Christensen et al. 1997; Drews et al. 1998; Drews and Yadegari 2002). L'identification de tels gènes aide non seulement à la compréhension analytique de la

génération gamétophytique mais contribue également à comprendre les processus cellulaires et les processus de développement fondamentaux utilisés tout au cours du cycle de vie de la plante. Une catégorie phénotypique supplémentaire est formée par des mutants qui produisent un sac embryonnaire d'apparence normale mais qui ne peuvent transmettre l'allèle mutant à la génération suivante à travers le gamétophyte femelle. Ces mutants touchent les fonctions reproductives contrôlées par le gamétophyte femelle et font l'objet des prochaines sections.

1.2.4. Les gènes gamétophytiques impliqués dans les fonctions reproductives

En ce qui a trait aux fonctions reproductives contrôlées par le gamétophyte femelle, les mutations gamétophytiques identifiées affectent des processus tels que le guidage du tube pollinique vers le micropyle de l'ovule (Hülskamp et al. 1995; Ray et al. 1997; Shimizu and Okada 2000; Higashiyama et al. 2003), la réception du tube pollinique (Huck et al. 2003; Rotman et al. 2003), l'initiation du développement de la graine au moment de la fécondation (Ohad et al. 1996; Chaudhury et al. 1997) ainsi que le contrôle du développement de l'embryon et de l'albumen suite à la fécondation (Chaudhury and Berger 2001).

1.2.4.1. Guidage du tube pollinique

Chez les angiospermes, les gamètes mâles sont non-motiles et doivent être transportés à proximité des gamètes femelles par le tube pollinique (TP) pour permettre la double fécondation de s'effectuer (Higashiyama 2002; Higashiyama et al. 2003). Dans les dernières étapes de la croissance du TP dans l'ovaire, et souvent à proximité d'un ovule non-fécondé, le TP réoriente sa croissance pour émerger à la surface du placenta et se rendre sur un funicule, sur lequel il croît jusqu'à proximité du micropyle pour finalement pénétrer à l'intérieur du micropyle de l'ovule

(Hülskamp et al. 1995; Ray et al. 1997; Shimizu and Okada 2000). La précision et la constance avec lesquelles les TP accomplissent un tel parcours pour atteindre leur cible distante impliquent une forme de communication entre le gamétophyte mâle et les structures femelles.

Une combinaison de signaux de source sporophytique et gamétophytique semble être impliquée dans l'attraction du TP de la surface du placenta au micropyle de l'ovule (Higashiyama 2002; Higashiyama et al. 2003; Weterings and Russell 2004). Par exemple, l'acide γ-amino butyrique (GABA) a été proposé comme candidat potentiel de signal d'attraction produit par les tissus sporophytiques chez *Arabidopsis* (Palanivelu et al. 2003). Des études génétiques ont de plus révélé l'importance du gamétophyte femelle en tant que source d'un signal de courte distance qui dirige le TP vers le micropyle de l'ovule. Il a été observé chez des mutants d'*Arabidopsis* produisant des ovules avec des téguments d'apparence normale que les TP ne sont pas attirés vers les ovules dont le gamétophyte femelle est absent ou anormal, mais qu'ils croient de façon consistante vers les ovules qui contiennent un gamétophyte femelle fonctionnel (Hülskamp et al. 1995; Ray et al. 1997; Shimizu and Okada 2000). La mise au point d'un système d'étude semi-*in vitro* chez *Torenia fournieri* combinée à des expériences d'ablation au laser de cellules spécifiques a permis de définir plus précisément que les synergides du sac embryonnaire représentent la source d'un signal de nature diffusible agissant sur courte distance et de façon directe sur le guidage du TP (Higashiyama et al. 1998). La présence généralisée et la structure caractéristique des synergides chez les angiospermes pourraient refléter l'universalité des synergides en tant que source de signal de guidage du TP (Higashiyama 2002).

Les ions calcium ont été proposés comme molécule d'attraction du TP et plusieurs études sont venues appuyer ce rôle potentiel (Weterings and Russell 2004). Cependant, le signal de guidage chez *Arabidopsis* et *Torenia* semble spécifique à l'espèce et agit sur courte distance (quelques centaines de μm *in vitro*), contrairement

aux ions calcium (Shimizu and Okada 2000; Higashiyama 2002). Récemment, Marton et al. (2005) ont identifié *Zea mays EGG APPARATUS 1* (*ZmEA1*), un gène codant pour un peptide qui présente plusieurs caractéristiques d'une molécule de signalisation spécifique qui serait impliquée dans le guidage du TP sur courte distance chez le maïs. Le gène *ZmEA1* montre entre autre une expression exclusive dans l'appareil ovulaire des ovules matures non-fécondés et un transport progressif de la protéine dans l'appareil filiforme et dans la région du nucelle entourant le micropyle au cours de la maturation de l'ovule. Dans des lignées transgéniques sous-exprimant *ZmEA1*, les TP perdent leur croissance directionnelle une fois arrivés à proximité du micropyle d'environ la moitié des ovules. ZmEA1 représente ainsi un bon candidat de molécule de guidage du TP mais aucun récepteur spécifique à ce signal n'a encore été identifié.

1.2.4.2. Réception du tube pollinique

Suite à son passage dans le micropyle de l'ovule, le TP pénètre dans le sac embryonnaire en passant par ou à proximité de l'appareil filiforme, une élaboration de la paroi cellulaire micropylaire des synergides (Higashiyama 2002). Une fois arrivé aux côtés de la synergide réceptive intacte ou dans le cytoplasme de la synergide réceptive déjà dégénérée (Willemse and van Went 1984; Russell 1992; Higashiyama 2002), la réception du TP s'effectue. La réception du TP implique l'arrêt de croissance du TP, la rupture de son extrémité et la libération des deux cellules spermatiques, qui migrent ensuite vers la cellule-œuf et la cellule centrale (Willemse and van Went 1984; Russell 1992; Higashiyama 2002). Chez *Arabidopsis*, la synergide réceptive dégénère suite à l'arrivée du TP dans le sac embryonnaire, produisant un gamétophyte femelle à trois cellules (FG8) (Christensen et al. 1997).

Selon des données génétiques, le gamétophyte femelle participe à la réception du TP. Chez les mutants gamétophytiques *feronia* (*fer*) (Huck et al. 2003) et *sirène*

(*srn*) (Rotman et al. 2003) d'*Arabidopsis*, le développement et la structure des sacs embryonnaires sont normaux. Cependant, une fois pénétré à l'intérieur du sac embryonnaire, le TP continu à croître et ne libère pas son contenu. Une prolifération similaire du TP dans le sac embryonnaire a été observée lors de croisements interspécifiques incongrues chez *Rhododendron* (Weterings and Russell 2004). Ces observations suggèrent que la réception du TP implique un processus de signalisation spécifique entre le TP et la synergide ou d'autres cellules du sac embryonnaire. Selon les phénotypes des mutants *fer* et *srn*, le sac embryonnaire pourrait soit émettre un signal qui induirait la réception du TP, soit percevoir un signal issu du TP qui entraînerait des changements, structuraux ou physiologiques, nécessaires à la réception du TP (Rotman et al. 2003). L'isolement des gènes *FER* et *SRN* permettra de mieux définir les mécanismes d'interaction entre les gamétophytes mâle et femelle.

1.2.4.3. Contrôle maternel du développement de la graine

Suite à la libération des gamètes mâles dans le sac embryonnaire, la double fécondation des gamètes femelles enclenche le développement de la graine et du fruit. La fusion d'un premier gamète mâle avec la cellule-œuf génère un zygote diploïde qui se développera en embryon, représentant la nouvelle génération sporophytique, alors que la fusion d'un second gamète mâle avec la cellule centrale génère la cellule initiale de l'albumen qui se développera en un tissu nourricier triploïde. La production d'une graine viable porteuse de la génération sporophytique suivante requiert le développement coordonné de l'embryon, de l'albumen, ainsi que des téguments de l'ovule en enveloppe de la graine (Russell 1992; Russell 1996). Des analyses génétiques ont montré que le gamétophyte femelle participe également au contrôle du développement de la graine à plusieurs niveaux, soit lors de l'étape de l'initiation et lors du développement subséquent de l'embryon et de l'albumen

(Drews et al. 1998; Drews and Yadegari 2002; Yadegari and Drews 2004; Brukhin et al. 2005).

1.2.4.4. Contrôle maternel de l'initiation du développement de la graine

Lors de la reproduction sexuée, l'initiation du développement de l'embryon et de l'albumen requiert normalement la fécondation des gamètes femelles par les gamètes mâles. Cependant, les mutants gamétophytiques femelles *fertilization-independent endosperm* (*fie* ou *fis3*) (Ohad et al. 1996; Chaudhury et al. 1997), *medea* (*mea* ou *fis1*) (Chaudhury et al. 1997; Grossniklaus et al. 1998) et *fertilization-independent seed2* (*fis2*) (Chaudhury et al. 1997), initient un développement spontané d'un albumen diploïde ainsi que de l'enveloppe de la graine et du fruit en absence de fécondation. Chez le mutant *multiple supressor of ira* (*msi1*), le développement d'une structure embryonnaire est initié en plus d'un albumen (Kohler et al. 2003a; Guitton and Berger 2005). Ces phénotypes suggèrent que les gènes mutés répriment en temps normal la prolifération cellulaire et ainsi le développement de l'albumen et/ou de l'embryon dans un sac embryonnaire non-fécondé. Les gènes *FIE*, *MEA* et *FIS2* sont exprimés principalement dans la cellule centrale du sac embryonnaire avant la fécondation (Vielle-Calzada et al. 1999; Luo et al. 2000; Yadegari et al. 2000) et codent pour des homologues de protéines homologues à celles des complexes du groupe *Polycomb* des métazoaires, qui forment un complexe répresseur de l'expression de gènes homéotiques (Grossniklaus et al. 1998; Luo et al. 1999; Ohad et al. 1999). De façon analogue, chez *Arabidopsis*, un tel complexe réprimerait l'expression du gène *PHERES1* (*PHE1*), qui code pour une protéine à domaine MADS et dont l'expression est induite dans les premiers stades du développement de l'albumen suite à la fécondation (Kohler et al. 2003b). Ces données montrent l'importance du gamétophyte femelle dans le contrôle de l'initiation du développement de l'albumen par l'expression d'un ensemble de protéines qui répriment l'initiation en absence de fécondation. La fécondation permettrait d'initier

le développement de l'albumen en inactivant ce complexe répressif par un mécanisme encore inconnu.

1.2.4.5. Contrôle maternel du développement de l'embryon et de l'albumen suite à la fécondation

Lors de la fécondation des gamètes femelles, l'apport du génome des gamètes mâles permet l'élaboration d'un embryon diploïde et d'un albumen triploïde. L'identification de certains mutants gamétophytiques femelles montrent que, une fois la fécondation effectuée et malgré la présence du génome paternel, le développement subséquent de l'embryon et de l'albumen nécessite la participation de gènes gamétophytiques femelles. Les mutations gamétophytiques femelles qui affectent le développement suite à la fécondation, lors du développement de l'embryon et de l'albumen, et dont les effets ne peuvent être contrebalancés par l'allèle provenant du génome des gamètes mâles, sont définies comme étant des mutations gamétophytiques à effet maternel et les gènes correspondant sont des gènes gamétophytiques à effet maternel. L'effet maternel d'une mutation gamétophytique peut être causé par différents mécanismes (Grossniklaus and Schneitz 1998): (1) la mutation perturbe le dosage génique (nombre de copie d'un gène) (2) la mutation affecte un gène exprimé par le gamétophyte femelle avant la fécondation et qui est spécifiquement requis pour le développement de l'embryon et/ou de l'albumen après la fécondation; (3) la mutation affecte un gène dont seul l'allèle contribué par le gamétophyte femelle est actif après la fécondation, l'allèle paternel étant inactivé par "*genomic imprinting*".

Plusieurs mutations gamétophytiques à effet maternel ont été identifiés (Brukhin et al. 2005; Pagnussat et al. 2005). En plus des mutants *fie*, *mea* et *fis2* mentionnés précédemment, dont les gènes maternels correspondants sont également requis suite à la fécondation (Ohad et al. 1996; Chaudhury et al. 1997; Grossniklaus

et al. 1998), les mutants *capulet1* (*cap1*) et *capulet2* (*cap2*) (Grini et al. 2002), *constitutive triple response1* (*ctr1*) (Christensen et al. 2002) et *prolifera* (*prl*) (Springer et al. 1995; Springer et al. 2000) d'*Arabidopsis* ainsi que le mutant *maternal effect lethal1* (*mel1*) (Evans and Kermicle 2001) du maïs en représentent quelques exemples. Chez tous ces mutants, le développement de l'embryon et/ou de l'albumen est anormal suite à la fécondation des gamétophytes mutants avec du pollen de type sauvage. Le gène *PRL* code pour un homologue du *DNA Replication Licensing Factor Mcm7*, requis pour la réplication de l'ADN (Springer et al. 1995; Springer et al. 2000), alors que le gène *CTR1* code pour une protéine kinase Raf Ser/Thr, impliquée dans la transduction du signal de l'éthylène (Christensen et al. 2002). L'identité des gènes affectés dans les mutants *cap1*, *cap2* et *mel1* n'est cependant pas connue. Parmi les mutants gamétophytiques à effet maternels identifiés, le mécanisme en cause dans l'effet maternel n'a été démontré que pour le mutant *mea*, qui serait dû à l'inactivation de l'allèle paternel par "*genomic imprinting*" (Vielle-Calzada et al. 1999; Yadegari et al. 2000).

Suite à la fécondation, les tissus sporophytiques entourant le sac embryonnaire subissent des changements morphologiques simultanément au développement de l'embryon et de l'albumen. Certaines données génétiques montrent la participation de gènes exprimés par les tissus sporophytiques de l'ovule dans le contrôle du développement de l'embryon et de l'albumen suite à la fécondation (Grossniklaus and Schneitz 1998). Ces gènes sont définies comme étant des gènes sporophytiques à effet maternel. Par exemple, l'expression du gène *SHORT INTEGUMENT1* (*SIN1*) d'*Arabidopsis* dans les tissus sporophytiques de l'ovule est requise pour le développement de l'embryon, et ce indépendamment du génotype de l'embryon ou de l'albumen (Ray et al. 1996). Des effets sporophytiques maternels sur le développement de l'albumen ont aussi été observés lors d'une sous-expression dans l'ovule spécifiquement des gènes MADS box *FLORAL BINDING PROTEIN 7* (*FBP7*) et *FBP11* chez le pétunia (Colombo et al. 1997). Le mécanisme d'action de

ces gènes sur le développement de l'embryon et/ou la graine n'est cependant pas déterminé.

1.3 Approche par génétique inverse (*reverse genetics*)

Notre compréhension des processus génétiques et moléculaires impliqués dans la mégagamétogénèse et les évènements entourant l'initiation du développement de la graine a jusqu'à récemment été principalement acquise par une approche de "*forward genetic*", à travers laquelle la compréhension d'un processus de développement passe par l'identification de mutations qui produisent un phénotype recherché, suivie par l'identification du gène muté correspondant (Drews and Yadegari 2002; Yadegari and Drews 2004; Brukhin et al. 2005). Cependant, cette approche semble montrer quelques limitations quant au nombre de gènes pouvant être identifiés et donc à une compréhension plus complète de ses bases moléculaires. Il a été estimé que plusieurs milliers de gènes sont exprimés par le gamétophyte femelle et que, parmi ceux-ci, seulement 600 pourraient être identifiés par criblage génétique de mutants (Christensen et al. 2002; Drews and Yadegari 2002). Cette limitation serait en partie due à la redondance fonctionnelle des gènes, un processus par lequel un membre de la famille de gènes a le potentiel de complémenter entièrement ou partiellement la fonction du gène muté ou sous-exprimé (Drews and Yadegari 2002; Dresselhaus 2006). De plus, les effets pléiotropiques lors du stade de développement sporophytique causés par des mutations sporophytiques pourraient masquer l'implication des gènes correspondants dans les processus reproductifs reliés au gamétophyte femelle.

Des approches basées sur le profil d'expression relié au gamétophyte femelle doivent ainsi être utilisées de façon complémentaire à l'approche génétique. Cependant, les problèmes à surmonter sont intrinsèques au système d'étude, étant donné la taille très réduite du gamétophyte femelle et la difficulté à le séparer nettement des téguments qui l'entourent. La création de lignées "*gene-trap*" et

"*enhancer-trap*" exprimant un gène rapporteur visuel a par exemple mené à l'identification et la caractérisation de quelques gènes exprimés dans le gamétophyte femelle (Springer et al. 1995; Sundaresan et al. 1995; Acosta-Garcia and Vielle-Calzada 2004). Plus récemment des études du transcriptome ont été menées. Chez *Arabidopsis*, pour qui le génome a été entièrement séquencé et la presque entièreté des gènes codés par son génome ont été microalignés (*microarrays*), des gènes spécifiquement ou préférentiellement exprimés dans le gamétophyte femelle (Yu et al. 2005) et des gènes potentiellement impliqués dans la régulation du développement reproductif (Hennig et al. 2004) ont été identifiés par comparaison des profils d'expression. Chez le maïs et le blé, la mise au point de techniques de micro-dissection *in vitro* pour isoler des gamétophytes femelles et de ses cellules isolées a permis la construction de banques d'ADNc ainsi que le séquençage d'un grand nombre d'ESTs correspondants (Kranz et al. 1991; Dresselhaus et al. 1994; Kumlehn et al. 2001; Le et al. 2005; Okamoto et al. 2005; Sprunck et al. 2005; Yang et al. 2006). Très peu de chevauchement a été trouvé entre les gènes identifiés dans les divers criblages génétiques et ceux issus des études sur le transcriptome jusqu'à présent (Yang et al. 2006), montrant la complémentarité de ces approches.

Les gènes ainsi identifiés peuvent servir de base dans une approche par génétique inverse ciblée, par laquelle la fonction biologique d'un gène individuel ou d'un groupe de gènes d'intérêt est déterminée par les phénotypes causés par une altération dans leurs niveaux d'expression dans des lignées transgéniques. Les gènes spécifiquement exprimés dans un type cellulaire peuvent servir de marqueur cellulaire et les promoteurs de ces gènes peuvent être utilisés pour réguler l'expression spécifique de transgènes.

1.4. Introduction au projet de recherche

Ce projet de doctorat s'inscrit à l'intérieur d'un projet plus global visant à identifier et à caractériser des gènes impliqués dans la régulation de processus

reproductifs dans les organes femelles par une approche de génétique inverse, avec un intérêt particulier pour les gènes potentiellement impliqués dans des voies de signalisation et dans la régulation génique. L'identification de tels gènes a tout d'abord été réalisée à travers un projet de séquençage d'ESTs générés par une méthode dérivée de la soustraction virtuelle, qui permet d'isoler des gènes faiblement représentés dans une population d'ARNm provenant d'un tissus d'intérêt (Li and Thomas 1998; Germain et al. 2005). Le faible niveau de représentation d'un gène peut résulter d'une expression limitée à un petit nombre de cellules dans les tissus analysés, ce qui est le cas par exemple des gamétophytes femelles dans les ovules, ou d'un niveau d'expression intrinsèquement faible dans les tissus analysés, ce qui peut être le cas notamment pour les gènes impliqués dans des voies de communication intercellulaire ou dans la régulation génique (Hu et al. 2003; Germain et al. 2005). Ces travaux ont été effectués chez *Solanum chacoense*, une espèce de pomme de terre sauvage et ainsi un proche parent d'espèces de grande importance économique telles que la pomme de terre et la tomate. *S. chacoense* est auto-incompatible, permettant un contrôle aisé du moment de la pollinisation, produit des ovaires contenant un très grand nombre d'ovules et possède une mégagamétogénèse de type monosporique *Polygonum*, comme la majorité des angiospermes (Clarke 1940; Maheshwari 1950; Dnyansagar and Cooper 1960; Estrada-Luna et al. 2004).

Cette thèse porte plus spécifiquement sur la caractérisation fonctionnelle des gènes *NOTCHLESS* (*NLE*) et *MIDASIN* (*MDN1*) chez *Solanum chacoense* (*Sc*) et/ou *Arabidopsis thaliana* (*At*). Le gène *ScNLE* a été isolé d'une soustraction virtuelle effectuée sur environ 2 000 clones provenant d'une banque d'ADNc de pistils récoltés 48 heures après pollinisation, une période correspondant aux évènements de la double fécondation et de l'initiation du développement de la graine chez *S. chacoense*. *ScNLE* est l'homologue du gène *NLE* de *Drosophila melanogaster* (*DmNLE*), qui code pour une protéine à WD-repeat impliquée dans la régulation de la voie de communication intercellulaire Notch (Royet et al. 1998). La voie Notch est utilisée dans plusieurs processus de différenciation cellulaire locaux lors du

développement des métazoaires (Kimble and Simpson 1997; Artavanis-Tsakonas et al. 1999), justifiant ainsi l'intérêt premier d'étudier la fonction du gène *NLE* chez les plantes, qui n'avait jusqu'à présent pas été déterminée. Le gène *MDN1* a été isolé par double-hybride lors de la recherche de protéines interagissant avec ScNLE dans cette étude. Ce résultat, combiné à ceux obtenus pour la levure par d'autres équipes de recherche, suggère que NLE jouerait un rôle dans la biogénèse des ribosomes.

Les trois prochains chapitres présentent les résultats de la caractérisation des gènes *NLE* et *MDN1* lors du développement végétal. Les chapitres II et III portent sur la caractérisation du gène *ScNLE* chez *Solanum chacoense*. Le chapitre II présente le gène *ScNLE* ainsi que la caractérisation de son rôle lors de la reproduction sexuée. Le chapitre III traite de la caractérisation du rôle de *ScNLE* lors du développement végétatif et sur l'isolement de ScMDN1 comme protéine interagissant avec ScNLE. Finalement, le chapitre IV porte sur la caractérisation fonctionnelle des gènes *AtNLE* et *AtMDN1* chez *Arabidopsis*.

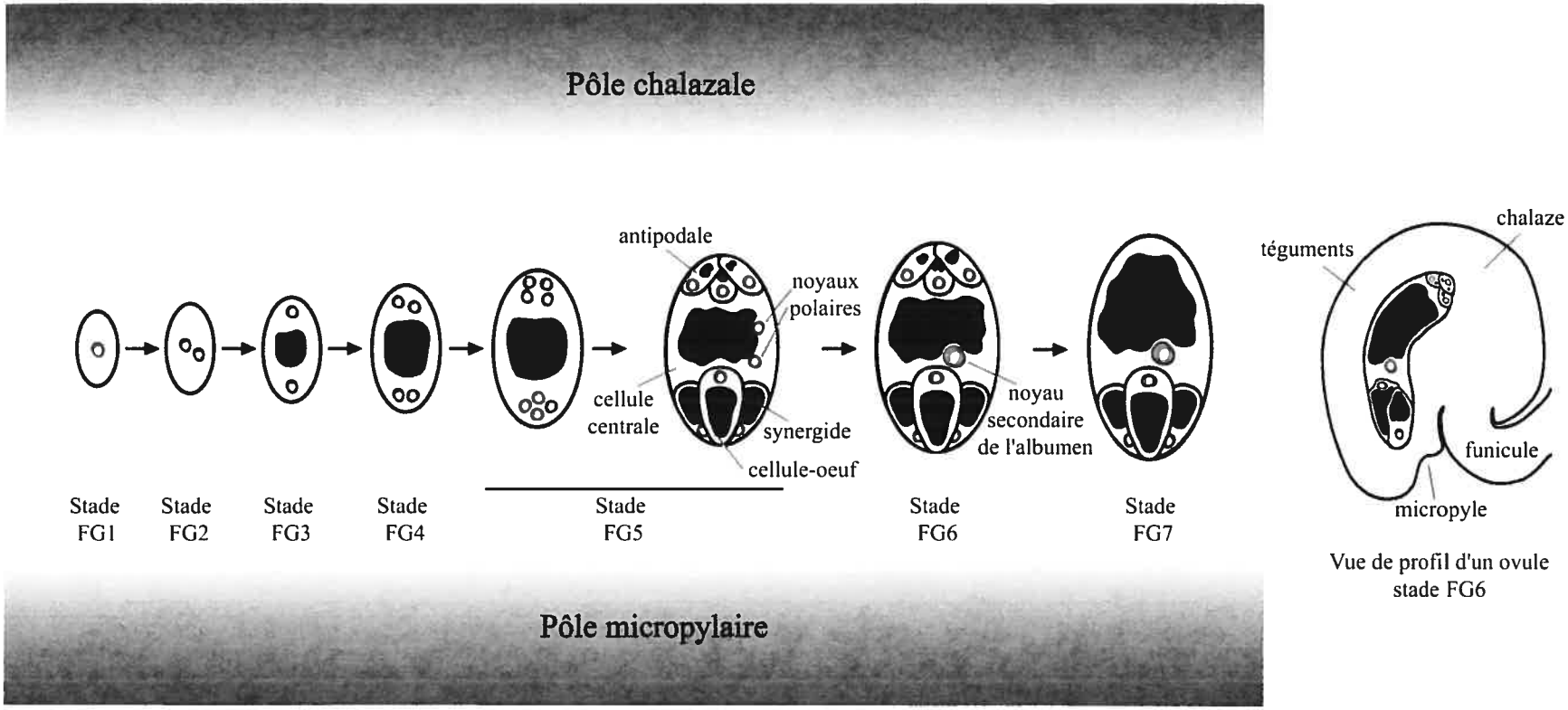

Figure 1-1. Représentation schématique des principaux stades de la mégasporogénèse de type *Polygonum* chez *Arabidopsis* et vue de profil d'un ovule au stage FG6. Les petits cercles gris foncé représentent les noyaux, les taches blanches à l'intérieur des noyaux représentent les nucléoles, les taches noires représentent les vacuoles. Les stades de la mégasporogénèse sont décrits de façon plus détaillée dans le texte. Tiré et modifié de Christensen et al., 1998.

Tableau 1-1. Catégories phénotypiques des mutants gamétophytiques femelles identifiés chez *Arabidopsis* et le maïs*

Catégorie de mutant	Nom du mutant	Références
Mitotique		
Stade à un noyau	*gfl*	(Christensen et al. 1997)
	gfa4, gfa5	(Feldmann et al. 1997)
	ada, tya	(Howden et al. 1998)
	fem2, fem3, fem9, fem12, fem26, fem29, fem35, fem37, fem38	(Christensen et al. 2002)
	agp18	(Acosta-Garcia and Vielle-Calzada 2004)
	eda8	(Pagnussat et al. 2005)
Autres stades	*prl*	(Springer et al. 1995)
	*ig**	(Huang and Sheridan 1996)
	hdd	(Moore et al. 1997)
	fem5, fem10, fem11, fem16, fem18-fem25, fem30, fem31, fem33, fem34, fem36	(Christensen et al. 2002)
	cki1	(Pischke et al. 2002; Hejatko et al. 2003)
	nomega	(Kwee and Sundaresan 2003)
	apc2	(Capron et al. 2003)
	rbr1	(Ebel et al. 2004)
	swa1	(Shi et al. 2005)
	eda1-eda7, eda9-eda23	(Pagnussat et al. 2005)
	lpat2	(Kim et al. 2005)
Caryogamie	*gfa2, gfa3, gfa7*	(Feldmann et al. 1997; Christensen et al. 1998)
	maa1, maa3	(Shimizu and Okada 2000)
	eda24-eda41	(Pagnussat et al. 2005)
Cellularisation	*gfa3, fem4*	(Christensen et al. 1998; Christensen et al. 2002)
	fem6- fem8, fem11, fem13, fem15	(Christensen et al. 2002)
	myb98	(Kasahara et al. 2005)
Fécondation	*fer*	(Huck et al. 2003)
	srn	(Rotman et al. 2003)
	une1-une18	(Pagnussat et al. 2005)
	*zmea1**	(Marton et al. 2005)
Effet maternel	*fis1 (mea), fis2, fis3 (fie)*	(Ohad et al. 1996; Chaudhury et al. 1997; Grossniklaus et al. 1998)
	*mel1**	(Evans and Kermicle 2001)
	prl	(Holding and Springer 2002)
	cap1, cap2	(Grini et al. 2002)
	ctr1	(Christensen et al. 2002)
	dme	(Choi et al. 2002)
	mee1-mee70	(Pagnussat et al. 2005)

CHAPITRE II :

Characterization of the plant NOTCHLESS homolog, a WD repeat protein involved in seed development

Article publié:

Sier-Ching Chantha[1], B. Starling Emerald[2], and Daniel P. Matton[1]* (2006).

Plant Molecular Biology 62(6): 897-912.

[1]Institut de Recherche en Biologie Végétale (IRBV), Département de sciences biologiques, Université de Montréal, 4101 rue Sherbrooke est, Montréal, QC, Canada, H1X 2B2.

[2]The Liggins Institute, Faculty of Medical and Health Sciences, The University of Auckland, Private Bag 92019, Auckland, New Zealand.

*Author for correspondance:

Tel: 1-514-872-3967

Fax: 1-514-872-9406

[redacted]

Keywords: Notchless, WD repeat protein, meristem, fertilization, ovule, seed.

Genbank accession number: ScNle AY428810.

Abbreviations: Days after pollination, DAP; Hours after pollination, HAP; SAM, shoot apical meristem.

PERMISSION DE L'ÉDITEUR

Dear Dr. Chantha,

With reference to your request (copy herewith) to re-use material on which Springer controls the copyright, our permission is granted free of charge, on the following conditions:

* it concerns original material which does not carry references to other sources,
* if material in question appears with credit to another source, authorization from and reference to that source is required as well, and permission is also obtained from the author (address is given on the imprint page or with the article);
* allows you non-exclusive reproduction rights throughout the world,
* permission includes use in an electronic form, on the condition that content is
  - password protected,
  - at Intranet or
  - in CD-ROM/E-book;
* full credit (book/journal title, volume, year of publication, page, chapter/article title, name(s) of author(s), figure number(s), original copyright notice) is given to the publication in which the material was originally published by adding: With kind permission of Springer Science and Business Media.

Permission free of charge does not prejudice any rights we might have to charge for reproduction of our copyrighted material in the future.

With best regards,

–

Alice Essenpreis
Springer
Rights and Permissions

–

Tiergartenstrasse 17 | 69121 Heidelberg GERMANY
FAX: +49 6221 487 8223
permissions.Heidelberg@springer.com
WWW.springer.com/rights

COAUTHORSHIP DECLARATION FOR AN ARTICLE

1. Student identification and academic program

Sier-Ching Chantha

Ph. D. Biology

2. Article description

S.C. Chantha, B.S. Emerald et D.P. Matton. Characterization of the plant Notchless homolog, a WD protein involved in seed development. *Plant Molecular Biology* DOI 10.1007/s11103-006-9064-4.

3. Coauthors declaration other than the student

As a coauthor of the above mentionned article, I agree that Sier-Ching Chantha includes this article in her Ph. D. thesis entitled " Caractérisation fonctionnelle des gènes *NOTCHLESS* et *MIDASIN* lors du développement végétal".

Bright Starling Emerald	[redacted]	4/09/06
Coauthor	Signature	Date

DÉCLARATION DES COAUTEURS D'UN ARTICLE

1. Identification de l'étudiant et du programme

Sier-Ching Chantha

Ph. D. Sciences biologiques

2. Description de l'article

S.C. Chantha, B.S. Emerald et D.P. Matton. Characterization of the plant Notchless homolog, a WD protein involved in seed development. *Plant Molecular Biology* (2006) DOI 10.1007/s11103-006-9064-4.

3. Déclaration des coauteurs autres que l'étudiante

À titre de coauteur de l'article identifié ci-dessus, je suis d'accord pour que Sier-Ching Chantha inclue cet article dans sa thèse de doctorat qui a pour titre "Caractérisation fonctionnelle des gènes *NOTCHLESS* et *MIDASIN* lors du développement végétal".

Daniel P. Matton [redacted] 19 Octobre 2006

Coauteur Date

2.1. ABSTRACT

We have isolated a plant *NOTCHLESS* (*NLE*) homolog from the wild potato species *Solanum chacoense* Bitt., encoding a WD-repeat containing protein initially characterized as a negative regulator of the Notch receptor in animals. Although no Notch signaling pathway exists in plants, the *NLE* gene is conserved in animals, plants and yeast. Overexpression of the plant *ScNLE* gene in *Drosophila* similarly affected bristle formation when compared to the overexpression of the endogenous *Drosophila NLE* gene, suggesting functional conservation. Expression analyses showed that the *ScNLE* gene was fertilization-induced and primarily expressed in ovules after fertilization, mainly in the integumentary tapetum (endothelium) of the ovule. Significant expression was also detected in the shoot apex. Promoter deletion analysis revealed that the *ScNLE* promoter had a complex modulatory architecture with both positive, negative, and tissue specific regulatory elements. Transgenic plants with reduced levels of *ScNLE* transcripts displayed pleitotropic phenotypes including a severe reduction in seed set, consistent with *ScNLE* gene expression pattern.

2.2. INTRODUCTION

In the life cycle of a flowering plant (angiosperm), a new sporophytic generation is established during seed development. Seed development is initiated by double-fertilization of the egg-cell and central cell of the female gametophyte, which is embedded within the maternal sporophytic integument(s) of the ovule, by the two sperm cells of the pollen. Double-fertilization triggers several developmental programs, mainly: the fertilized egg-cell initiates embryogenesis, the fertilized central cell forms a triploid nucleus that divides to give rise to the endosperm, and the integument starts differentiating into the seed coat. In coordination with seed development, the ovary develops into a fruit (Gillaspy *et al.*, 1993). The molecular mechanisms underlying fertilization and initiation of seed development events, such as pollen tube guidance, pollen tube reception, and interactions between the different seed components (embryo, endosperm, ovule integument), likely involves intercellular signaling (Chaudhury *et al.*, 1997; Huck *et al.*, 2003; Marton *et al.*, 2005; Ohad *et al.*, 1996; Rotman *et al.*, 2003). In animals, numerous cell fate decisions and developmental processes rely on cellular signaling through the Notch pathway. Determining whether initially equivalent cells will adopt epidermal or neural identity in *Drosophila* and controlling germline proliferation in *Caenorhabditis elegans* represent only few examples (reviewed in Artavanis-Tsakonas *et al.*, 1999; Kimble and Simpson, 1997). The Notch pathway occurs between adjacent signaling cell (ligand-expressing) and receiving cell (receptor-expressing). The skeleton of this pathway is made of three conserved core components: a transmembrane DSL (Delta, Serrate, Lag-2) ligand, a transmembrane Notch-type receptor, and a downstream CSL (CBF-1, Su(H), Lag-1) transcriptional effector. The DSL ligand extracellular domain of a signaling cell first interacts with the Notch-type extracellular domain of a receiving cell. This interaction leads to the activation of the Notch intracellular domain (NICD) by releasing it from the plasma membrane. The NICD is then translocated into the nucleus where it serves as a

coactivator of a CSL transcription factor to modulate gene expression. The receiving cell thus acquires an identity that differs from its adjacent signaling cell.

Several proteins are known to be positive or negative regulators of the Notch signaling activity (reviewed in Kadesch, 2000). Among these, the *Drosophila melanogaster* NOTCHLESS (DmNLE) protein was shown to be a modifier of Notch activity by genetic studies and to interact with the intracellular domain of Notch by GST pull-down and immunoprecipitation assays (Royet *et al.*, 1998). Some mutant alleles of the *Drosophila* Notch receptor (called *notchoid*) cause the formation of notches on the edge of the fly's wings. The *DmNLE* gene was isolated in a genetic screen as a dominant mutant that could suppress this notching, explaining the origin of its name. How DmNLE regulates Notch signaling activity remains however unclear. Interestingly, the mouse *NLE* homolog was found as a candidate gene for a maternal factor present in oocytes that causes the DDK syndrome, which is defined by embryonic lethality of embryos from crosses between DDK females and non-DDK males (Le Bras *et al.*, 2002).

The *NLE* gene encodes a WD-repeat (WDR) protein. The main feature of WDR proteins is the WD motif, which is almost exclusively found in eukaryotes. This motif is defined as a stretch of 44 to 60 amino acids usually containing the Trp-Asp (WD) dipeptide at its C-terminus and a Gly-His (GH) dipeptide 11-24 residues downstream from its N-terminus, but exhibiting only a limited amino acid sequence conservations at each other individual position (Smith *et al.*, 1999; Yu *et al.*, 2000). The WD motifs are repeated in tandem from 4 to 16 times within a polypeptide and fold together into a propeller-shape platform that serves in coordinating simultaneous and/or sequential protein-protein interactions with multiple partners (Smith *et al.*, 1999). Despite being structurally related, members of the WDR protein superfamily are however functionally very diverse. They are in fact involved in a vast array of molecular mechanisms such as signal transduction, RNA processing, cytoskeletal

dynamics, chromatin modification and transcriptional mechanisms, to name a few examples (reviewed in Neer *et al.*, 1994; van Nocker and Ludwig, 2003).

In *Arabidopsis*, van Knocker & Ludwig (2003) identified 237 WDR proteins and classified them into 143 distinct families according to sequence similarities. Among these, some well characterized WDR proteins were shown to regulate various development processes in plants. For example, FIE and MSI1 are two WDR proteins that together associate with MEA in a higher protein complex to repress gene transcription in the central cell of the embryo sac (Kohler *et al.*, 2003). Their activity is required to repress the initiation of endosperm development in the absence of fertilization. Loss-of-function mutations in these genes lead to precocious endosperm formation without the need for fertilization (Chaudhury *et al.*, 1997; Kohler *et al.*, 2003; Ohad *et al.*, 1996). *Msi1* mutants also initiate parthenogenetic development of the embryo (Guitton and Berger, 2005). Also involved in embryo and seedling development, mutations in the TANMEI/EMB2757 WDR protein have recently been shown to produce pleiotropic phenotypes (Yamagishi *et al.*, 2005). LEUNIG is another WDR protein reported to function as a putative transcriptional co-repressor in the regulation of the *AGAMOUS* floral homeotic gene expression (Conner and Liu, 2000). One more example is COP1, a protein that possesses in addition a RING-finger motif and is proposed to act as an E3 ubiquitin ligase in the ubiquitin-proteasome degradation pathway (Osterlund *et al.*, 2000). Because *cop1* mutants show a photomorphogenic development when grown in the dark, COP1 is defined as a negative regulator of photomorphogenic development in the dark (Deng *et al.*, 1991). Other WDR proteins are involved in cell cycle regulation, such as CCS52, a mitotic inhibitor that is required for endoreduplication (Cebolla *et al.*, 1999). These few examples demonstrate the importance of WDR proteins in the regulation of diverse aspects of plant development.

In this report we describe the characterization of a plant homolog of the *DmNLE* gene in *Solanum chacoense* (*ScNLE*). Based on the analysis of the

Arabidopsis genome, most of the known components of the Notch signaling pathway are absent from plants (Wigge and Weigel, 2001). However overexpression experiments of the plant *Nle* homolog in *Drosophila* showed that ScNLE retains the capability to interact with the Notch receptor. In *S. chacoense*, *ScNLE* expression is associated to the shoot apex and is also transiently induced by fertilization in some structures of the ovary such as the endothelium of ovules. Analysis of transgenic plants underexpressing *ScNLE* suggests a specific role in fertilization and/or post-fertilization events for this gene as well as a general role in shoot development.

2.3. MATERIAL AND METHODS

2.3.1. Plant material and growth conditions

We used the diploid (2n=2x=24) *Solanum chacoense* Bitt. (Potato Introduction Station, Sturgeon Bay, WI) self-incompatible genotypes G4 (S_{12} and S_{14} self-incompatibility alleles) as female progenitor and V22 (S_{11} and S_{13} alleles) as pollen donor. Plants were maintained by *in vitro* propagation on 1/2X MS medium with charcoal (1/2X MS salts, 1X MS vitamins, 20% sucrose, 0.5% deactivated charcoal, 0.6% agar, pH 5.8) at 20-22°C with a photoperiod of 16 h light and 8 h dark. Plants from 1 to 2 months old were transferred to soil and were grown in a greenhouse with an average of 14 h of light/day for flower and fruit development analyses.

2.3.2. Isolation and gel blot analysis of RNA and DNA

Isolation of total RNA, poly(A)$^+$ mRNA and genomic DNA as well as gel blot analyses were performed as described previously (Lagacé *et al.*, 2003; Lantin *et al.*, 1999). For RNA gel blot analysis, 10 µg of total RNA for each tissue samples were separated on gel. For DNA gel blot analysis, 10 µg samples of genomic DNA were completely digested separately with 5 U/µl of HindIII, EcoRV, and EcoRI restriction enzymes in an overnight incubation, as recommended by the supplier (New England Biolabs, Mississauga, ON). Probes were derived from full length *ScNLE* cDNA labelled with α-[^{32}P]-dATP (ICN Biochemicals, Irvine, CA) using the High Prime DNA Labeling kit (Roche Diagnostics, Laval, QC). Membranes were exposed at –85°C with intensifying screens on Kodak Biomax MR film (Interscience, Markham, ON).

2.3.3. Library construction and virtual subtraction

The cDNA library was made from 5 µg of poly(A)$^+$ mRNA isolated from pistils 48 HAP with the ZAP express® vector system (Stratagene, LaJolla, CA) (Lantin *et al.*, 1999). In order to enrich the screened library for non-redundant and weakly expressed transcripts, a negative selection screen was performed (Germain *et al.*, 2005).

2.3.4. *In situ* hybridization

Tissue samples were fixed, dehydrated and embedded in paraffin as described previously (Lantin *et al.*, 1999). *In situ* detection of *ScNLE* on 10 µm thick sections was performed as described previously (Lantin *et al.*, 1999). Sense and antisense digoxigenin-11-UTP (Roche Diagnostics) labeled riboprobes were synthesized from the *ScNLE* cDNA cloned in the pBK-CMV vector using T3 and T7 RNA polymerases (RNA transcription kit, Stratagene) after linearization of the plasmid with XhoI or EcoRI, respectively.

2.3.5. *ScNLE* constructs for underexpression

For gene suppression using the antisense strategy, a ~1500 bp fragment of *ScNLE* cDNA was cloned in the antisense orientation in the pBIN35S double-enhancer vector using the HindIII restriction sites (Bussiere *et al.*, 2003). For gene suppression using the double-stranded RNA interference strategy, a ~650 bp fragment of *ScNLE* cDNA was cloned in the sense and antisense orientations in the pDarth vector (O'Brien *et al.*, 2002) from PCR products obtained with the NLE14 (5'-GAGA**GGATCC**AAACCACGCAGGGGAAGCTA-3') and NLE18 (5'-GAGAGGCGC**GGTACC**CTATCCCATCCATAGCTTCAG) primers containing the

BamHI and XhoI restriction sites respectively, and with the NLE19 (5'-GAGA**CTCGAG**AAACCACGCAGGGGAAGCTA-3') and NLE22 (5'-GAGA**GGCGCGCC**CTATCCCATCCATAGCTTCAG-3') primers containing the XhoI and AscI restriction sites respectively. Plant transformation with *Agrobacterium tumefaciens* strain LBA4404 was carried out as described previously (Matton *et al.*, 1997).

2.3.6. Semi-quantitative RT-PCR

Apex RNA samples were purified from DNA contamination by treatment with RNase-free DNase I on RNeasy® columns (Qiagen, Mississauga, ON), according to the manufacturer's instructions, and quantified. RNA samples were reverse transcribed with M-MLV reverse transcriptase (Invitrogen Canada, Burlington, ON) according to the manufacturer's instructions, using 0.1 µg/µl oligo dT_{20}, 2 U/µl RNaseOUT™ (Invitrogen Canada), and 0.1 µg/µl total RNA. PCR mixtures contained 1/20 vol of cDNA sample, 1 µM forward and reverse primers, 200 µM dNTP, 1X Taq buffer and 0.025 U/µl HotStartTaq DNA polymerase (Qiagen). Endogenous *ScNLE* was amplified with the NLE20 (5'-GAGAGGTACCCCTCTATTTCCTCTTAAGAG-3') and NLE3 (5'-TAGCGTTTTCAGGGAGGTAC-3') primers and *ACTIN* was amplified with the Act-1F (5'-CTGARGCMCCYCTTAAYCCCAAG-3') and Act-1R (5'-GTGRCTSACACCATCACCAGAGT-3') degenerated primers. PCR reactions were performed under the following conditions: 1 cycle of 95 °C / 15 min; varying number of cycles of 94 °C / 30 sec, 57 °C / 30 sec, 72 °C / 30 sec; 1 cycle of 72 °C / 5 min. PCR products were run on an 1 % agarose gel, stained with ethidium bromide and bands were scanned. For quantitative measurements, densitometric scans were performed and *ScNLE* amplification products were normalized with their corresponding *ACTIN* amplication products using the ImageQuant software of a Typhoon 9200 phosphor imager (GE Healthcare).

2.3.7. *ScNLE* promoter cloning

A genome walking technique was used to isolate the promoter of the *ScNLE* gene. Genomic DNA of *S. chacoense* was isolated with the DNeasy® Plant Mini Kit (Qiagen). Adaptor-ligated genomic DNA libraries construction and PCR-based DNA walking were performed according to a modified protocol of the Universal GenomeWalker™ Kit (Clontech, Palo Alto, CA). Three micrograms of genomic DNA aliquots were separately digested with restriction enzymes *Dra*I, *Eco*RV, *Nae*I, *Pvu*II, *Stu*I, and *Sma*I restriction enzymes. Blunt-ended DNA fragments were then ligated to the GenomeWalker adaptors. Primary PCR amplifications were performed with adaptor-specific AP1 and gene-specific NLE26 (5'-TTGCCTTCTGGGTCTGCCAACTGACATATG-3') primers using a manual hot start (40 µl PCR mix: 1 µl DNA library; 21.68 µl deionized H_2O; 1X XL buffer II (Perkin Elmer); 0.2 mM dNTP mix; 1.1 mM $Mg(OAc)_2$; 0.1 µM AP1 primer; 0.1 µM NLE26 primer. 10 µl hot start mix: 5.97 µl deionized H_2O; 1X XL buffer II; 2 U r*Tth* DNA Polymerase (Perkin Elmer)). PCR program: 96°C, 5 min; 7 cycles - 94 °C, 25 sec, 72 °C, 3 min; 32 cycles - 94 °C, 25 sec, 67 °C, 3 min; 67 °C, 7 min. Secondary PCR amplifications were performed with nested adaptor-specific AP2 and gene-specific NLE27 (5'-AGCTTCCACTTCCACTTCCATCGTTTCTGC-3') primers (40 µl PCR mix: 1 µl primary PCR product; 21.68 µl deionized H_2O; 1X XL buffer II; 0.2 mM dNTP mix; 1.1 mM $Mg(OAc)_2$; 0.1 µM AP2 primer; 0.1 µM NLE27 primer, 10 µl hot start mix: 5.97 µl deionized H2O; 1X XL buffer II; 2 U r*Tth* DNA Polymerase). PCR program: 94°C, 5 min; 5 cycles - 94 °C, 25 sec, 72 °C, 3 min; 20 cycles - 94 °C, 25 sec, 67 °C, 3 min; 67 °C, 7 min. DNA fragments obtained from secondary PCR were gel-extracted with the QIAquick® Gel Extraction kit (Qiagen) and cloned with the TOPO TA cloning® system (Invitrogen) according to the manufacturer's instructions. Cloned DNA fragments were sequenced to confirm identity.

2.3.8. Promoter-GUS fusion constructs

Four regions of the *ScNLE* promoter were PCR amplified from *S. chacoense* genomic DNA using PWO DNA Polymerase (Roche Diagnostics). The vector pCambia-1291Z (CAMBIA, Canberra, Australia) was used to create translational fusions with the GUS reporter gene. The upstream primers used for amplifying promoter DNA fragments of various sizes were: NLE31 (-1171) 5'-GAGA**GAATTC**TTGGAGCGTGTTTTATCAAG-3'; NLE30 (-695) 5'-GAGA**GAATTC**AGCTATATTAGCTCACCGTTC-3'; NLE29 (-400) 5'-GAGA**GAATTC**TGCCAAATGTGAAACAATGTC-3'; and NLE36 (-113) 5'-GAGA**GAATTC**ATCTTTGCAAAGCTGAAA-3'. These upstream primers were tagged with the EcoRI restriction site sequence (in bold in the above mentioned primers). The downstream primer NLE28 (5'-GAGA**CCATGG**CACTGTTTGTTGCTTCTCTC-3') is tagged with the NcoI restriction site (in bold) and was used in all the PCR amplifications. The 3' nucleotide position for all the promoter regions cloned corresponds to +58. PCR products were digested with and ligated to the EcoRI and NcoI sites of pCambia1291Z. The amplified sequences and junctions of the construct were confirmed by sequencing. Plant transformation with *Agrobacterium tumefaciens* strain LBA4404 was carried out as described previously (Matton *et al.*, 1997).

2.3.9. GUS staining

Tissues were collected and immediately fixed in 90% ice-cold acetone and incubated 20 min at room temperature. Tissues were rinsed twice with a GUS working solution (50 mM sodium phosphate, pH 7.2, 2 mM $K_3Fe(CN)_6$, 2 mM $K_4Fe(CN)_6$, and 0.2% Triton X-100) for 20 min each at room temperature. After

rinsing, tissues were vacuum infiltrated for 40 min with 5-bromo-4-chloro-3-indolyl ß-D-glucuronide cyclohexylamine (X-Gluc) salt, added to GUS working solution to a final concentration of 2 mM, and then incubated at 37 °C overnight. The reaction was terminated and tissues were cleared in 70% ethanol added fresh once a day for a week.

2.3.10. Microscopy

Plant material embedded in paraffin was prepared for sectioning as described for *in situ* hybridization. Tissues stained for GUS expression were fixed in formaldehyde-acetic acid (3.7 % formaldehyde, 5 % acetic acid, and 50 % ethanol) for 2 h and dehydrated through an ethanol series and embedded in paraffin. Paraffin blocks were trimmed to reveal internal tissues and surface-exposed tissues were counter-stained with safranin to localize GUS coloration (Kim *et al.*, 2002). Sectioned tissues were visualized under a dissecting microscope. For flower bud morphology analysis, sections 10 µm thick were rehydrated and stained with safranine overnight, thoroughly washed in water and then stained with Astra blue for 20 min. After two washes in water, sections were dehydrated and mounted in Permount.

2.3.11. DNA sequencing and analysis

Approximately 200 ng (5 µl) of plasmid DNA and 15 µl of reaction mixture containing 8.5 µl of water, 3.5 µl 5X sequencing buffer, 2 µl primer at 0.8 µM, and 1 µl Big Dye Terminator Ready Reaction Mix (PE Applied Biosystems) was used for the sequencing reaction. Sequencing reactions were preformed on a GeneAmp PCR System 9700 (PE Applied Biosystems), and the cycling conditions were: 96 °C, 10 sec; 50 °C, 5 sec, 60 °C, 4 min for 25 cycles. DNA sequencing was performed on an

Applied Biosystem ABI 310 automated sequencer. Sequence alignments were performed with the ClustalW module of the MacVector 7.2.3 software (Accelrys). Database searches were conducted with the BLAST program at The Arabidopsis Information Resource (www.arabidopsis.org) and at the National Center for Biotechnology Information (www.ncbi.nlm.nih.gov).

2.3.12. *Drosophila* transformation

Details on overexpression experiments in *Drosophila* have been described previously (Royet *et al.*, 1998).

2.4. RESULTS

2.4.1. Isolation of the *NLE* gene in *Solanum chacoense*

Key regulatory genes involved in development, as opposed to housekeeping genes, are generally weakly expressed and highly tissue-specific (Hu *et al.*, 2003). We have initiated a negative selection screen targeting weakly expressed genes, with the aim of identifying regulatory genes involved in fertilization and seed initiation in *Solanum chacoense* (a close relative of the potato and tomato) (Germain *et al.*, 2005). *S. chacoense* is self-incompatible and pollination time can therefore be easily controlled. Pollen tubes reach the first ovules in the ovary around 36 hours after pollination (HAP) and fertilization is completed for all ovules around 42-48 HAP (Clarke, 1940; Williams, 1955; and our unpublished observations). The selection screen was initially carried on 2000 clones obtained from a cDNA library of pistils collected 48 HAP. A total of 250 clones were selected and sequenced. A homolog of the *Drosophila melanogaster NLE* gene (*DmNLE*) was isolated and named *ScNLE* (for *Solanum chacoense NLE*). The *DmNLE* gene was initially isolated in a suppressor screen in a viable Notch receptor mutant background and was characterized as a regulator of Notch signaling activity (Royet *et al.*, 1998).

The longest ScNLE cDNA isolated consisted of 1827 bp (excluding the poly A tail) and likely represented the full-length or near full-length ScNLE mRNA since it corresponded to the size of the mRNA detected in gel blot analyses (~1.8 kb). The *ScNLE* cDNA contained a single long open reading frame (ORF) with two in frame initiation codons at positions 65 (AGAUUAAUGGCA) and 77 (AAACGAUGGAA) from the first nucleotide of the cDNA. The second AUG thus shows higher similarity with the plant translation start site consensus sequence for the dicots (aaA(A/C)aAUGGCu) (Joshi *et al.*, 1997). Furthermore, sequence comparison with amino acid sequences from plant NLE orthologs (data not shown) suggests that the

second ATG represents the most probable translational initiation start site. Thus, the deduced ScNLE protein is 482 aa long and has a predicted molecular weight of 53.2 kDa.

ScNLE gene copy number was determined by DNA gel blot analysis (Figure 2-1B). Three hybridizing fragments could be detected from HindIII (4.5, 2.0 and 1.3 kb), two from EcoRV (7.0 and 3.0 kb), and two from EcoRI (5.0 and 4.2 kb) restriction enzymes. Since there are two HindIII (position 233 and 1799) and one EcoRV (position 1393) sites in the cDNA sequence, this suggests that *ScNLE* is a single copy gene in *S. chacoense*. Accordingly, analysis of the *Arabidopsis* genome sequence revealed the presence of only one copy of the *AtNLE* gene (At5g52820).

2.4.2. Sequence analysis of ScNLE protein

A BLAST search of the GenBank protein database revealed that ScNLE exhibits highest overall similarities with plant sequences obtained from *Arabidopsis thaliana* (76% identity, 88% similarity; BAB10430) and *Oryza sativa* (78% identity, 89% similarity; ABA94577). Moreover, ScNLE showed high overall sequence conservation with orthologs from *Xenopus laevis* (56% identity, 74% similarity; AAC62236), *Saccharomyces cerevisiae* (47% identity, 68% similarity; NP_009997 or Ycr072cp) and *Drosophila melanogaster* (52% identity, 71% similarity; AAF51479).

The NLE protein contains a Nle domain followed by a WD-repeat (WDR) domain (Figure 2-1A). The Nle domain was defined as a region with a high degree of sequence conservation in the N-terminal portion of NLE homologs (Royet *et al.*, 1998). *S. chacoense* and *D. melanogaster* Nle domains are 42% identical (64% similar). Use of predictive tools (http://BMERC-www.bu.edu/wdrepeat) allowed the identification of eight WD repeats in the WDR domain of ScNLE (Figure 2-1A). A

WD motif is defined as a stretch of 44 to 60 aa that typically contains the GH dipeptide 11-24 residues from its N-terminus and the WD dipeptide at its C-terminus, but that exhibits only a limited amino acid sequence conservation at each individual position (Smith *et al.*, 1999; Yu *et al.*, 2000). Seven of the eight WD repeats in ScNLE range from 41 to 48 aa in length. The fifth WD motif is unusually long (78 aa) and Royet et *al.* (1998) considered this fifth repeat as representing two different WD repeats lacking the signature residues. Our analyses indicated instead that this region represents a unique WD repeat that contains a small insertion. Surface-exposed residues in a WD repeat are predicted to be grouped in the variable regions I and II (Smith *et al.*, 1999) (Figure 2-1A). These regions are responsible for most protein variability and would determine the specificity of protein interaction with protein partners. Despite a high overall homology between corresponding WD repeat of ScNLE and DmNLE, ranging from 43% to 72% identity, comparison of their corresponding variable regions I and II revealed a variation in the degree of sequence identity, with very low conservation found in some of these regions. On the basis of these observations, protein partners of ScNLE and DmNLE have likely diverged in plant and animal organisms.

2.4.3. ScNLE is a partial functional homolog of DmNLE in *Drosophila*

To determine whether the high overall amino acid sequence identity between ScNLE and DmNLE reflects conservation in protein function, the plant ScNLE protein was overexpressed in the thorax of fruit flies by driving a UAS::ScNLE construct under the control of apterous::GAL4 (ap-GAL4). In *Drosophila*, modulating the Notch signaling pathway influences, among other things, the number of thoracic cells that differentiate into bristle instead of epidermal cell. The overexpression of *DmNLE* in *Drosophila* was reported to cause a significant reduction in the number of bristles formed on the thorax (196.0 ± 3.0, n=17) compared to ap-GAL4 control lines (214.2 ± 2.7, n=9) (Royet *et al.*, 1998).

Interestingly, the overexpression of *ScNLE* also caused a significant reduction in the number of thoracic bristles formed, with an average of 187.9 ± 8.1 bristles per thorax (n=16, $p<0.001$) (Figure 2-1C). This result indicates that ScNLE is able to accomplish, at least partially, the same function as DmNLE protein when overexpressed in flies. However, some strong *ScNLE* overexpressing lines obtained from these experiments and were associated with phenotypes never observed in *DmNLE* overexpressing lines. Strong *ScNLE* overexpressing lines produced much less bristles comprising large, medium, and also unusual tiny bristles (Figure 2-1C). Furthermore, the fly's thorax seemed to collapse, suggesting the loss of some internal tissues. Since these additional phenotypes were not observed with *DmNLE* overexpression, it is likely that ScNLE and DmNLE are not fully functional homologous proteins, as can be expected.

2.4.4. *ScNLE* expression pattern in *Solanum chacoense*

ScNLE mRNAs expression pattern was determined in plant tissues by RNA gel blot analyses. We first focused on *ScNLE* expression pattern in ovaries since *ScNLE* cDNA was isolated from a pollinated pistil cDNA library. Figure 2-2A shows a broad time-course analysis using isolated ovules. Weak expression signal was detected in ovules from unpollinated flowers (0 h). Interestingly, the expression was strongly and transiently increased two days after pollination (DAP), decreasing to basal levels by four DAP. A more detailed time-course analysis was also carried out with pollinated ovaries (Figure 2-2B). *ScNLE* expression was weak from 0 to 30 hours after pollination (HAP) and was significantly increased at 36 HAP. Peak expression was reached around 42 HAP (Figure 2-2B) and then slowly declined to basal levels (Figure 2-2A). This transient increase in *ScNLE* gene expression around 36 to 42 HAP corresponds exactly to the intense period of basipetal fertilization of the multiple ovules present in the ovary and to the initiation of seed development in some Solanaceous species, including *S. chacoense* (Clarke, 1940; Williams, 1955),

and our unpublished results). To confirm that the strong increase in *ScNLE* expression was fertilization-dependent and not only a consequence of pollination, we took advantage of the gametophytic self-incompatibility system present in *S. chacoense*. Following a self-incompatible pollination, pollen tubes are normally stopped in the top 2/3 of the style and no increase in *ScNLE* mRNA levels could be observed in ovaries (Figure 2-2B). This result confirmed that the increase in *ScNLE* expression was fertilization-dependent.

We also tested for *ScNLE* expression in various plant tissues. Figure 2-2C shows that no signal was detected in the vegetative tissues tested, including tubers, roots, stems and leaves, nor in floral organs such as petals, anthers and pollen grains or tubes. RNAs from ovaries 3 DAP served as a positive control in this RNA gel blot. Although no expression could be initially detected in vegetative tissues, shoot apices containing the shoot apical meristem (SAM) and organ primordia were also tested (see also transgenic phenotype section below). As for other tissues tested, a single band of ~1.8 kb, corresponding to the length of the longest *ScNLE* cDNA isolated, was also detected in the shoot apex (Figure 2-2C).

2.4.5. *In situ* detection of *ScNLE*

In situ hybridization was used to further examine *ScNLE* mRNA expression pattern in ovaries 48 HAP, a time point corresponding to high *ScNLE* expression levels in RNA gel blot analysis (Figure 2-2A). Hybridization signals were more strongly associated to the outermost cell layers of the placenta and to the endothelium (also called the integumentary tapetum) of ovules, which is the innermost cell layer of the integument (Solanaceous ovules are unitegmic) (Figure 2-3A) as well as in the zygote (Figure 2-3C). *ScNLE* expression was also strongly detected in the vascular tissues of the receptacle and of the ovary (Figure 2-3A) as well as of the funiculus (Figure 2-3D).Uniform and weaker expression of *ScNLE* was detected in inner

placenta cells (Figure 2-3A). Equivalent tissues were hybridized with a *ScNLE* sense probe as negative controls and no signal could be detected in these tissues (Figure 2-3B, E), confirming the specificity of the *ScNLE* hybridization pattern obtained. Such expression pattern suggests that *ScNLE* plays a role in some specific response immediately following fertilization.

2.4.6. Analysis of cis-regulatory regions required for expression of *ScNLE* in ovary

As a first step in defining the cis-regulatory regions required for specific expression pattern of *ScNLE* in the ovary, a promoter deletion analysis was performed. A 1171 bp fragment upstream of the translational initiation site (numbered as +1) was isolated by a genome walking technique. A series of 5' deletions with end points at -1171, -695, -400, and -113 from the translation start site, and comprising a part of the coding region (+58), were fused in-frame to the *uidA* reporter gene encoding the β-glucuronidase (GUS) protein (Figure 2-4). The resulting chimeric gene constructs were subsequently transformed into WT *S. chacoense* plants. At least five stable trangenic plants of each construct were analyzed for the expression patterns of GUS activity. Variability in the patterns of GUS activity within the different lines generated from the same construct was observed, which is consistent with results obtained in other studies and could be attributed to position effects (Honma and Goto, 2000; Tilly *et al.*, 1998). A summary of the deletion constructs and the relative intensities of GUS staining observed in more than half of the samples, unless specified otherwise, is reported in Figure 2-4. Typical GUS staining patterns from tissue sections are shown in Figure 2-5. With construct PNLE-1171 in flowers 48 HAP, obvious GUS staining was found in a region of the receptacle below the ovary (Figure 2-5A). This stained region of the receptacle comprised mainly the vascular tissues of the receptacle as suggested by a more precise localization in lightly stained samples (Figure 2-5D). Staining was weak and

uniform in the placenta with a darker outermost cell layer (Figures 2-5B, C). Finally, in about one third of the ovaries analyzed, the funiculus of ovules was also stained (Figures 2-5B, C). GUS activity was not detected, or sometimes only faintly detected, in petals and anthers (Figure 2-5E), confirming results obtained by RNA gel blot analysis (Figure 2-2C). The observed pattern of PNLE-1171 GUS staining recapitulated only partially the pattern of endogenous *ScNLE* transcripts revealed by *in situ* RNA hybridization (Figure 2-3). In accordance, GUS activity was detected in the vascular tissues of the receptacle, in the placenta and the funiculus. However, the absence of GUS staining in the endothelium of ovules and in the vascular tissues of the ovary as well as the presence of GUS staining in the receptacle outside the vascular tissues differed from the *ScNLE* expression pattern determined by *in situ* hybridization (compare Figures 2-3 and 2-5A). Therefore, the -1171 bp region upstream of the *ScNLE* gene contains some, but not all, of the regulatory elements necessary for normal (wild-type) expression pattern observed in the ovary, as determined by *in situ* hybridization. These results also suggest that a silencer element is required to inhibit *ScNLE* expression in the receptacle and that additional regulatory elements, either upstream of the -1171 position, or downstream of the +58 position, are also required for expression of the *ScNLE* gene in the endothelium of ovules and vascular tissues of the placenta (Figure 2-6A).

Further deletion analyses uncovered other aspects of *ScNLE* gene expression regulation. Promoter deletion up to -695 gave identical GUS staining patterns as for the PNLE-1171 construct (Figure 2-5F), suggesting that the regulatory elements driving the expression pattern in the ovary 48 HAP observed with the PNLE-1171 construct are not comprised in the -1171 to -695 region of *ScNLE* promoter. Further deletion to -400 however led to the loss of specificity of GUS expression in the ovary (Figure 2-5G). GUS distribution with the PNLE-400 construct was more extended in the receptacle and was also uniformly distributed in all the tissues of the ovary. Therefore, the -695 to -400 region of *ScNLE* promoter seems to comprise a silencer element for repression of *ScNLE* expression in several tissues of the ovary 48 HAP,

such as in external regions of the receptacle, in the carpel wall, and in the ovule's integument, to allow a specific expression pattern of the gene (Figure 2-6A). A further deletion to -113 abolished GUS expression in all ovary tissues 48 HAP except the placenta (Figure 2-5H), suggesting that the -113 to +58 region and the -195 to -113 region contain positive regulatory elements essential for *ScNLE* expression in the placenta and the other ovary tissues, respectively (Figure 2-6A).

RNA gel blot analyses showed that *ScNLE* expression in ovules and ovaries was very weak in unpollinated mature flowers (0 HAP) and was strongly increased around fertilization time (48 HAP) (Figures 2-2A, B). We next wanted to determine whether a regulatory element responsible for this increase in *ScNLE* expression was present in the 1171 bp promoter region analyzed. RNA gel blots made with total RNA extracted from ovaries at time 0 and 48 HAP after fertilization collected from the same transgenic lines used to study GUS staining patterns were probed with a labeled *GUS* insert and, as internal control, with a *ScNLE* probe to detect the expression of the endogenous *ScNLE* gene. A summary of the results is reported in Figure 2-4. Equal loading of the samples was confirmed by probing with ribosomal 18S (data not shown). With construct PNLE-1171, a considerable increase in *GUS* expression levels from 0 HAP, where expression was barely detectable, to 48 HAP recapitulated the pattern of endogenous *ScNLE* expression levels, suggesting that the promoter region analyzed contained regulatory element(s) that respond to the fertilization event. Deletion of region -1171 to -695 led to higher expression of *GUS* in ovaries 0 HAP when compared to endogenous *ScNLE* expression, suggesting that this region comprises a negative regulatory element for repression of *ScNLE* expression in the ovary in absence of fertilization (Figures 2-4 and 2-6A). Despite the appearance of *GUS* expression in ovaries 0 HAP when region -1171 to -695 was removed, *ScNLE* promoter deletion down to -400 generally still led to an increase in *GUS* expression levels from 0 to 48 HAP. With the PNLE-695 construct in ovaries 48 HAP, *GUS* was expressed at similar levels to endogenous *ScNLE* whereas with the PNLE-400 construct, *GUS* expression was stronger than that of the endogenous

ScNLE, a result that is consistent with loss of tissue-specific activity of *ScNLE* promoter and hence, widespread distribution of *GUS*, as shown previously with this construct (Figures 2-4 and 2-5G). Further promoter deletion to -113 however completely abolished the increase in *GUS* expression levels from 0 to 48 HAP, leading to equal *GUS* expression levels at 0 and 48 HAP, lower than endogenous *ScNLE*. These results altogether suggest that region -400 to -113 of *ScNLE* promoter comprises a positive regulatory element that responds to fertilization in the ovary (Figure 2-6A).

2.4.7. Analysis of cis-regulatory motifs in *NLE* promoter sequences

To link the cis-regulatory regions we have identified to candidate transcription factors, we searched the *ScNLE* promoter for different sequence motifs recognized by transcription factors that had been shown to be expressed in ovary tissues by *in situ* hybridization. Because orthologous genes frequently have common expression patterns, we also determined whether these sequence motifs were common to available putative *NLE* promoters from different plant species (*Arabidopsis thaliana*, *Oryza sativa* var. *japonica*, *Populus trichocarpa*). Regions of about the same length, upstream of the predicted translation start site were analyzed (in all cases the exact transcription initiation has not been experimentally determined). Figure 2-6B illustrates the relative position of the putative cis-regulatory elements identified by using visual inspection or the plant cis-acting regulatory DNA element database (PLACE; Higo *et al.*, 1999). None of the *NLE* promoters analyzed have an obvious TATA box but all of them possess a putative basic promoter CAAT box. In the *ScNLE* promoter, the CAAT box is located in the -400 to -113 region, which was found to be essential for driving the expression of GUS in several tissues of the ovary 48 HAP (Figures 2-5G-H, 2-6). Four sequences showing a nine in ten match to the CArG box (consensus $CC[A/T]_6GG$), bound by MADS domain proteins (Acton *et al.*, 1997; Huang *et al.*, 1993), were identified in the -1171 to -695 and -695 to -400

region of *ScNLE* promoter, which were shown to be required for fertilization-dependent response and tissue-specific repression of GUS expression, respectively (Figures 2-5F-G, 2-6). The core binding sequence of the *Arabidopsis* PRHA homeodomain transcription factor (TAATTG) (Plesch *et al.*, 1997) was additionally found in the same region. In *A. thaliana*, two putative CArG boxes and three PRHA binding sites were identified within the first 927 bp of the extended promoter. In *P. trichocarpa*, two putative CArG boxes and one PRHA binding site were found within 1194 bp whereas in *O. sativa*, one putative CArG box and no PRHA binding site were found within 1166 bp. Finally, several AAAG sequences, representing the core binding site of Dof transcription factors (Yanagisawa, 2004), are scattered along all the *NLE* promoter sequences analyzed,. In the *ScNLE* promoter, these are present in all the deletion regions analyzed. Dof transcription factors are known to interact with bZIP (Conlan *et al.*, 1999) and MYB (Diaz *et al.*, 2005; Diaz *et al.*, 2002) binding proteins. No core sequence for bZIP binding (ACGT) have been found in the 1171 bp upstream region of *ScNLE* promoter but several sequence motifs recognized by different MYB transcription factors have been found by the PLACE database (data not shown) in the all the *NLE* promoters analyzed.

2.4.8. Reducing *ScNLE* expression levels in *S. chacoense* caused reduced fertility

To investigate the function of *ScNLE* during plant reproductive development, we generated transgenic *ScNLE* underexpressing lines and analyzed the phenotypes associated with ovary development following fertilization. WT *S. chacoense* plants were transformed with part of the *ScNLE* cDNA either in the antisense orientation (asNLE lines) or as a double-stranded RNA construct (RNA interference construct, iNLE lines) driven by the strong and constitutive CaMV 35S promoter. Among the transgenic lines obtained, a total of four lines, namely asNLE3, asNLE5, iNLE5 and iNLE6, showed similar pleiotropic phenotypes including dwarfism (Figure 2-7A) and defects in seed and fruit development (Figures 2-7 E-G). RT-PCR analyses using

primers that annealed to a region of *ScNLE* cDNA not included in the transgene constructs revealed that all four lines had a reduced endogenous *ScNLE* transcripts in apex tissues relative to WT (Figure 2-7B). Severity of the phenotypes in these lines did not however correlate with the severity in *ScNLE* expression reduction. While asNLE5 and iNLE6 showed the strongest phenotypes and an average of 88% and 62% of WT transcript levels, respectively, the asNLE3 had intermediate phenotypes with 28 % of transcripts, and iNLE5 was mildly affected in some developmental aspects despite a reduction of transcripts to 32%. This absence of correlation is consistent with results obtained in previous studies showing that the production of abnormal phenotypes induced by RNAi is not always correlated with a significant decrease in transcript levels (Acosta-Garcia and Vielle-Calzada, 2004; Kerschen *et al.*, 2004). Furthermore, the phenotypes were stably maintained over time.

In the extreme case of iNLE6 line, flower buds sometimes initiated but always dropped at very early stages of their formation. This phenomenon was also observed for the asNLE5 line with the exception that some of the buds could reach maturity. Because asNLE3 and asNLE5 showed the more obvious post-fertilization defects, phenotype analyzes were carried on these lines. Flowers that were formed from these underexpressing lines produced apparently normal ovule-containing ovaries (Figures 2-7C, D). However, when asNLE3 and asNLE5 flowers were cross-pollinated with WT compatible pollen, their fruits were always smaller than those produced from WT plants during the course of their development (Figure 2-7E). At maturity, at 36 DAP, volume of asNLE3 and asNLE5 fruits were about 55% and 40%, respectively, of the WT fruits. Both asNLE3 and asNLE5 mature fruits had higher proportions of small aborted ovules and aborted seeds than the WT. More exhaustive dissection of asNLE5 mature fruits revealed 30% of small aborted ovules, 60% of flat aborted seeds of varied sizes, and 10% of bulging embryo-containing seeds (Figure 2-7G). In contrast, WT seeds contained an average of 1% aborted ovules, 25% aborted seeds and 74% embryo-containing seeds (Figure 2-7F). High occurrence of natural seed failure has been reported in numerous Solanaceous species (Clarke, 1940;

Dnyansagar and Cooper, 1960; Kapil and Tiwari, 1978). The high proportions of unfertilized ovules and aborted seeds obtained in the asNLE5 underexpressing line suggest that *ScNLE* plays an essential role in reproductive processes in the female organs.

2.5. DISCUSSION

Using a negative selection screen for weakly expressed mRNAs in fertilized ovaries we have isolated in the wild potato species *Solanum chacoense*, a homolog of the *Drosophila NOTCHLESS* (*NLE*) gene, which encodes a WDR protein. *DmNLE* was isolated in *Drosophila* through a genetic screen for modifiers of Notch signaling activity, and its name comes from the analysis of loss-of-function *nle* mutant alleles that dominantly suppress the wing notching caused by some Notch alleles (Royet *et al.*, 1998). Overexpression of *NLE* in *Xenopus* and *Drosophila* also exerts a dominant-negative effect in that it also increases Notch activity. In *Drosophila*, genetic and biochemical evidences show that DmNLE modifies Notch signaling activity through a direct interaction with the Notch receptor intracellular domain (Royet *et al.*, 1998). Although the Notch pathway is not present in plants and yeasts, *NLE* is nonetheless highly conserved between animals, plants and yeast, suggesting therefore functional conservation of the gene in these organisms.

In this study, we have demonstrated that the plant *ScNLE* gene can affect bristle formation similarly to *DmNLE* when overexpressed in the fruitfly (Figures 2-1 B-C). This finding is interesting as it requires that ScNLE is able to interact with the *Drosophila* Notch intracellular domain and possibly with other regulatory components of the pathway. Therefore, ScNLE and DmNLE are likely to share an analogous mode of action and to be part of cellular processes common to both plants, yeast and animals. The additional and unique phenotypes produced by strong *ScNLE* overexpressing flies (Figure 2-1C) could be attributed to a difference in protein-protein interaction efficiency between the plant ScNLE protein and Notch pathway components. This hypothesis is supported by the weak sequence conservation between several corresponding surface-exposed regions (regions I and II in Figure 2-1A) of ScNLE and DmNLE. These regions are thought to confer specificity of interaction with protein partners and WD repeats having more similar surface-exposed regions are more likely to share common binding partners (Smith *et al.*,

1999). Because most of the Notch pathway components do not exist in plants (and yeast), the conserved cellular function of NLE would have adapted to serve separately animal-specific and plant-specific developmental processes. Accordingly, plants and animals use divergent signaling pathways (Wigge and Weigel, 2001). With about 417 members in *Arabidopsis*, receptor-like kinases (RLKs) constitute the largest family of transmembrane receptor in higher plants (Shiu and Bleecker, 2001) and therefore represent a most probable candidate if ScNLE regulates the activity of a receptor in plants. Such a situation would then be a reminder of AGB1, a WDR protein orthologous to the Gβ subunit of the heterotrimeric G protein. In animals, G protein associates with the intracellular domain of G Protein-Coupled Receptors (GPCRs). In plants, although the homolog of the Gβ subunit GPA1 was reported to interact with a GPCR-type of receptor (GCR1) (Pandey and Assmann, 2004), genetic evidences also suggest that AGB1 would interact with ERECTA, a leucine-rich repeat receptor-like kinase (LRR-RLK) (Lease *et al.*, 2001).

The importance of the *NLE* gene during plant growth and development was also revealed in this study carried in *S. chacoense*. The expression pattern of the gene and the pleiotropic phenotypes caused by its underexpression showed that *ScNLE* is used reiteratively in multiple developmental processes, which may not be surprising since WDR proteins are able to mediate interactions with multiple binding partners in a sequential and/or simultaneous manner (Smith *et al.*, 1999).

In addition of being involved in plant vegetative development, we have shown that *ScNLE* plays other roles during fertilization and/or post-fertilization events. *ScNLE* mRNA expression was up-regulated immediately following fertilization and this increase was transient, with *ScNLE* expression going down to basal levels within two days after the initial up-regulation. Moreover, expression of *ScNLE* in the ovary 48 HAP showed localization in specific tissues including the placenta, the vascular tissues and the endothelial cells of ovules. We further demonstrated that underexpressing *ScNLE* led to the production of smaller fruits that contained mostly

aborted ovules and aborted seeds. While these data clearly indicate a role for *ScNLE* during fertilization and/or early post-fertilization events, how the gene influences these processes still needs to be defined. In flowering plants, seeds and fruits develop from ovules and ovaries, respectively, in response to double-fertilization of the embryo sac by the two spermatic cells of a pollen (Goldberg *et al.*, 1989). A period of intensive cell division characterizes the first stage of fruit development following fertilization (Tanksley, 2004). The endothelium of ovules, which is a specialized tissue layer of the integument closest to the embryo sac, appears to perform diverse functions depending on the stage of seed development, from coordinating growth of the ovule to later feeding and protecting the developing embryo sac and embryo (Kapil and Tiwari, 1978). Therefore, the transient up-regulation of *ScNLE* in the ovary could perhaps participate in a cellular process triggered by fertilization and that is essential in the initiation of seed and fruit development, such as cell proliferation. Once the program initiated, high *ScNLE* activity would be dispensable and down-regulated. Although *NLE* is likely involved in plant fertilization response, preliminary screening of *AtNLE* RNAi lines in *Arabidopsis* indicates that development of the female gametophyte is arrested after megaspore formation, suggesting that megagametogenesis could also be impaired in aborted ovules of *ScNLE* underexpressing lines (Gray-Mitsumune, M. and Matton, D. P., unpublished observation).

Similarly to *ScNLE*, several genes that have been shown to be expressed in the endothelium of ovules and other tissues of the ovary are also expressed in the shoot apex (Bowman *et al.*, 1991; Lu *et al.*, 1996; Porat *et al.*, 1998). Although the overall morphology of the ovaries produced by *ScNLE* underexpressing lines looked similar to the WT, it can not be excluded that more subtle defects in ovary formation arising from the plant apex (meristem) could contribute in part to the post-fertilization phenotypes observed in these lines. Therefore, the specific function of *ScNLE* in the ovary in response to fertilization would need to be ascertained in transgenic plants

with *ScNLE* underexpression driven by an inducible promoter system or a tissue-specific promoter.

We carried out a 5' deletion analysis as a first step in trying to delineate the cis regions regulating the specific activity of the *ScNLE* promoter in the ovary following fertilization (48 HAP). This analysis revealed that *ScNLE* expression pattern is driven by a mosaic of positive, negative, and tissue specific regulatory elements acting through different regions of the promoter. Region -400 to -113 was found to be essential for most of the positive regulation of *ScNLE*, since its deletion completely abrogated transcription of *uidA* reporter gene in every tissues of the ovary except the placenta, in which expression seemed to be conferred by the -113 to +58 region. The -400 to -113 region was however unable to confer the tissue-specific expression pattern of endogenous *ScNLE* as determined by *in situ* hybridization. Instead, region -695 to -400 seemed to contain negative regulatory elements for restricting the activity of the *ScNLE* promoter in some of the determined tissues (placenta, funiculus), since its removal led to a widespread and unspecific distribution of GUS throughout the ovary. A similar active repression conferring cell-specific expression was shown for the pollen generative cell-expressed gene *LGC1* (Singh *et al.*, 2003). Despite the analysis of more than 1 kb of promoter region, the 1171 bp *ScNLE* region analyzed did not completely recapitulate the expression pattern of the endogenous *ScNLE* gene as revealed by *in situ* hybridization, such as the presence of transcripts in the endothelium of ovules and vascular tissues of the placenta, and the absence of expression in the receptacle outside the vascular tissues. There are several explanations for such discrepancies. For example, the GUS staining in the receptacle outside the vascular tissues could have been the result of leakage of the GUS enzyme or of the X-gluc reaction product from the vascular tissues of the receptacle to surrounding tissues because of strong GUS accumulation. Moreover, the promoter region analyzed does probably not contain all the regulatory elements required for complete and proper *ScNLE* expression pattern. Although numerous examples of promoter analysis have shown that promoter regions with a size in range of several

hundreds bp to 1 kb upstream of the gene reproduce faithful expression patterns of reporter genes *in vivo*, other studies have shown the requirement of sequences further upstream (Lee *et al.*, 2005), downstream of the gene (Larkin *et al.*, 1993), as well as in introns (Sieburth and Meyerowitz, 1997).

Regions required for *ScNLE* promoter responsiveness to fertilization were also determined. RNA gel blot analyses carried out with both isolated ovules (containing few placental tissue contamination) and whole ovaries clearly showed that endogenous *ScNLE* expression level is very weak in ovaries at 0 HAP, in absence of fertilization, but is highly increased from 36 to 48 HAP, corresponding to a period of intense fertilization in *S. chacoense*. Our *ScNLE* promoter deletion analyzes pointed to an initial active repression of *ScNLE* expression in the ovary in absence of fertilization, that is conferred by a regulatory element in the -1171 to -695 region, since removal of this region led to considerably higher basal *GUS* expression levels in ovaries 0 HAP compared to endogenous *ScNLE*. Also, *ScNLE* responsiveness to fertilization is likely controlled by a positive regulatory element located in the -400 to -113 region of the promoter, since the presence of this region allowed an increase in *GUS* expression levels in ovaries from 0 to 48 HAP but its removal abolished such increase in fertilized ovaries. The expression of *GUS* driven by the determined regulatory regions fused to a minimal 35S promoter should confirm their respective roles in the regulation of *ScNLE* gene expression in the ovary.

We analyzed the *ScNLE* promoter sequence for regulatory motifs with the aim of correlating the identified regulatory regions to transcription factors whose expression in space and time has been shown by *in situ* hybridization to overlap, at least in part, with that of *ScNLE*. These transcription factors would represent candidate positive and negative regulators controlling *ScNLE* promoter activity. Several regulatory motifs were found. For example, deletion of the putative CAAT box, a basic promoter element, and of a Dof transcription factor binding site (AAAG motif) could explain the major loss of *ScNLE* promoter activity when region -400 to -

113 was deleted. Since the core Dof recognition motif is short, finding numerous AAAG motifs distributed along *ScNLE* promoter is not significant by itself. The DAG1 Dof transcription factor have however been shown to be expressed in the vascular tissues of the gynoecium and in the funiculus after fertilization in *Arabidopsis* (Papi *et al.*, 2000). Similarly, PRHA homeodomain transcription factor, for which one putative binding site was identified in *ScNLE* promoter sequence, is associated to developing vascular tissues (Plesch *et al.*, 1997). In addition, we found four very close matches to the CArG box motif, recognized by MADS domain transcription factors (Acton *et al.*, 1997; Huang *et al.*, 1993), of which two are located in the -1171 to -695 region required for most of *ScNLE* promoter responsiveness to fertilization. Interestingly, numerous MADS-box genes of tomato, a close relative of *S. chacoense*, were shown to be induced soon after fertilization in a combination of tissues in the ovary including vascular tissues, placenta, and the endothelium of ovules (Busi *et al.*, 2003). Most of all these identified putative binding sites were also found in the putative *NLE* promoter of three other plant species. The final determination of the functions of these putative binding sites will however require site-directed mutagenesis altering these sequences to be performed.

2.6. ACKNOWLEDGEMENTS

We are indebt to Dr. Stephen Cohen from the European Molecular Biology Laboratory, Heidelberg, Germany, where part of the work was realized in his laboratory on *Drosophila* transgenic experiments. We also thank Roselyne Labbé, Édith Lafleur and Éric Chevalier for technical assistance. This work was supported by the Natural Sciences and Engineering Research Council of Canada (NSERC) and from the Canada Research Chair program. S. C. Chantha is the recipient of Ph. D. fellowships from NSERC and from Le Fonds Québécois de la Recherche sur la Nature et les Technologies (FQRNT, Québec). D. P. Matton holds a Canada Research Chair in Functional Genomics and Plant Signal Transduction.

(A)

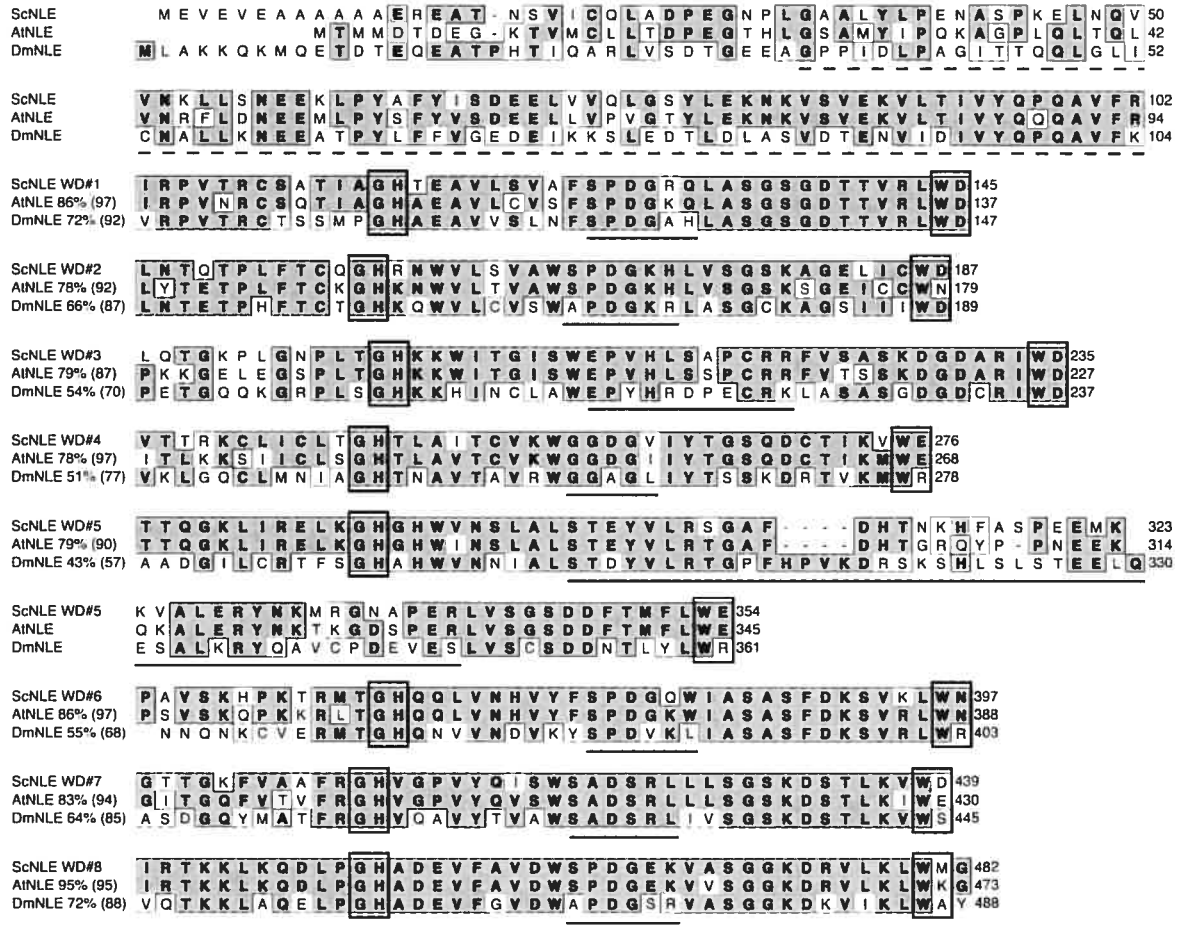
ScNLE
AtNLE
DmNLE
ScNLE WD#1
AtNLE 86% (97)
DmNLE 72% (92)
ScNLE WD#2
AtNLE 78% (92)
DmNLE 66% (87)
ScNLE WD#3
AtNLE 79% (87)
DmNLE 54% (70)
ScNLE WD#4
AtNLE 78% (97)
DmNLE 51% (77)
ScNLE WD#5
AtNLE 79% (90)
DmNLE 43% (57)
ScNLE WD#5
AtNLE
DmNLE
ScNLE WD#6
AtNLE 86% (97)
DmNLE 55% (68)
ScNLE WD#7
AtNLE 83% (94)
DmNLE 64% (85)
ScNLE WD#8
AtNLE 95% (95)
DmNLE 72% (88)

(B)

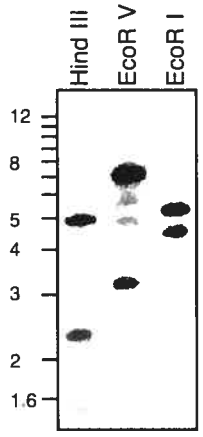
Hind III
EcoR V
EcoR I
12
8
5
4
3
2
1.6

(C)


(L)
(M)
(R)

Figure 2-1. NLE sequence and gene copy number analysis, and overexpression experiment in *Drosophila*. (A) Alignment of ScNLE, AtNLE, and DmNLE amino acid sequences. The NLE domain is indicated with a dashed line. The eight WD motifs that constitute the WDR domain are numbered on the left with percentage of sequence identity and similarity (in parenthesis) compared to ScNLE. The conserved dipeptides GH and WD of each WD motif are boxed. The variable regions I comprise the amino acids preceding the GH of each WD motif. The variable regions II are underlined. Sequence identity is highlighted in dark gray and similarity in light gray. Dashes indicate gaps introduced to maximize homology. (B) DNA gel bot analysis of the *ScNLE* gene. Genomic DNA (10 μg) was digested with the restriction enzymes indicated on top and probed with the complete 1.8 kb 32P-labelled *ScNLE* cDNA. Molecular weight markers are indicated in kb on the left. (C) Effects of overexpression of *ScNLE* on thoracic bristle formation in *Drosophila*. SEM images of the thorax of an ApGal4/+ line (left); a weak overexpressing *ScNLE* line ApGal4/UAS-*ScNLE* (middle); and a strong overexpressing *ScNLE* line ApGal4/UAS-*ScNLE* (right).

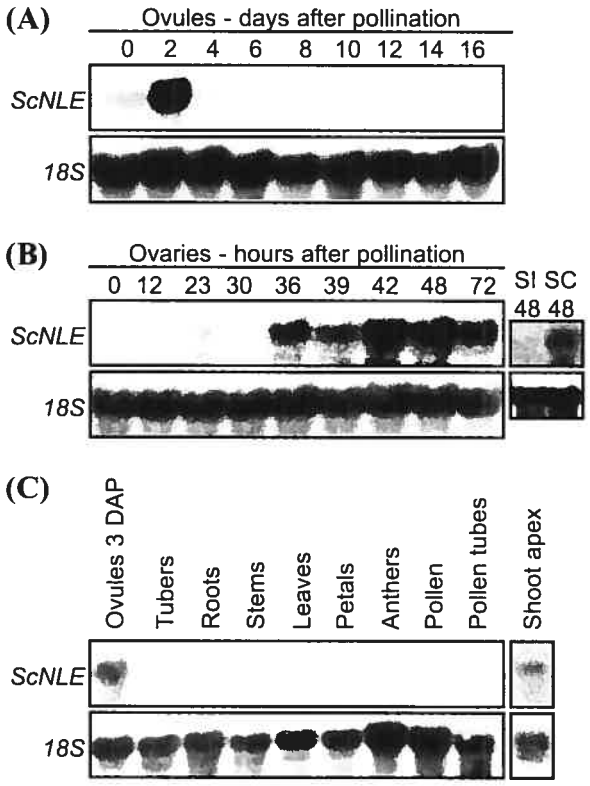

Figure 2-2. RNA expression analysis of *ScNLE* transcript levels. Ten microgram of total RNA from various tissues were probed with a 32P-labelled *ScNLE* cDNA. (A) Ovules at different time points in days after pollination (DAP). (B) Ovaries (including ovules) at different time points in hours after pollination (HAP) and comparison between a compatible (SC) and an incompatible (SI) pollination 48 HAP. (C) Mature plant tissues and the shoot apex.

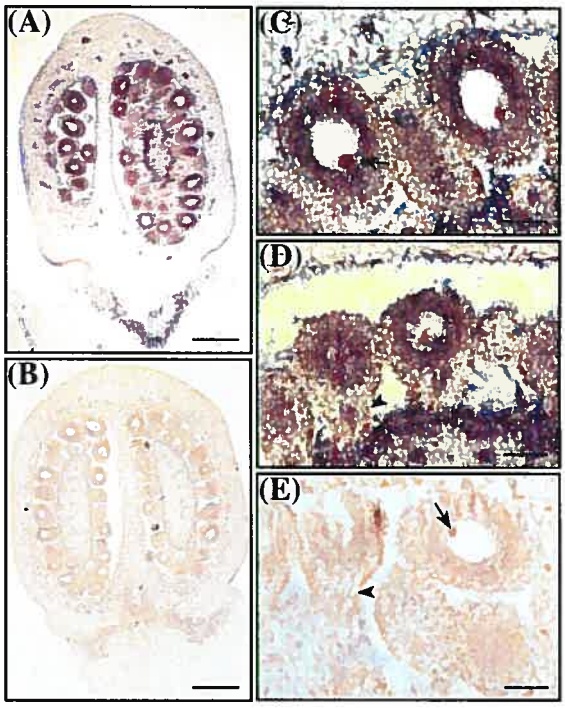

Figure 2-3. *In situ* localization of *ScNLE* transcripts. (A) Ovary 48 HAP, longitudinal section, *ScNLE* antisense probe. (B) Ovary 48 HAP, longitudinal section, *ScNLE* sense probe. (C, D) Ovules 48 HAP, *ScNLE* antisense probe. Magnified view of portions of (A). Arrows indicate the zygote in (C) and the funiculus in (D). (E) Ovules 48 HAP, *ScNLE* sense probe. Magnified view of portions of (B). Arrow indicates the zygote and arrowhead indicates the funiculus. (A, B) Bar = 500 μm. (C, D, E) Bar = 100 μm.

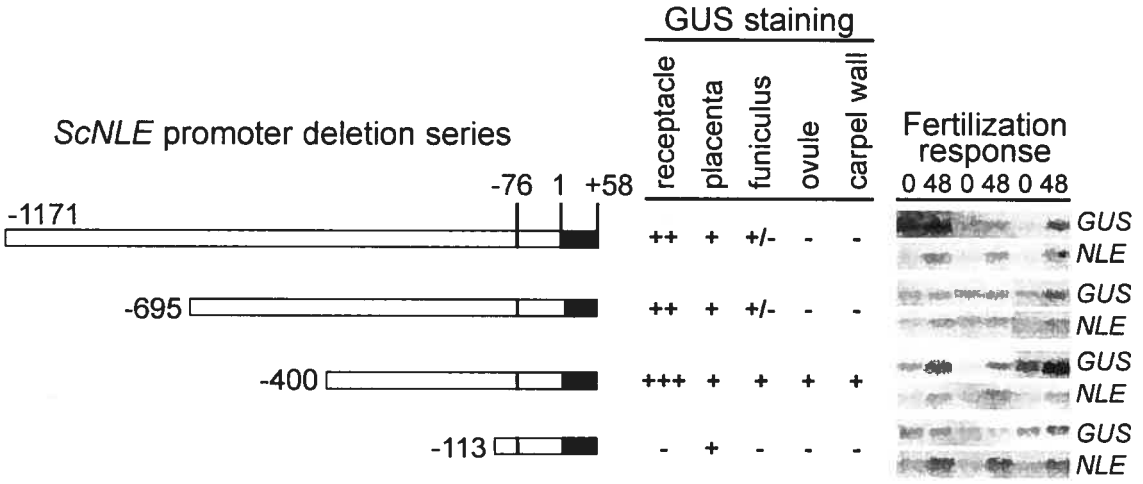

Figure 2-4. *ScNLE* promoter deletion analysis. Left: Schematic representation of the *ScNLE* promoter deletion series fused to the *uidA* reporter gene. Numbers indicate nucleotide position: +1 corresponds to the first nucleotide of the ATG initiation codon, -76 represents the 5' end of the longest *ScNLE* cDNA isolated, and numbers on the left of the schemes refer to the 5' end nucleotide positions of the promoter regions cloned. A portion of the *ScNLE* coding region corresponding to the first 19 N-terminal amino acids (black box) have been included in the constructs to create a translational fusion with the *GUS* reporter gene. Middle: Summary of GUS expression patterns obtained with corresponding constructs in ovaries 48 HAP. Relative levels of GUS staining represented by: -, not detected; +, low; ++, moderate; +++, high; +/-, coloration observed in one third of the samples only. All other relative levels corresponds to observations made in more than half of the lines tested. Right: RNA gel blot analysis of regulatory regions required for the increase in *ScNLE* expression induced by fertilization using the *GUS* reporter gene.

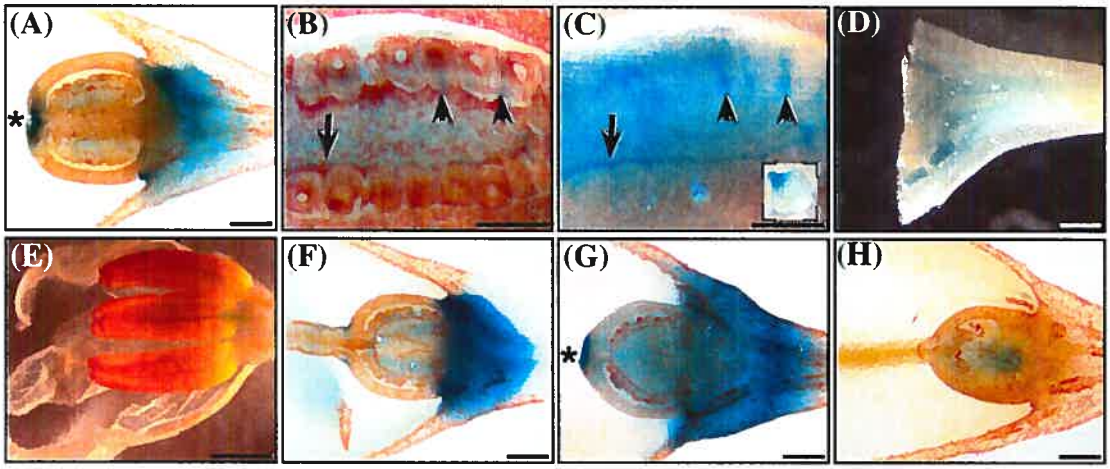

Figure 2-5. GUS expression patterns in ovary and other floral organs 48 HAP conferred by 5' deletions of the *ScNLE* promoter. (A) PNLE-1171, ovary 48 HAP, longitudinal section. (B, C) PNLE-1171, magnified view of a portion of (A) showing GUS expression in the funiculus (arrowhead) and outermost cell layer of the placenta (arrow). Bar = 200 μm. (C) Identical to (B) without safranin coloration. (D) PNLE-1171, whole-mount image of a lightly stained receptacle. Bar = 500 μm. (E) PNLE-1171, whole-mount image of anthers and petals. Bar = 2 mm. (F) PNLE-695, ovary 48 HAP, longitudinal section. (G) PNLE-400, ovary 48 HAP, longitudinal section. (H) PNLE-113, ovary 48 HAP, longitudinal section. (A, F, G, H) Longitudinal sections of ovaries were counter-stained with safranin (red coloration). Bar = 500 μm. (A, G) Asterisks indicate blue coloration on top of the carpel wall at the style junction observed only in a small subset of samples.

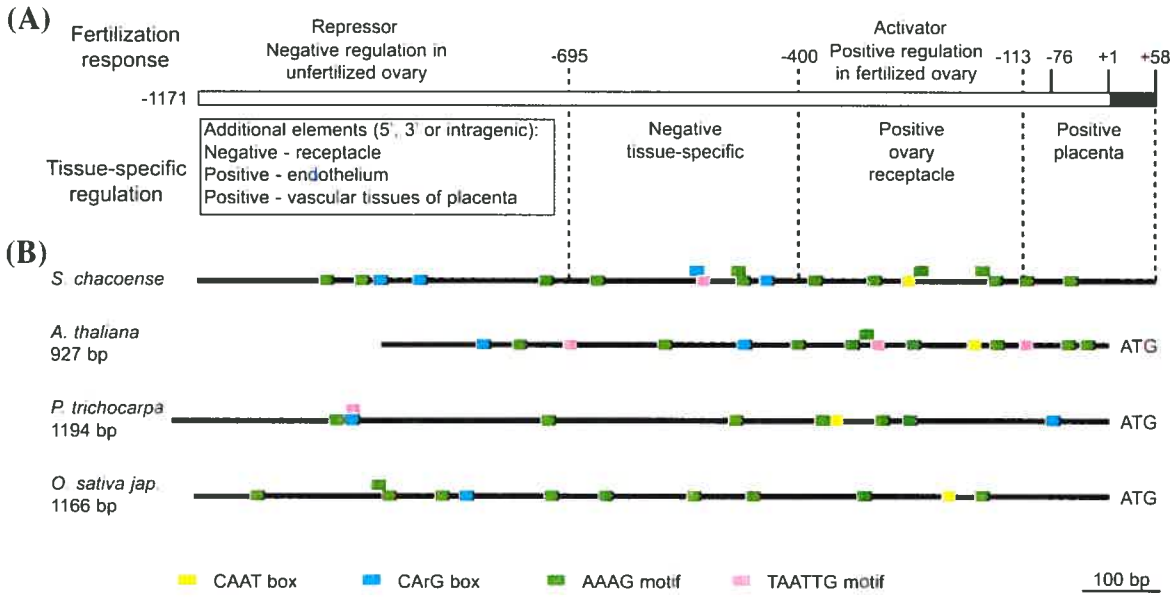

Figure 2-6. Putative *cis*-regulatory regions and elements in the *NLE* promoter. (A) Summary of the regulatory regions for *ScNLE* gene expression in the ovary 48 HAP as determined by promoter deletion analysis. (B) Relative location of putative *cis*-regulatory elements in *Solanum chacoense NLE* promoter linked to the regulatory regions reported in (A) and also found in *NLE* promoters of *Arabidopsis thaliana*, *Populus trichocarpa* and *Oryza sativa* (var. *japonica*).

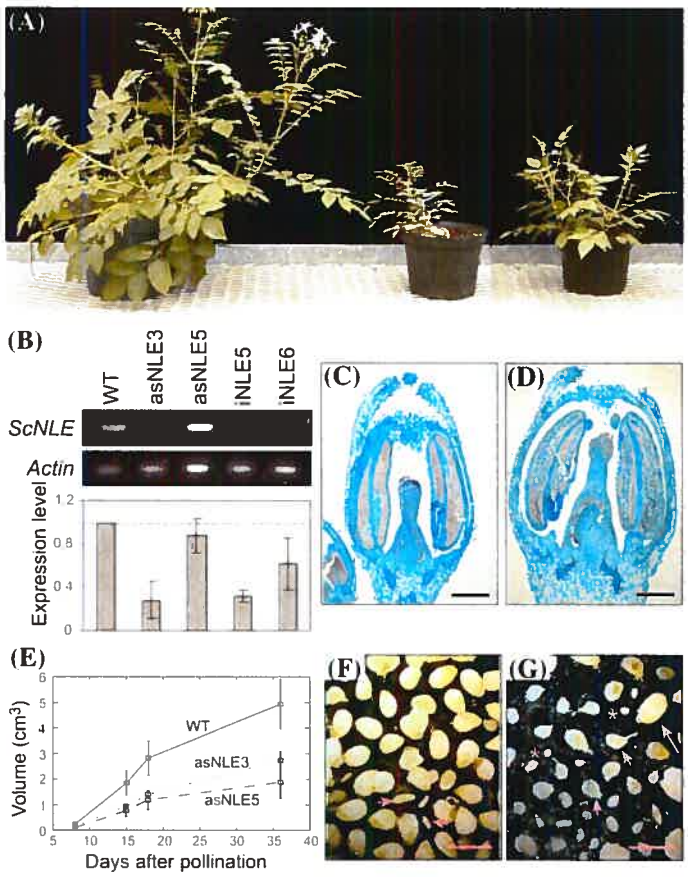

Figure 2-7. Phenotypic analysis of *ScNLE* underexpressing lines. (A) 10 week-old WT (left), asNLE3 (middle), and asNLE5 (right) lines. Bar = 5 cm. (B) RT-PCR analysis of *ScNLE* mRNA expression levels in WT and *ScNLE* antisense (as) and double-stranded RNA (i) lines (top). *ACTIN* served as an internal control (middle). Relative quantification of *ScNLE* expression levels (bottom). (C, D) Longitudinal sections of representative flowers before anthesis from (C) WT and (D) asNLE5 lines. Bar = 500 µm. (E) Fruit growth. Fruit volumes of WT, asNLE3 and asNLE5 underexpressing lines were measured 8, 5, 18, and 36 days after pollinisation (n=10). (F, G) Seeds isolated from fruits of (F) WT and (G) asNLE5 lines. Stars indicate small aborted ovules, arrowheads indicate flat aborted seeds, arrows indicate mature seeds. Bar = 4 mm.

2.7. REFERENCES

Acosta-Garcia G., Vielle-Calzada J.P. 2004. A classical arabinogalactan protein is essential for the initiation of female gametogenesis in Arabidopsis. Plant Cell 16: 2614-2628

Acton T.B., Zhong H., Vershon A.K. 1997. DNA-binding specificity of Mcm1: operator mutations that alter DNA-bending and transcriptional activities by a MADS box protein. Mol Cell Biol 17: 1881-1889

Artavanis-Tsakonas S., Rand M.D., Lake R.J. 1999. Notch signaling: cell fate control and signal integration in development. Science 284: 770-776

Bowman J.L., Drews G.N., Meyerowitz E.M. 1991. Expression of the Arabidopsis floral homeotic gene AGAMOUS is restricted to specific cell types late in flower development. Plant Cell 3: 749-758

Busi M.V., Bustamante C., D'angelo C., Hidalgo-Cuevas M., Boggio S.B., Valle E.M., Zabaleta E. 2003. MADS-box genes expressed during tomato seed and fruit development. Plant Mol Biol 52: 801-815

Bussiere F., Ledu S., Girard M., Heroux M., Perreault J.-P., Matton D.P. 2003. Development of an efficient cis-trans-cis ribozyme cassette to inactivate plant genes. Plant Biotechnology Journal 1: 423-435

Cebolla A., Vinardell J.M., Kiss E., Olah B., Roudier F., Kondorosi A., Kondorosi E. 1999. The mitotic inhibitor ccs52 is required for endoreduplication and ploidy-dependent cell enlargement in plants. Embo J 18: 4476-4484

Chaudhury A.M., Ming L., Miller C., Craig S., Dennis E.S., Peacock W.J. 1997. Fertilization-independent seed development in Arabidopsis thaliana. Proc Natl Acad Sci U S A 94: 4223-4228

Clarke A.E. 1940. Fertilization and early embryo development in the potato. Am. Potato J. 17: 20-25

Conlan R.S., Hammond-Kosack M., Bevan M. 1999. Transcription activation mediated by the bZIP factor SPA on the endosperm box is modulated by ESBF-1 in vitro. Plant J 19: 173-181

Conner J., Liu Z. 2000. LEUNIG, a putative transcriptional corepressor that regulates AGAMOUS expression during flower development. Proc Natl Acad Sci U S A 97: 12902-12907

Deng X.W., Caspar T., Quail P.H. 1991. cop1: a regulatory locus involved in light-controlled development and gene expression in Arabidopsis. Genes Dev 5: 1172-1182

Diaz I., Martinez M., Isabel-Lamoneda I., Rubio-Somoza I., Carbonero P. 2005. The DOF protein, SAD, interacts with GAMYB in plant nuclei and activates transcription of endosperm-specific genes during barley seed development. Plant J 42: 652-662

Diaz I., Vicente-Carbajosa J., Abraham Z., Martinez M., Isabel-La Moneda I., Carbonero P. 2002. The GAMYB protein from barley interacts with the DOF transcription factor BPBF and activates endosperm-specific genes during seed development. Plant J 29: 453-464

Dnyansagar V.R., Cooper D.C. 1960. Development of the seed of Solanum phureja. American Journal of Botany 47: 176-186

Germain H., Rudd S., Zotti C., Caron S., O'brien M., Chantha S.C., Lagace M., Major F., Matton D.P. 2005. A 6374 Unigene Set Corresponding to Low Abundance Transcripts Expressed Following Fertilization in Solanum chacoense Bitt, and Characterization of 30 Receptor-like Kinases. Plant Mol Biol 59: 515-532

Gillaspy G., Ben-David H., Gruissem W. 1993. Fruits: A Developmental Perspective. Plant Cell 5: 1439-1451

Goldberg R.B., Barker S.J., Perez-Grau L. 1989. Regulation of gene expression during plant embryogenesis. Cell 56: 149-160

Guitton A.E., Berger F. 2005. Loss of function of MULTICOPY SUPPRESSOR OF IRA 1 produces nonviable parthenogenetic embryos in Arabidopsis. Curr Biol 15: 750-754

Higo K., Ugawa Y., Iwamoto M., Korenaga T. 1999. Plant cis-acting regulatory DNA elements (PLACE) database: 1999. Nucleic Acids Res 27: 297-300

Honma T., Goto K. 2000. The Arabidopsis floral homeotic gene PISTILLATA is regulated by discrete cis-elements responsive to induction and maintenance signals. Development 127: 2021-2030

Hu W., Wang Y., Bowers C., Ma H. 2003. Isolation, sequence analysis, and expression studies of florally expressed cDNAs in Arabidopsis. Plant Mol Biol 53: 545-563

Huang H., Mizukami Y., Hu Y., Ma H. 1993. Isolation and characterization of the binding sequences for the product of the Arabidopsis floral homeotic gene AGAMOUS. Nucleic Acids Res 21: 4769-4776

Huck N., Moore J.M., Federer M., Grossniklaus U. 2003. The Arabidopsis mutant feronia disrupts the female gametophytic control of pollen tube reception. Development 130: 2149-2159

Joshi C.P., Zhou H., Huang X., Chiang V.L. 1997. Context sequences of translation initiation codon in plants. Plant Mol Biol 35: 993-1001

Kadesch T. 2000. Notch signaling: a dance of proteins changing partners. Exp Cell Res 260: 1-8

Kapil R.N., Tiwari S.C. 1978. The integumentary tapetum. The botanical review 44: 457-490

Kerschen A., Napoli C.A., Jorgensen R.A., Muller A.E. 2004. Effectiveness of RNA interference in transgenic plants. FEBS Lett 566: 223-228

Kim M.K., Choi J.W., Jeon J.H., Franceschi V.R., Davin L.B., Lewis N.G. 2002. Specimen block counter-staining for localization of GUS expression in transgenic arabidopsis and tobacco. Plant Cell Rep 21: 35-39

Kimble J., Simpson P. 1997. The LIN-12/Notch signaling pathway and its regulation. Annu Rev Cell Dev Biol 13: 333-361

Kohler C., Hennig L., Bouveret R., Gheyselinck J., Grossniklaus U., Gruissem W. 2003. Arabidopsis MSI1 is a component of the MEA/FIE Polycomb group complex and required for seed development. Embo J 22: 4804-4814

Lagacé M., Chantha S.C., Major G., Matton D.P. 2003. Fertilization induces strong accumulation of a histone deacetylase (HD2) and of other chromatin-

remodeling proteins in restricted areas of the ovules. Plant Mol Biol 53: 759-769

Lantin S., O'brien M., Matton D.P. 1999. Pollination, wounding and jasmonate treatments induce the expression of a developmentally regulated pistil dioxygenase at a distance, in the ovary, in the wild potato Solanum chacoense Bitt. Plant Mol Biol 41: 371-386.

Larkin J.C., Oppenheimer D.G., Pollock S., Marks M.D. 1993. Arabidopsis GLABROUS1 Gene Requires Downstream Sequences for Function. Plant Cell 5: 1739-1748

Le Bras S., Cohen-Tannoudji M., Guyot V., Vandormael-Pournin S., Coumailleau F., Babinet C., Baldacci P. 2002. Transcript map of the Ovum mutant (Om) locus: isolation by exon trapping of new candidate genes for the DDK syndrome. Gene 296: 75-86

Lease K.A., Wen J., Li J., Doke J.T., Liscum E., Walker J.C. 2001. A mutant Arabidopsis heterotrimeric G-protein beta subunit affects leaf, flower, and fruit development. Plant Cell 13: 2631-2641

Lee J.Y., Baum S.F., Alvarez J., Patel A., Chitwood D.H., Bowman J.L. 2005. Activation of CRABS CLAW in the Nectaries and Carpels of Arabidopsis. Plant Cell 17: 25-36

Lu P., Porat R., Nadeau J.A., O'neill S.D. 1996. Identification of a meristem L1 layer-specific gene in Arabidopsis that is expressed during embryonic pattern formation and defines a new class of homeobox genes. Plant Cell 8: 2155-2168

Marton M.L., Cordts S., Broadhvest J., Dresselhaus T. 2005. Micropylar pollen tube guidance by egg apparatus 1 of maize. Science 307: 573-576

Matton D.P., Maes O., Laublin G., Xike Q., Bertrand C., Morse D., Cappadocia M. 1997. Hypervariable Domains of Self-Incompatibility RNases Mediate Allele-Specific Pollen Recognition. Plant Cell 9: 1757-1766

Neer E.J., Schmidt C.J., Nambudripad R., Smith T.F. 1994. The ancient regulatory-protein family of WD-repeat proteins. Nature 371: 297-300

O'brien M., Kapfer C., Major G., Laurin M., Bertrand C., Kondo K., Kowyama Y., Matton D.P. 2002. Molecular analysis of the stylar-expressed Solanum chacoense small asparagine-rich protein family related to the HT modifier of gametophytic self-incompatibility in Nicotiana. Plant J 32: 985-996

Ohad N., Margossian L., Hsu Y.C., Williams C., Repetti P., Fischer R.L. 1996. A mutation that allows endosperm development without fertilization. Proc Natl Acad Sci U S A 93: 5319-5324

Osterlund M.T., Hardtke C.S., Wei N., Deng X.W. 2000. Targeted destabilization of HY5 during light-regulated development of Arabidopsis. Nature 405: 462-466

Pandey S., Assmann S.M. 2004. The Arabidopsis putative G protein-coupled receptor GCR1 interacts with the G protein alpha subunit GPA1 and regulates abscisic acid signaling. Plant Cell 16: 1616-1632

Papi M., Sabatini S., Bouchez D., Camilleri C., Costantino P., Vittorioso P. 2000. Identification and disruption of an Arabidopsis zinc finger gene controlling seed germination. Genes Dev 14: 28-33

Plesch G., Stormann K., Torres J.T., Walden R., Somssich I.E. 1997. Developmental and auxin-induced expression of the Arabidopsis prha homeobox gene. Plant J 12: 635-647

Porat R., Lu P., O'neill S.D. 1998. Arabidopsis SKP1, a homologue of a cell cycle regulator gene, is predominantly expressed in meristematic cells. Planta 204: 345-351

Rotman N., Rozier F., Boavida L., Dumas C., Berger F., Faure J.E. 2003. Female control of male gamete delivery during fertilization in Arabidopsis thaliana. Curr Biol 13: 432-436

Royet J., Bouwmeester T., Cohen S.M. 1998. Notchless encodes a novel WD40-repeat-containing protein that modulates Notch signaling activity. Embo J 17: 7351-7360

Shiu S.H., Bleecker A.B. 2001. Receptor-like kinases from Arabidopsis form a monophyletic gene family related to animal receptor kinases. Proc Natl Acad Sci U S A 98: 10763-10768

Sieburth L.E., Meyerowitz E.M. 1997. Molecular dissection of the AGAMOUS control region shows that cis elements for spatial regulation are located intragenically. Plant Cell 9: 355-365

Singh M., Bhalla P.L., Xu H., Singh M.B. 2003. Isolation and characterization of a flowering plant male gametic cell-specific promoter. FEBS Lett 542: 47-52

Smith T.F., Gaitatzes C., Saxena K., Neer E.J. 1999. The WD repeat: a common architecture for diverse functions. Trends Biochem Sci 24: 181-185

Tanksley S.D. 2004. The genetic, developmental, and molecular bases of fruit size and shape variation in tomato. Plant Cell 16 Suppl: S181-189

Tilly J.J., Allen D.W., Jack T. 1998. The CArG boxes in the promoter of the Arabidopsis floral organ identity gene APETALA3 mediate diverse regulatory effects. Development 125: 1647-1657

Van Nocker S., Ludwig P. 2003. The WD-repeat protein superfamily in Arabidopsis: conservation and divergence in structure and function. BMC Genomics 4: 50

Wigge P.A., Weigel D. 2001. Arabidopsis genome: life without notch. Curr Biol 11: R112-114

Williams E.J. 1955. Seed failure in the Chippewa variety of *Solanum tuberosum*. Bot. Gaz. 10: 10-15

Yamagishi K., Nagata N., Yee K.M., Braybrook S.A., Pelletier J., Fujioka S., Yoshida S., Fischer R.L., Goldberg R.B., Harada J.J. 2005. TANMEI/EMB2757 encodes a WD repeat protein required for embryo development in Arabidopsis. Plant Physiol 139: 163-173

Yanagisawa S. 2004. Dof domain proteins: plant-specific transcription factors associated with diverse phenomena unique to plants. Plant Cell Physiol 45: 386-391

Yu L., Gaitatzes C., Neer E., Smith T.F. 2000. Thirty-plus functional families from a single motif. Protein Sci 9: 2470-2476

CHAPITRE III :

Underexpression of the plant *NOTCHLESS* gene, encoding a WD repeat protein, causes pleitropic phenotype during plant development

Article accepté pour publication:
Sier-Ching Chantha[1] and Daniel P. Matton[1]* (2006).
Planta, DOI 10.1007/s00425-006-0420-z.

[1]Institut de Recherche en Biologie Végétale (IRBV), Département de sciences biologiques, Université de Montréal, 4101 rue Sherbrooke est, Montréal, QC, Canada, H1X 2B2.

Keywords: Notchless, WD repeat protein, meristem, stomata, Midasin.

Genbank Accession number: ScNle AY428810.

Abbreviations: Days after pollination, DAP; Hours after pollination, HAP; SAM, shoot apical meristem.

DÉCLARATION DES COAUTEURS D'UN ARTICLE

1. Identification de l'étudiant et du programme

Sier-Ching Chantha

Ph. D. Sciences biologiques

2. Description de l'article

Sier-Ching Chantha and Daniel P. Matton. Underexpression of the plant *NOTCHLESS* gene, encoding a WD repeat protein, causes pleitropic phenotype during plant development. *Planta* (2006) Manuscript ID Planta-2006-08-0487.R1. Accepté pour publication, octobre 2006.

3. Déclaration des coauteurs autres que l'étudiante

À titre de coauteur de l'article identifié ci-dessus, je suis d'accord pour que Sier-Ching Chantha inclue cet article dans sa thèse de doctorat qui a pour titre "Caractérisation fonctionnelle des gènes *NOTCHLESS* et *MIDASIN* lors du développement végétal".

Daniel P. Matton	[redacted]	19 Oct. 2006
Coauteur	Signature	Date

3.1. ABSTRACT

WD-repeat proteins are involved in a breadth of cellular processes. While the WD-repeat protein encoding gene *NOTCHLESS* has been involved in the regulation of the Notch signaling pathway in *Drosophila*, its yeast homolog Rsa4p was shown to participate in 60S ribosomal subunit biogenesis. The plant homolog *ScNLE* was previously characterized in *Solanum chacoense* (*ScNLE*) as being involved in seed development. However, expression data and reduced size of *ScNLE* underexpressing plants suggested in addition a role during shoot development. We here report the detailed phenotypic characterization of *ScNLE* underexpressing plants during shoot development. *ScNLE* was shown to be expressed in actively dividing cells of the shoot apex. Consistent with this, *ScNLE* underexpression caused pleiotropic defects such as a reduction in aerial organ size, a reduction in some organ numbers, delayed flowering, and an increase in stomatal index. Analysis of adaxial epidermal cells revealed that both cell number and cell size were reduced in mature leaves of *ScNLE* underexpressing lines. Two-hybrid screens with the Nle domain and the WD-repeat domain of ScNLE allowed the isolation of homologs of yeast *MIDASIN* and *NSA2* genes, the products of which are involved in 60S ribosomal subunit biogenesis in yeast. A ScNLE-GFP chimeric protein was localized in both the cytoplasm and nucleus. These data altogether suggest that ScNLE likely plays a role in 60S ribosomal subunit biogenesis, which is essential for proper cellular growth and proliferation during plant development.

3.2. INTRODUCTION

In animals, adult organs are initiated during embryogenesis while in plants, new organs are continuously generated post-embryonically through meristematic cell sources. The shoot apical meristem (SAM) is pivotal for shoot development as it maintains a population of undifferentiated cells while also contributing the cells required for lateral organ primordia and stem formation throughout plant development (Esau 1977). Cells initially recruted to organ primordia retain their meristematic competence but only for a limited period of time. Subsequent gradual loss of cell meristematic competence during organ maturation is combined with cell growth/expansion and differentiation. The final size of a plant organ therefore reflects both cell number and cell size composition (Mizukami 2001).

Cell growth and cell division require the expression of a large number of genes involved in basic cellular functions. Members of the WD-repeat (WDR) protein superfamily, found almost exclusively in eukaryotes, have been involved in cellular processes as diverse as cytoskeletal dynamics, vesicular traffiking, nuclear export, RNA processing, chromatin modification, signal transduction, and ribosome biogenesis, to name a few examples (Neer et al. 1994;van Nocker and Ludwig 2003). Although functionally diversified, WDR proteins are structurally related by sharing the WD-repeat as a common sequence motif, which is repeated from four to eight times within a protein (Smith et al. 1999). They are thought to fold altogether into a propeller-like structure that would serve as a stable platform to coordinate the specific interaction of multiple protein partners in simultaneous and/or in a successive manner (Smith et al. 1999), a feature that could allow WDR proteins to integrate molecular mechanisms and pathways.

In *Arabidopsis*, 237 WRD proteins were grouped into 143 distinct families, the majority of which are evolutionary conserved in animals, plants and yeast, suggesting that many of them are components of basic cellular mechanisms (van

Nocker and Ludwig 2003). Only few of these members have been characterized to date for their function during plant growth and development. One intriguing WDR member is the homolog of the *Drosophila melanogaster NLE* (*DmNLE*) gene. *DmNLE* was first characterized as a modifier of the transmembrane Notch receptor activity in *Drosophila* (Royet et al. 1998). The DmNLE protein was shown to interact directly with the cytoplasmic domain of Notch, but the mechanism by which it regulates the activity of the receptor remains unclear. In animals, numerous cell fate decisions and developmental processes rely on cellular signaling through the Notch pathway (Kimble and Simpson 1997). In plants and yeast however, a Notch-type receptor and other components associated to the signaling pathway appear to be absent (Wigge and Weigel 2001). The yeast *NLE* homolog gene product, also known as Rsa4p and YCR072p, was later found as a trans-acting factor associated to pre-60S ribosomal particles throughout their maturation, from the nucleolus to the cytoplasm (Bassler et al. 2001;Gavin et al. 2002;Nissan et al. 2002). Yeast NLE/Rsa4p was shown to be required for proper rRNA processing and intra-nuclear transport of pre-60S ribosomal particles (de la Cruz et al. 2005). Most of the trans-acting factors involved in ribosome biogenesis have been characterized in *Saccharomyces cerevisiae* but the conservation of almost all these factors in higher eukaryotes suggest that ribosome biogenesis process is conserved in plants, animals, and fungi (Tschochner and Hurt 2003). However, reports on the role of genes encoding trans-acting factors involved in ribosome maturation during plant development are scarce.

A plant *NLE* homolog was previously isolated in a subtractive screen as a gene that is transiently up-regulated by fertilization in the ovaries of *Solanum chacoense*, a wild potato species, and was characterized for its function in post-fertilization processes (Chantha et al. 2006). *ScNLE* was shown to be expressed in diverse tissues of the ovary after fertilization, including the endothelium of ovules, placenta, and vascular tissues. Underexpressing *ScNLE* in transgenic plants led to the production of smaller fruits containing high proportions of aborted ovules and seeds. However, this also led to the production of smaller plants, suggesting an involvement

of *ScNLE* during shoot development as well. We herein report a detailed characterization of the defects associated to shoot development and aerial organ formation in *ScNLE* underexpressing lines. We propose that these developmental defects originate from the requirement of *ScNLE* for proper cell growth and cell proliferation, and an implication in a basic cellular process. Results from our two-hybrid screens also provide further support to the participation of the *NLE* gene in ribosome biogenesis in plants.

3.3. MATERIAL AND METHODS

3.3.1. Plant material and growth conditions

The diploid (2n=2x=24) *Solanum chacoense* Bitt. (Potato Introduction Station, Sturgeon Bay, WI) self-incompatible genotypes were line G4 (S_{12} and S_{14} self-incompatibility alleles) as female progenitor and line V22 (S_{11} and S_{13} alleles) as pollen donor. Plants were maintained by *in vitro* propagation on ½X MS medium with charcoal (0.5X MS salts, 1X MS vitamins, 20% sucrose, 0.5% deactivated charcoal, 0.6% agar, pH 5.8) at 20-22°C with a photoperiod of 16 h light and 8 h dark. Plants from 1 to 2 months old were transferred to soil and were grown either in a greenhouse with an average of 14 h of light/day for flower analyses or in a growth chamber at 20-22 °C with a photoperiod of 16 h light and 8 h darkness for comparative examination of vegetative growth parameters.

3.3.2. *In situ* hybridization and GUS analysis

For *in situ* hybridization, tissue samples were fixed, dehydrated and embedded in paraffin as described previously (Lantin et al. 1999). *In situ* detection of *ScNLE* on 10 µm thick sections was performed as described previously (Lantin et al. 1999). Sense and antisense digoxigenin-11-UTP (Roche Diagnostics, Laval, QC) labeled riboprobes were synthesized from the *ScNLE* cDNA cloned in the pBK-CMV vector using T3 and T7 RNA polymerases (RNA transcription kit, Stratagene, LaJolla, CA) after linearisation of the plasmid with XhoI or EcoRI, respectively. For GUS analysis, details on *ScNLE* promoter cloning and GUS staining are provided in Chantha et al. (2006).

3.3.3. Microscopy

Plant material embedded in paraffin was prepared for sectioning as described for *in situ* hybridization. For leaf cell morphology analysis, sections were rehydrated and stained with safranine overnight, thoroughly washed in water and then stained with Astra blue for 20 min. After two washes in water, sections were dehydrated. Methods for *ScNLE* promoter-GUS fusion construct and GUS staining are detailed in (Chantha et al. 2006). Tissue sections 10 µm thick were mounted in Permount. Adaxial epidermal cells were analyzed from nail polish peels. Nail polish was applied on the central region of terminal leaves surface and, once dried, peeled by using adhesive tape. Peels were sticked on microscope slides. Images were acquired with a digital camera installed on a Leitz light microscope.

3.3.4. *ScNLE* constructs for underexpression

For gene suppression using the antisense strategy, a ~1500 bp fragment of *ScNLE* cDNA was cloned in the antisense orientation in the pBIN35S double-enhancer vector using the HindIII restriction sites (Bussiere et al. 2003). For gene suppression using the double-stranded RNA interference strategy, a ~650 bp fragment of *ScNLE* cDNA was cloned in the sense and antisense orientations in the pDarth vector (O'Brien et al. 2002) from PCR products obtained with the NLE14 (5'-GAGAGGATCCAAACCACGCAGGGGAAGCTA-3') and NLE18 (5'-GAGAGGCGCGGTACCCTATCCCATCCATAGCTTCAG) primers containing the BamHI and XhoI restriction sites respectively, and with the NLE19 (5'-GAGACTCGAGAAACCACGCAGGGGAAGCTA-3') and NLE22 (5'-GAGAGGCGCGCCCTATCCCATCCATAGCTTCAG-3') primers containing the XhoI and AscI restriction sites respectively. Plant transformation with *Agrobacterium tumefaciens* strain LBA4404 was carried out as described previously (Matton et al. 1997).

3.3.5. Two-Hybrid cDNA libraries synthesis

Isolation of total RNA and poly(A)$^+$ mRNA were performed as described previously (Lantin et al. 1999). An AD-cDNA target library was synthetized from 5 µg of poly(A)$^+$ mRNA isolated from ovaries collected 18 to 72 HAP in the pAD-GAL4-2.1 phagemid vector by using the HybriZap®-2.1 XR library construction kit (Stratagene), according to the manufacturer's instructions. The activation domain-tagged primary cDNA library contained $1.6x10^6$ independent clones. A MYR-cDNA target library was synthetized from 5 µg of poly(A)$^+$ mRNA isolated from depericarped ovaries collected 2 to 6 DAP in the pMyr XR vector using the CytoTrap® XR Library construction kit (Stratagene), according to the manufacturer's instructions.

3.3.6. *ScNLE* constructs for two-hybrid screens

For all the two-hybrid constructs, sequences were amplified from *ScNLE* cDNA using PWO DNA Polymerase (Roche Diagnostics). All constructs were sequenced to confirm that fusions were in-frame and unmutated.

The vector pBD GAL4 Cam (Stratagene) was used to construct C-terminal fusions of three ScNLE regions with the Binding Domain of GAL4 and generate the following bait proteins: BD-dNLE (Nle domain), BD-dWD (WDR domain) and BD-ScNLE (complete ScNLE protein). Primers used for PCR amplification were tagged with EcoRI and SalI restriction site sequences in the forward and reverse primers respectively. The Nle domain (aa 2 to 115) was amplified with the NLE4 (5'-CG**GAATTC**GAAGTGGAAGTGGAAGCT-3') and NLE6 (5'-CGTA**GTCGAC**CAGCAATTGTGGCCGAA-3') primers. The WDR domain (aa

101 to 482) was amplified with the NLE23 (5'- GAGA**GAATTC** TTTCGAATCCGCCCTGTCAC-3') and NLE8 (5'- CAT**GTCGAC**CTATCCCATCCATAGCTTCAG-3') primers. The full ScNLE coding region, excluding the initiation codon, was amplified with the NLE4 and NLE8 primers. PCR products were digested with and ligated to the EcoRI and SalI sites of pBD GAL4 Cam.

The vector pSos (Stratagene) was used to construct C-terminal fusions of the three same ScNLE regions (mentioned above) with Sos to generate the following bait proteins: Sos-dNLE, Sos-dWD and Sos-ScNLE. The primers used for PCR amplification were tagged with the BamHI and SalI restriction site sequences in the forward and reverse primers respectively. The Nle domain was amplified with the NLE11 (5'-CG**GGATCC**GAAGTGGAAGTGGAAGCT-3') and NLE6 primers. The WDR domain (nt 402 to stop codon; aa 110 to 482) was amplified with the NLE12 (5'- GAGA**GGATCC**GTTCGGCCACAATTGCTGGT-3') and NLE8 primers. The full ScNLE ORF was amplified with the NLE11 and NLE8 primers. PCR products were digested with and ligated to the BamHI and SalI sites of pSos.

3.3.7. Two-Hybrid screening

GAL4 system: Bait plasmids were separately transformed into yeast strain PJ69-4A (kindly provided by Phillip James, University of Wisconsin Medical School, Madison, WI, USA) (James et al. 1996). Yeast strains carrying BD fusion plasmids were transformed with the pAD-GAL4-2.1 library according to a modified version of the high efficiency lithium acetate method of (Agatep et al. 1998). Transformed cells were plated on synthetic complete (SC) medium -Leu -Trp -His supplemented with 1 mM 3-amino-1',2',4'-triazole (3AT) and incubated at 30°C for 14 days. Colonies were replica-plated on SC medium –Leu -Trp -Ade and incubated at 30°C for an additional 14 days. Autoactivating target plasmids were eliminated by segregation

analysis and plasmid DNA was extracted from positive colonies (Parchaliuk et al. 1999). Yeast plasmid DNA was transformed into electrocompetent XL1-blue MRF' (Stratagene) and cells with pAD target plasmid were selected on LB agar plates containing 100 μg/ml ampicillin. Positive target plasmids were separately transformed back into PJ69-4A harboring the pBD-GAL4 Cam, pBD-dNLE, pBD-dWD, or pBD-ScNLE plasmid for reconstruction of two-hybrid positives. A rapid LiAc transformation protocol was used for yeast transformation with bait and positive target plasmids (Gietz and Woods 2002).

Sos Recruitment system: Bait plasmids were cotransformed with pMyr target library in the temperature-sensitive yeast strain cdc25H according to the CytoTrap instruction manual (Stratagene). Transformed cells were plated on SC/glucose medium -Ura -Leu and incubated at 25°C for two days. Colonies were replica-plated on SC medium/galactose -Ura -Leu and incubated at 37°C for ten days. Positive colonies were selected and positive interaction clones were confirmed as specified in the CytoTrap instruction manual. The cDNA inserts isolated from positive colonies were sequenced.

3.3.8. Isolation and gel blot analysis of RNA

Isolation of total RNA as well as gel blot analyses were performed as described previously (Lagace et al. 2003;Lantin et al. 1999). 10 μg of total RNA for each tissue samples were separated on gel. Probes were derived from partial *ScMDN1* cDNA labelled with α-[^{32}P]-dATP (ICN Biochemicals, Irvine, CA) using the High Prime DNA Labeling kit (Roche Diagnostics, Laval, QC). A ^{32}P-labelled *18S* probe was used as a control. Membranes were exposed at –85°C with intensifying screens on Kodak Biomax MR film (Interscience, Markham, ON).

3.3.9. Protoplast transformation and GFP visualization

ScNLE-eGFP was expressed as a translational fusion under the control of the CaMV 35S promoter. Protoplasts were derived from *Nicotiana tabacum* leaf mesophyll cells as described previously (Koop et al. 1996). Protoplasts were transformed with 40 µg of plasmid with a Cell PORATOR apparatus (Gibco BRL, Burlington, ON) with voltage adjusted to 225 V and the capacitor to 1000 µF. Live protoplasts were observed on microscope slides 24 h after incubation in culture medium. Images were acquired using a Leica TCS SP1 laser scanning confocal microscope. An argon laser emitting at 488nm was used as the light source. GFP fluorescence and chlorophyll autofluorescence were detected in separate channels at 500-530 nm and 670-700 nm, respectively. The laser intensity was limited in order to minimize photobleaching. Under these conditions, no GFP fluorescence was detected in control untransformed protoplasts. For display, GFP and chlorophyll images were pseudo-colored in green and red respectively and overlaid using the Leica Confocal Software (LCS). The corresponding Nomarski images were acquired simultaneously.

3.3.10. DNA sequencing and analysis

Approximately 200 ng (5 µl) of plasmid DNA and 15 µl of reaction mixture containing 8.5 µl of water, 3.5 µl 5X sequencing buffer, 2 µl primer at 0.8 µM, and 1 µl Big Dye Terminator Ready Reaction Mix (PE Applied Biosystems) was used for the sequencing reaction. Sequencing reactions were preformed on a GeneAmp PCR System 9700 (PE Applied Biosystems), and the cycling conditions were: 96 °C, 10 sec; 50 °C, 5 sec, 60 °C, 4 min for 25 cycles. DNA sequencing was performed on an Applied Biosystem ABI 310 or 3100 automated sequencer. Sequence alignments were performed with the ClustalW module of the MacVector 7.2.3 software (Accelrys). Database searches were conducted with the BLAST program at The Arabidopsis Information Resource (www.arabidopsis.org) and at the National Center

for Biotechnology Information (www.ncbi.nlm.nih.gov). Cellular localizations were predicted using PSORT (psort.nibb.ac.jp) and SignalP (www.cbs.dtu.dk/services/SignalP).

3.4. RESULTS

3.4.1. *ScNLE* is expressed in actively dividing cells of the apex

ScNLE has previously been shown by RNA gel blot analysis to be expressed in the shoot apex (Chantha et al. 2006). *In situ* hybridization was performed to define more precisely its expression pattern. In shoot apex sections, *ScNLE* localization was associated to actively dividing cells (Fig. 3-1). *ScNLE* transcripts were detected in the shoot apical and axillary meristems (Fig. 3-1A), in inflorescence meristems (Fig. 3-1B), in growing zones of young developing leaves, in floral organ primordia, as well as in the procambium (Fig. 3-1A, B). Analysis of plants transformed with a translational fusion of an about 1100 bp *ScNLE* promoter fragment to GUS revealed identical staining patterns in the shoot apex in addition to expression in the veins of young leaves (Fig. 3-1D). Such expression pattern suggests that *ScNLE* plays a role in actively dividing cells during shoot development and aerial organ formation.

3.4.2. Reducing *ScNLE* expression levels in *S. chacoense* caused a pleiotropic phenotype

To investigate the function of *ScNLE* during shoot development, we analyzed the phenotypes of four transgenic lines underexpressing *ScNLE* that were generated previously with antisense or double-stranded RNA constructs (Chantha et al. 2006). These lines, namely asNLE3, asNLE5, iNLE5, and iNLE6, shared similar pleiotropic phenotypes although with different degrees of severity, with asNLE5 and iNLE6 showing overall the strongest developmental defects.

ScNLE underexpression lead to a considerable array of developmental alterations. The most striking effect was an overall reduction in plant size (see Fig. 2-

7A in Chantha et al., 2006) that was reflected by a reduction in the size of all the aerial organs examined. Height of *ScNLE* underexpressing plants, represented by stem length, was constantly lower than the WT (Fig. 3-2A) and stem width was correspondingly smaller (Fig. 3-2D). Moreover *ScNLE* underexpressing plants produced smaller leaves, with both reduced blade width and length (Fig. 3-2C). Measurement of total leaf surface area produced by 9 week-old plants revealed that this reduction represented ~12% in iNLE5 to ~85% in asNLE3 (248 ± 11.5 to 41.9 ± 19.4 cm^2, n=10 and 6, respectively) of the WT value (281 ± 21.3 cm^2, n=10). Young asNLE3 plants were chlorotic and had an etiolated phenotype that could explain the discrepancy between severe reduction in leaf size (Fig. 3-2C) and mild phenotype on plant height (Fig. 3-2A). However asNLE3 plants recovered from this chlorosis defect in later development stages but still maintained the reduced size and other phenotypes discussed below. The significant reduction in total leaf surface area (t-test, $p < 0.001$) was not caused by lower numbers of leaves produced per plant since the rates of leaf production were similar or even higher in *ScNLE* underexpressing plants compared to the WT throughout plant development (Fig. 3-2B). Reduction in size was also observed for flower organs (Fig. 3-2E). These observations altogether show that *ScNLE* underexpression caused an overall reduction in aerial organ size.

Reducing *ScNLE* expression also reduced the number of some organs formed. For example, *ScNLE* underexpressing plants produced compound leaves with fewer leaflets than WT leaves at equivalent positions (Fig. 3-2C). Moreover, their stems did not produce the ridges normally formed along the mature WT stem that are apparently associated to larger vascular bundles in *S. chacoense* (Fig. 3-2D). In *ScNLE* underexpressing lines, the size of the vascular bundles seemed to be insufficient to trigger the formation of such ridges. Flowers of *ScNLE* underexpressing lines also showed a variety of organ defects. In the case of the strong iNLE6 line, flower buds were formed but always dropped at very early stages of their formation. The asNLE5 line, and at a lesser extend the iNLE5 line, produced flowers with four sepals and petals in high proportions while most WT flowers produce five

sepals and five petals (Fig. 3-2E). Petal fusion was also affected, being completely unfused in asNLE5 and iNLE5 flowers while WT petals were partially fused at their base (Fig. 3-2E). *ScNLE* underexpressing lines also showed reduced fertility. Pollen grains that are normally easy to collect from WT mature dehisced anthers by simple mechanical stimulation, could not be obtained from asNLE5 and iNLE5 anthers. Transition to flowering was also considerably delayed from several days or weeks depending on the *ScNLE* underexpressing line.

This pleiotropic shoot phenotype in addition to the expression of *ScNLE* in the shoot apical meristem (SAM) suggested that possible defects in the SAM could have resulted from *ScNLE* underexpression. We therefore analyzed the morphology of the SAM through longitudinal sections of the shoot apex. SAMs of *ScNLE* underexpressing lines showed a typical layered organization although their cell layers were less uniform than in the WT (Fig. 3-2F). Moreover, SAMs from underexpressing lines were somewhat less protuberant than the WT dome-shaped SAM and therefore seemed smaller (Fig. 3-2F). This reduction in SAM size may be attributable to a reduced number of meristematic cells since cell size was unaffected (data not shown). All *ScNLE* underexpressing plants continuously produced lateral organs during shoot development, suggesting that meristem maintenance is however not impaired.

3.4.3. *ScNLE* underexpression leads to alterations in cell size and in cell number

A change in organ size can reflect an alteration in cell size, in cell number, or both. To assess the contributions of cell size and cell number in the production of smaller leaves in *ScNLE* underexpressing lines, adaxial pavement cells of mature leaf blade were analyzed. Comparison with the WT revealed that asNLE3, asNLE5, and iNLE6 lines produced smaller cells (Fig. 3-3A, B). Surprisingly, the iNLE5 milder underexpressing line produced slightly larger cells (Fig. 3-3A, B). Cell area

measurement showed a significant decrease (*t*-test, $p < 0.001$) from ~70% to ~45% in the asNLE3 and iNLE6 lines (1380 ± 544.6 and 2455 ± 504.1 μm^2, n=120 and 150, respectively) compared to the WT (4316 ± 863.4 μm^2, n=150) (Fig. 3-3B). Average cell size in iNLE5 line was slightly but significantly larger (4939 ± 940, n=150, *t*-test, $p < 0.001$) than the WT (Fig. 3-3B). Similar results were also obtained with pith cells measured in transversal sections of stems (data not shown). Measurement of adaxial pavement cell area of very young leaves indicated that cells originally produced by *ScNLE* underexpressing lines and the WT were not significantly different in size (3-3B). Since cells originally contributed by the SAM are of similar size, as mentioned above, defects in cell size in *ScNLE* underexpressing leaves occured later during their maturation.

Some observations stemming from our analyses suggested that the reduction in leaf size in *ScNLE* underexpressing lines were not solely caused by a reduction in cell size. iNLE5 epidermal cells were slightly bigger (Fig. 3-3B) but their leaves were significantly smaller than the WT (Fig. 3-2C). Moreover, reductions in epidermal cell size in the other *ScNLE* underexpressing lines were not as severe as the reduction in their leaf size. We therefore suspected that cell number could also be affected in transgenic lines underexpressing *ScNLE*. Calculations with the terminal leaflet surface area and the average cell area of mature leaves showed that the average number of adaxial pavement cells was significantly reduced (*t*-test, $p<0.0001$) by about 35% in all *ScNLE* underexpressing lines compared to the WT (Fig. 3-3C). Therefore, reduction in cell number contributed to reduced organ size in all *ScNLE* underexpressing lines whereas reduction in cell size contributed only in lines expressing a more severe phenotype. Since surface areas of young leaves in *ScNLE* underexpressing lines were smaller than in the WT (Fig. 3-2C) while cell sizes were similar at that stage (Fig. 3-3B), reduced cell number is suggested to originate early during leaf formation, before defects in cell size could be detected.

3.4.4. *ScNLE* underexpression increased stomatal index

While analyzing the adaxial surface of mature leaves for cell size and cell number determination, we were struck by the high density of stomata found in *ScNLE* underexpressing lines (Fig. 3-4A, B). Stomatal density, which represents the number of stomata per surface unit, on the adaxial epidermis of mature leaves from all the *ScNLE* underexpressing lines was significantly higher than the WT, with lines asNLE3, asNLE5, and iNLE6 showing more than a fourfold increase (Table 3-1). Because stomatal density does not take into account the differences in the size of pavement cells, stomatal index [si = nb of stomata/(nb of pavement cells + nb of stomata)*100] was also determined. Stomatal index was significantly higher in all *ScNLE* underexpressing lines, being almost up to three-fold higher in iNLE6 adaxial epidermis compared to the WT (Table 3-1). Therefore, the ratio of pavement cells per stomata (ratio P/S) was decreased in *ScNLE* underexpressing lines (Table 3-1). To see whether this increase in stomatal index also applied to other organs, we analyzed stomata production on the stem. Stomatal index was also significantly higher on the stem of *ScNLE* underexpressing plants but at a lesser extent than on the leaf (Table 3-1). These results confirmed that underexpressing *ScNLE* increased the ratio of stomata produced.

To examine whether the structure of internal leaf tissues was affected, transverse sections of mature leaves were analyzed by light microscopy. Leaves typically contain a single layer of elongated parenchyma cells underlying the adaxial epidermis and several layers of spongy parenchyma, composed of cells and air spaces (Fig. 3-4C). All these cell layers were present in *ScNLE* underexpressing leaves, although spongy parenchyma cells in asNLE3, asNLE5, and iNLE6 (Fig. 3-4D) were less densely packed compared to the WT, possibly as a consequence of the production of considerably more stomata.

3.4.5. Yeast two-hybrid screens identified MDN1 as a binding partner of ScNLE

In order to better determine in which cellular process the ScNLE protein could be involved during plant development, yeast two-hybrid screens were performed to identify ScNLE interacting partners. The Nle domain (dNLE) and the WDR domain (dWD) of ScNLE, both predicted to be involved in protein-protein interactions, were separately used as baits (Fig. 3-5A). Both the nuclear GAL4 system and the cytoplasmic Sos Recruitment (SR) system were used as complementary two-hybrid screening approaches. In the GAL4 system, an AD-cDNA target library of ovaries collected 18 to 72 HAP was screened with the BD-dNLE and BD-dWD bait constructs in the yeast strain PJ69-4A. In the SR system, a MYR-cDNA target library of ovaries collected 2 to 6 DAP was screened with the Sos-dNLE and Sos-dWD bait constructs in the yeast strain cdc25H. Several candidates were identified of which a homolog of the yeast *MIDASIN* gene (*MDN1*, also known as YLR106c and REA1) was predominantly retrieved with the Nle domain in both two-hybrid systems. Six out of eleven (6/11) and thirteen out of fifteen (13/15) positive clones representing *ScMDN1* were isolated from screens carried with BD-dNLE (Fig. 3-5B) and Sos-dNLE respectively. Interestingly, when the AD-cDNA library was further screened with full-length ScNLE fused to BD, three out of the five positive clones also represented *ScMDN1* (Fig. 3-5B). However the WDR domain of ScNLE alone did not interact with ScMDN1 when cotransformed in yeast (Fig. 3-5B). These results suggest that ScNLE interacted with ScMDN1 through its Nle domain.

MDN1 represents the largest ORF found in the the yeast genome, with a predicted sequence of 4910 aa and molecular mass of 560 kDa (Garbarino and Gibbons 2002) and was shown to be a trans-acting factor involved in 60S ribosomal subunit maturation (Galani et al. 2004;Nissan et al. 2004). All the *ScMDN1* clones isolated were therefore only partial cDNAs representing the C-terminal portion of the protein (Fig. 3-5C). The length of the clones varied from 1 427 bp to 2 784 bp. The longest cDNA sequence coded for a 816 aa ORF that spanned almost completely the

D/E-rich domain and the whole MIDAS domain (M-domain) of MDN1 (Fig. 3-5C). The shortest cDNA encoded a 364 aa ORF that included only a small C-terminal portion of the D/E-rich domain and the whole M-domain (Fig. 3-5C). Because all the clones comprised the MIDAS domain but not always the D/E-rich domain, the MIDAS domain is likely to be the one involved in ScMDN1 interaction with ScNLE.

In addition, a homolog of the yeast NSA2 (also known as YER126p) was identified in three out of six (3/6) positive clones in a screen carried with the WDR domain fused to Sos (Sos-dWR) using the SR system. Interestingly, NSA2 was also isolated as a trans-acting factor associated to pre-60S ribosomal particles in yeast (Nissan et al. 2002).

3.4.6. *ScMDN1* expression pattern in plant organs

We next performed RNA gel blot analyses to determine *ScMDN1* expression pattern within the plant. We first examined *ScMDN1* expression in various plant organs. Signal was detected in stems, leaves, and shoot apices (including the shoot apical meristem and organ primordia) but not in tubers, roots, petals, anthers and pollen grains (Fig. 3-6A). Because the expression of ScNLE was previously shown to be induced by fertilization in ovules and ovaries (Chantha et al. 2006), we also analyzed *ScMDN1* expression pattern in these organs in time-course studies following pollination. Figure 6B shows a broad time-course analysis using isolated ovules. Signal was detected in ovules from unpollinated flowers and 2 days after pollination (DAP) but was very weak or undetectable by four DAP onwards. A more detailed time-course analysis was carried out with pollinated ovaries (Figure 6C). *ScMDN1* expression was weaker from 12 to 30 hours after pollination (HAP), increased at 42 and 48 HAP, and then decreased to basal levels at 72 HAP. In some Solanaceous species, including *S. chacoense* (Clarke 1940;Williams 1955), and our unpublished results), the period comprised between 36 to 42 HAP corresponds to the intense

basipetal fertilization of the multiple ovules present in the ovary and to initiation of seed development.

3.4.7. A NLE-GFP fusion protein is localized in the cytoplasm and nucleus

Analysis of the ScNLE protein sequence using various prediction tools did not identify any intracellular targeting sequences (e.g. NLS, transit sequence, signal sequence) and therefore predicted a cytoplasmic localization. In order to find out experimentally the cellular localization of ScNLE protein, we expressed a ScNLE-GFP fusion protein driven by the constitutive CaMV 35S promoter in tobacco protoplasts. Surprisingly, the ScNLE-GFP fusion product was not restricted to the cytoplasm but was also found in the nucleus (Fig. 3-7). Cytoplasmic localization can be seen as a thin ring appressed to the plasma membrane due to the presence of a large vacuole. We therefore considered that ScNLE is distributed in both the cytoplasm and the nucleus.

3.5. DISCUSSION

The *ScNLE* gene was originally isolated in a subtractive screen as a gene that is transiently up-regulated in the ovary by fertilization and was previously characterized for its function during post-fertilization events in *Solanum chacoense* (Chantha et al. 2006). Localization of the gene in the shoot apex as well as reduction in plant size associated with *ScNLE* underexpression however suggested that *ScNLE* is also involved in shoot development, which was the focus of the present study. Also, we provide some evidence that the *ScNLE* gene product, as his yeast homolog, is involved in 60S ribosomal subunit maturation in plants.

Detailed expression studies and phenotypic analysis of underexpressing plants revealed here that *ScNLE* functions in a process that affects cell proliferation and cell enlargement during shoot development. *ScNLE* was shown to be expressed in actively dividing structures of the shoot apex, such as the shoot and floral meristems, organ primordia, and the procambium (Fig. 3-1). Morever, underexpressing *ScNLE* led to pleiotropic defects during shoot development, the most prominent ones being an overall reduction in plant aerial organ size and a reduction in some organ numbers (Fig. 3-2). The final size of a plant organ is determined by cell number (cell proliferation) and cell size (cell enlargement) composition (Mizukami 2001). Analysis of adaxial leaf epidermal pavement cells revealed that aerial organ defects in *ScNLE* underexpressing plants are the consequence primarily of reduced cell number and also of reduced cell size. Reduction in cell number originated very early during leaf formation, possibly at the stage of cell recruitement from the shoot apical meristem (SAM) to primordium anlagen, since *ScNLE* underexpressing plants produced smaller SAMs that contained normal-sized cells (Fig. 3-2F and data not shown). Also, reduction in cell number was detected very early during development of *ScNLE* underexpressing leaves, at a stage when sizes of adaxial pavement cells were still indistinguishable from the WT (Fig. 3-3B). While a reduction in cell number was common to all *ScNLE* underexpressing lines, changes in cell size were

not as simply correlated: the less defective iNLE5 line produced larger than normal cells whereas all the other underexpressing lines produced smaller than normal cells. In plants, final organ size would be determined at the whole organ level through a total organ-size checkpoint that coordinates cell proliferation with cell enlargement to ensure that organs reach a determined size (Tsukaya 2002). There are several examples of plant cell cycle progression mutants in which a reduction in cell number in an organ is compensated by an increase in cell size, similarly to what was observed in the iNLE5 underexpressing line (Autran et al. 2002;De Veylder et al. 2001;Hemerly et al. 1995;Mizukami and Fischer 2000;Ullah et al. 2001;Wang et al. 2000). The lack of compensatory cell enlargement in the more severely affected *ScNLE* underexpressing lines therefore suggests that *ScNLE* is not merely involved in the regulation of cell cycle progression but is also required for proper cell enlargement. As discussed below, an implication of *ScNLE* in a basic cellular process such as ribosome biogenesis could give an explanation to the phenotypic consequences of underexpressing *ScNLE*.

Another phenotype associated with *ScNLE* underexpression is a significant increase in the stomatal index (Fig. 3-4). Stomatal formation has been extensively studied in *Arabidopsis* and similar patterning mechanisms likely apply to other dicots (Geisler et al. 2000). Stomata originate from a meristemoid, a cell with limited stem-cell capacity. The firsts meristemoids produced in an organ originate from some specialized protodermal cells called meristemoid mother cells (MMC). An asymmetric division of the MMC gives rise to a smaller, usually triangular shape meristemoid and a larger neighboring cell. The meristemoid can itself reiterate this pattern of asymmetric division, but only for a limited rounds of cell division, and eventually differentiates into a round guard mother cell (GMC). The GMC finally divides symmetrically to form the pair of guard cells of a stomata. Most of the neighboring cells of a stomatal complex differentiate into pavement cells, but some can reinitiate a stomatal lineage by dividing asymmetrically to give rise to satellite meristemoids. In *Arabidopsis*, almost half of the pavement cells of a leaf are

generated through the asymmetric divisions of meristemoids (Geisler et al. 2000). Considering our data on reduced cell proliferation in *ScNLE* underexpressing plants, an increase in stomatal index could be attributed to reduced meristematic maintenance capacity of meristemoid cells. Meristemoids would go through a fewer number of cell divisions before differentiating into GMC and hence less pavement cells would be generated per meristemoid, thus resulting in an increase of the stomatal index.

The *NLE* gene was first isolated as a regulator of the Notch receptor activity in *Drosophila* (Royet et al. 1998) and later, the yeast *NLE* homolog (YCR072c or Rsa4c) was repeatedly found as a non-ribosomal protein associated to pre-60S ribosomal particles (Bassler et al. 2001;Gavin et al. 2002;Nissan et al. 2002). Although no Notch signaling pathway exists in plants and yeasts (Wigge and Weigel 2001), the *NLE* gene is evolutionary conserved in eukaryotes and orthologues are expected to perform similar cellular functions. Ribosome biogenesis seems to be a highly conserved cellular process throughout animals, plants and yeasts (Tschochner and Hurt 2003). In this study, the identification of a homolog of the yeast *MDN1* gene product as a potential protein partner of ScNLE provides further support to the implication of the *NLE* gene in 60S ribosomal subunit biogenesis. With a molecular weight of 560 kDa, MDN1 represents the largest protein identified in the yeast genome. MDN1 consists of an N-terminal ATPase domain, comprised of six AAA^+-type promoters, that is separated by a long middle domain from the C-terminal M-domain (Garbarino and Gibbons 2002). The ScNLE-ScMDN1 interaction would involve the Nle domain of ScNLE and the M-domain of ScMDN1, since all the *ScMDN1* clones isolated from the two-hybrid screens contained at least the M-domain but not necessarily the adjacent upstream D/E-rich domain (Fig. 3-5C). Consistent with this, M-domains are involved in protein-protein interactions and function in multiprotein complexes (Whittaker and Hynes 2002).

Although the ScNLE-ScMDN1 interaction was not confirmed with other protein-protein interaction assays, we believe it is meaningful for the following reasons. Firstly, ScMDN1 was consistently isolated from two different two-hybrid systems, and therefore does not represent an artifact associated to the screening system itself. Secondly, despite the high number of clones screened, ScMDN1 was the only candidate with a M-domain retrieved. M-domains are present in several other plant proteins and are known to be involved in protein-protein interactions (Liu et al. 2005;Whittaker and Hynes 2002). Thirdly, we have shown that *ScMDN1* shows overlapping expression pattern (Fig. 3-6) with that determined for *ScNLE* in a previous study (Chantha et al. 2006). Moreover, an ScNLE-GFP protein localized in the nucleus (Fig. 3-7C), which is in the same cellular compartment as the yeast MDN1 (Galani et al. 2004;Garbarino and Gibbons 2002) and would therefore provide the potential for these proteins to interact *in planta*. Lastly, yeast NLE/Rsa4p and MDN1 were repeatedly isolated in the same protein complexes by tandem affinity purification – mass spectrometry using different tagged trans-acting factors of pre-60S ribosomal particles (Bassler et al. 2001;Galani et al. 2004;Nissan et al. 2002). The NSA2 protein (YER126p) was also found as a non-ribosomal constituent of these affinity purified pre-60S ribosomal particles (Gavin et al. 2002;Nissan et al. 2002). Interestingly, a homolog of yeast NSA2 was isolated several times with the WDR domain of ScNLE in our two-hybrid screens, bringing further support to the possible involvement of ScNLE in 60S ribosomal subunit biogenesis in plants.

In yeast, 60S ribosomal subunits undergo initial assembly in the nucleolus and then go through different steps of maturation in the nucleoplasm before they are exported to the cytoplasm for final maturation (Tschochner and Hurt 2003). While MDN1 is enriched in a late nucleoplasmic pre-60S ribosomal particle, close to export to the cytoplasm but from which it is released before export (Bassler et al. 2001;Galani et al. 2004), yeast NLE/Rsa4p has been identified in nucleolar, nucleoplasmic and cytoplamic pre-60S particles (Bassler et al. 2001;Nissan et al. 2002). Consistent with this, ScNLE-GFP was here shown to be localized in both the

nucleus and cytoplasm of plant cells (Fig. 3-6), which is also consistent with the subcellular localization determined for the human NLE (Scherl et al. 2002), and yeast NLE/Rsa4p (de la Cruz et al. 2005) orthologs. In yeast, pre-60S particles that are successively formed on their maturation path are composed of substantially different pre-rRNAs species, ribosomal proteins and trans-acting factors (Tschochner and Hurt 2003). Based on the structural nature of NLE as a WDR protein, it has been proposed that yeast NLE/Rsa4p could act as a molecular platform for the interaction of other trans-acting factors involved in the maturation of pre-60S particles, from early steps in the nucleolus to final dissociation in the cytoplasm (de la Cruz et al. 2005). Taking into account our yeast two-hybrid results and the evolutionary conservation of ribosome biogenesis, NSA2 and MDN1 could represent such trans-acting factors that transiently assemble to pre-60S particles through NLE/Rsa4p to accomplish their function.

Depletion of NLE/Rsa4p and MDN1 in yeast causes defects in pre-rRNA processing and pre-60S subunits transport, leading to the reduction of mature 60S subunit formed (de la Cruz et al. 2005;Galani et al. 2004). Because ribosomes are fondamental for global cellular functions, misregulations in ribosomal biogenesis can be expected to cause general developmental defects. In yeast, both *MDN1* and *NLE/Rsa4* are required for cell viability (Giaever et al. 2002). This also seems to be the case for *ScNLE* since fully suppressed plants could not be isolated from transgenic *S. chacoense* lines expressing either an antisense or a RNAi *ScNLE* construct (Chantha et al. 2006). Depletion of NLE/Rsa4p protein in yeast leads to a strong slow-growth phenotype (de la Cruz et al. 2005), which can be compared to the cellular enlargement and proliferation defects observed here on leaf adaxial pavement cells and hence could cause the pleitropic developmental defects in *ScNLE* underexpressing lines. In a previous study, *ScNLE* expression was shown to be upregulated in ovaries by fertilization, an event that induces an intense period of cellular division that initiates fruit development, and its underexpression was shown to cause ovule and seed abortion (Chantha et al. 2006). Reports on the role of genes

encoding trans-acting factors involved in ribosome maturation during plant development are scarce. An insertion mutation in the *SLOW WALKER1* (*SWA1*) gene, encoding a ribosome trans-acting factor, causes a delay in female gameogenesis (Shi et al. 2005). Mutating or silencing of plant ribosomal protein genes produced developmental phenotypes similar to the ones observed in *ScNLE* underexpressing plants, such as reduced organ size and organ number, late flowering and reduced cell proliferation (Lahmy et al. 2004;Popescu and Tumer 2004;Weijers et al. 2001).

In conclusion, our data indicate that *ScNLE* is essential for normal cell proliferation and cell enlargement during plant development. The pleiotropic defects in shoot development resulting from underexpressing *ScNLE* is likely the consequence of defects in 60S ribosomal biogenesis.

3.6. ACKNOWLEDGEMENTS

We are grateful to Alexandre Joyeux for providing the GFP vector and for assistance with the confocal microscope. This work was supported by the Natural Sciences and Engineering Research Council of Canada (NSERC) and from the Canada Research Chair program. S. C. Chantha is the recipient of Ph. D. fellowships from NSERC and from Le Fonds Québécois de la Recherche sur la Nature et les Technologies (FQRNT, Québec). D. P. Matton holds a Canada Research Chair in Functional Genomics and Plant Signal Transduction.

Table 3-1. Stomatal density and stomatal index in WT and various *ScNLE* underexpressing lines

Line	Adaxial leaf			Stem	
	Stomatal density[a]	Stomatal index (%)[b]	Ratio P/S*	Stomatal density[a]	Stomatal index (%)[b]
WT	7,0 ± 2,6	5,8 ± 1,8	17,8 ± 5,2	2,9 ± 1,1	1,6 ± 0,4
asNLE3[c]	34,0 ± 7,7	9,4 ± 2,5	10,3 ± 3,1	6,1 ± 2,1	3,3 ± 1,1
asNLE5	30,2 ± 5,9	9,0 ± 1,6	10,8 ± 2,0	2,8 ± 0,7	2,1 ± 0,6
iNLE5[c]	7,9 ± 1,5[e]	7,7 ± 1,0[d]	12,3 ± 2,0	9,1 ± 3,8	3,2 ± 0,8
iNLE6[c]	40,9 ± 7,1	15,9 ± 1,1	5,3 ± 0,4	5,2 ± 1,5[d]	2,4 ± 0,3

*P = number of pavement cells / S = number of stomata, ± SD (n= 8 to 13)

[a]Mean total number of stomata per surface unit (0,407 mm^2 field) ± SD (n= 8 to 13)

[b][si = S / (P + S)*100] ± SD (n= 8 to 13)

[c]All the values were significantly different from the corresponding WT value (t-test, $p < 0.001$) except for [d, e]

[d]Significantly different from the WT (Student's t-test, $p < 0.01$)

[e]Not significantly different from the WT

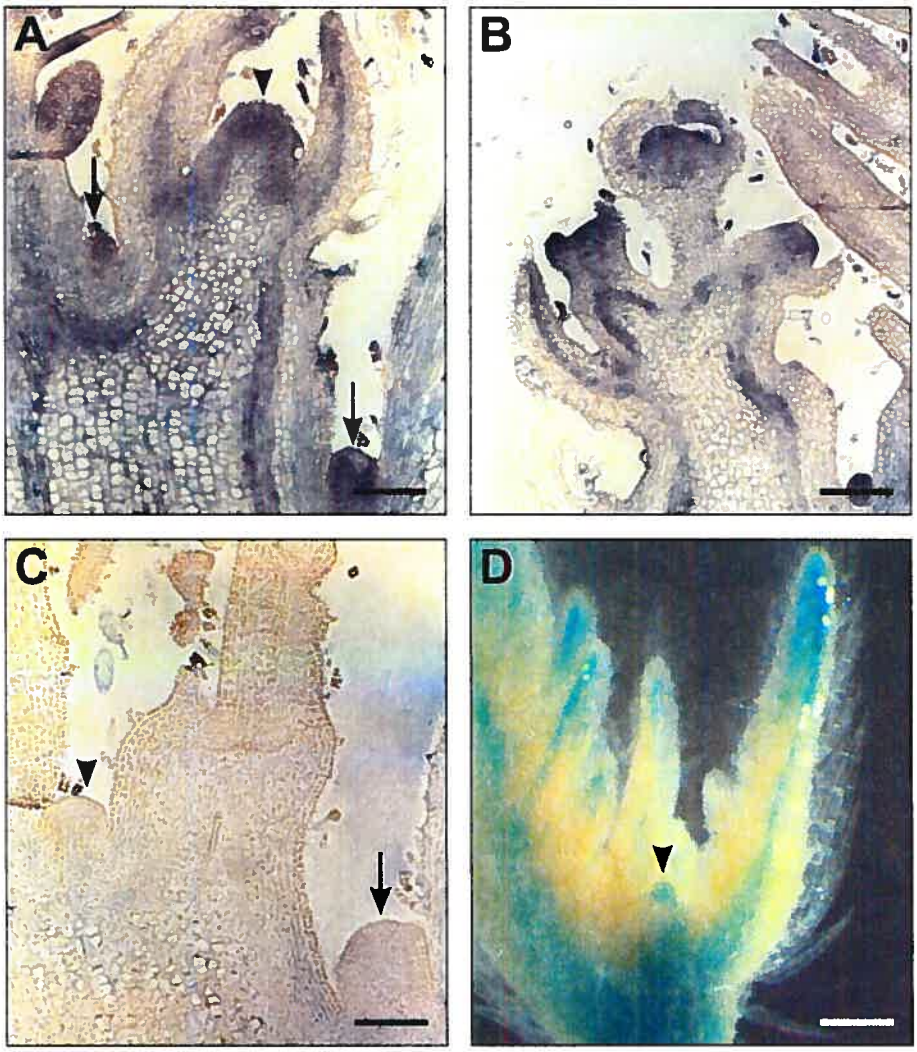

Figure 3-1. *In situ* localization of *ScNLE* transcripts in the apex. (A) Vegetative apex, longitudinal section, *ScNLE* antisense probe. (B) Inflorescence apex, longitudinal section, *ScNLE* antisense probe. (C) Vegetative apex, longitudinal section, *ScNLE* sense probe. (A - C) Bar = 100 μm. (D) GUS staining pattern conferred by *ScNLE* promoter. In (A, C, D) arrowheads indicate shoot apical meristems and arrows indicate axillary meristems. Bar = 250 μm.

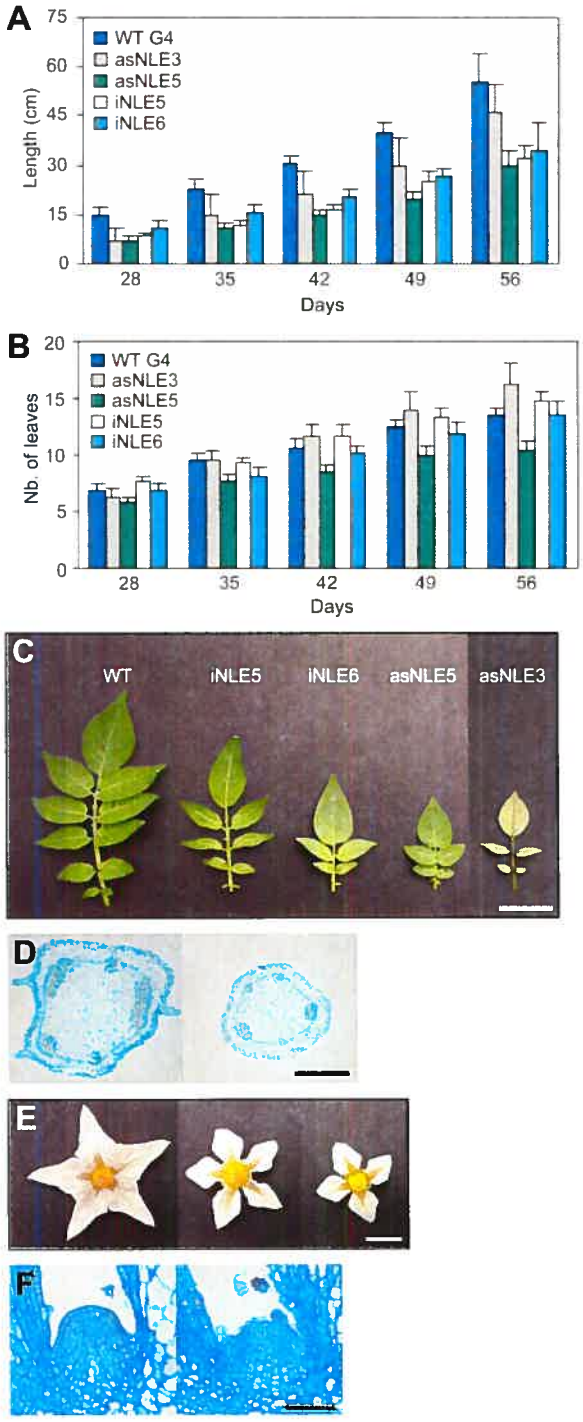

Figure 3-2. Sporophytic phenotypes associated to *ScNLE* underexpressing lines. (A) Stem elongation. Stem lengths of WT and *ScNLE* underexpressing lines were measured 28, 35, 42, 49 and 56 days after transfer of plants from *in vitro* culture to soil (n=10). (B) Leaf production. Number of opened leaves produced per plant (n=10). (C) 2nd youngest fully opened leaves of indicated genotype plant. Bar = 2 cm. (D) Transversal sections of WT (left) and iNLE6 (right) stems. Bar = 1 mm. (E) Morphology of representative flowers of WT (left) and iNLE5 line. Bar = 1 cm. (F) Longitudinal sections of WT (left) and iNLE6 (right) apices. Bar = 50 µm.

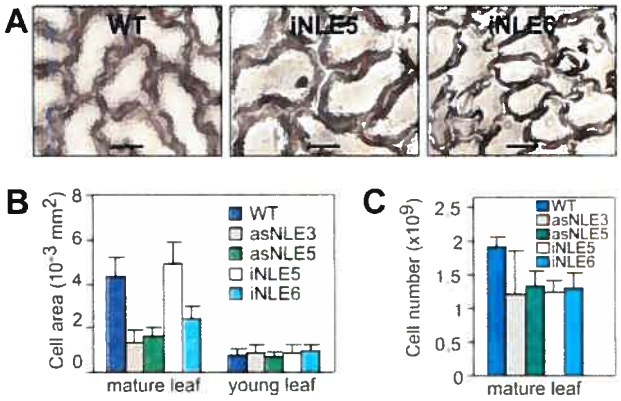

Figure 3-3. Adaxial epidermal pavement cell size and cell number in *ScNLE* underexpressing lines. (A) Cell imprints of mature leaf from WT (left), iNLE5 (middle) and iNLE6 (right) lines. Bar = 10 µm. (B) Average cell area of mature and young leaflets of WT and *ScNLE* underexpressing lines. For each line, a total of 150 epidermal cells were measured from 10 equivalent terminal leaflets coming from 10 independent plants. (C) Total number of cells of mature terminal leaflet. For each line, 10 equivalent terminal leaflet areas were measured and divided by corresponding mean cell areas determined in (B).

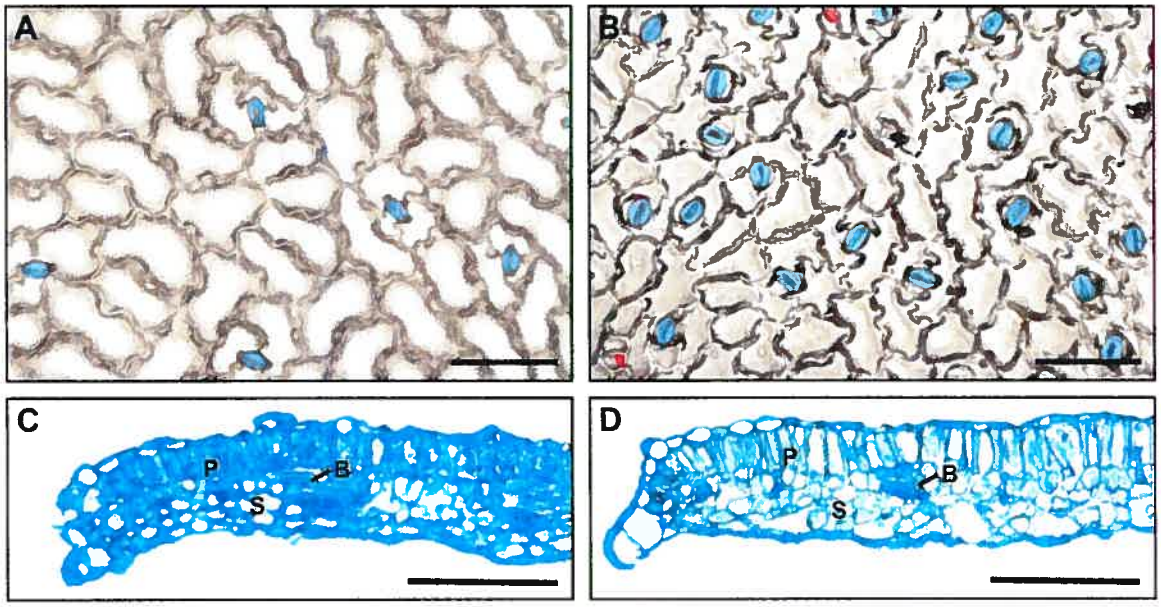

Figure 3-4. Stomata production and leaf internal tissues of a *ScNLE* underexpressing line. (A, B) Adaxial epidermal cell imprints of a WT (A) and a iNLE6 (B) mature leaf. Stomata are colored in blue and meristemoids are colored in red. (C, D) Transversal sections of mature leaf blades of WT (C) and iNLE6 line (D). Bars = 100 μm. P, palisade parenchyma; S, spongy parenchyma; B, bundle sheath.

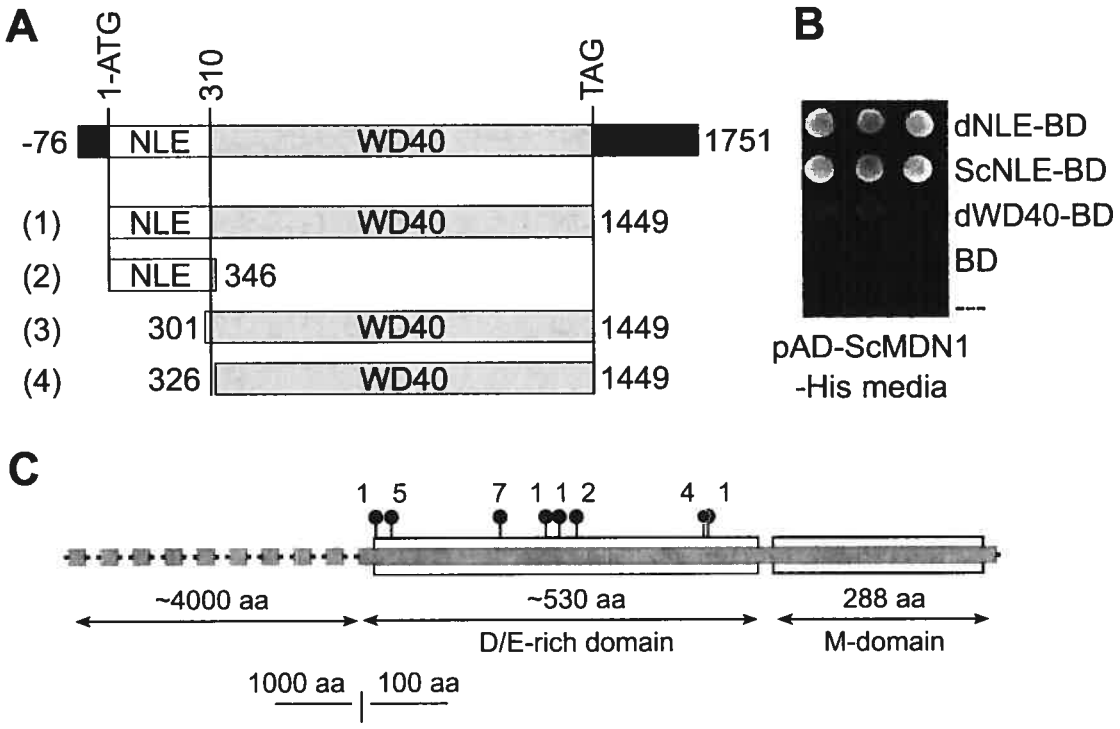

Figure 3-5. ScNLE two-hybrid interactions. (A) Schematic representation of *ScNLE* cDNA (up). Numbers on top represent nucleotide positions, number 1 corresponding to the first nucleotide of the ATG initiation codon. (1) to (4) represent regions fused to Gal4 BD and/or Sos. Numbers on the left and right refer respectively to 5' and 3' ends of cloned cDNA regions. (1) Full ScNLE; (2) Nle domain; (3) WDR domain cloned in pBD-Gal4; (4) WDR domain cloned in pSos. (B) Interactions of pAD-ScMDN1 C-terminal region with different portions of ScNLE fused to Gal4 BD or with Gal4 BD alone in yeast, on -His selection medium. (C) Schematic representation of ScMDN1 with emphasis on its C-terminal region. Circles with associated numbers represent N-terminal position and number of corresponding cDNA clones retrieved from two-hybrid screens with the Nle domain or complete ScNLE protein fused to Gal4-BD or Sos.

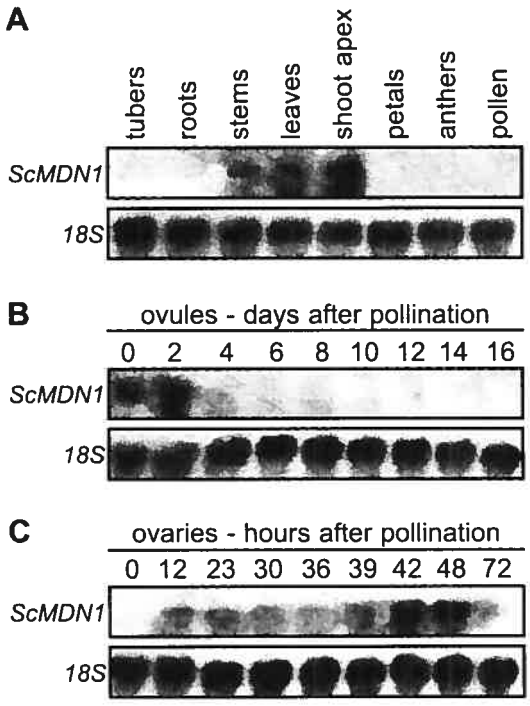

Figure 3-6. RNA expression analysis of *ScMDN1* transcript levels. Ten µg of total RNA from various tissues were probed with a 32P-labelled *ScMDN1* partial cDNA. (A) Diverse plant tissues. (B) Ovules at different time points in days after pollination (DAP). (C) Ovaries at different time points in hours after pollination (HAP). A 32P-labelled *18S* probe was used as a control.

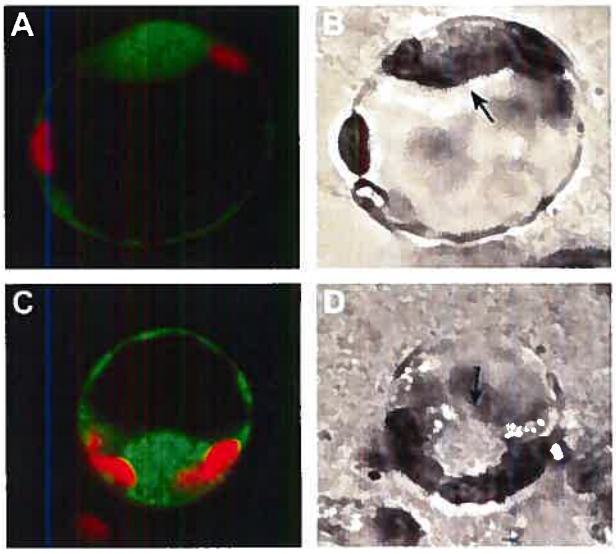

Figure 3-7. Transient expression of ScNLE-GFP in tobacco protoplasts. Confocal microscope images of (A) GFP control expression and (C) ScNLE-GFP chimeric protein expression. Green represents GFP fluorescence. Red represents chlorophyll fluorescence. (B) and (D) Differential interference contrast microscope images of (A) and (C), respectively. Arrows indicate the nucleus.

3.7. REFERENCES

Agatep R, Kirkpatrick RD, Parchaliuk DL, Woods RA, Gietz RD (1998) Transformation of Saccharomyces cerevisiae by the lithium acetate/single-stranded carrier DNA/polyethylene glycol (LiAc/ss-DNA/PEG) protocol. Technical Tips Online (http://tto.trends.com).

Autran D, Jonak C, Belcram K, Beemster GT, Kronenberger J, Grandjean O, Inze D, Traas J (2002) Cell numbers and leaf development in Arabidopsis: a functional analysis of the STRUWWELPETER gene. Embo J 21: 6036-49.

Bassler J, Grandi P, Gadal O, Lessmann T, Petfalski E, Tollervey D, Lechner J, Hurt E (2001) Identification of a 60S preribosomal particle that is closely linked to nuclear export. Mol Cell 8: 517-29.

Bussiere F, Ledu S, Girard M, Heroux M, Perreault J-P, Matton DP (2003) Development of an efficient cis-trans-cis ribozyme cassette to inactivate plant genes. Plant Biotechnology Journal 1: 423-435.

Chantha SC, Emerald BS, Matton DP (2006) Characterization of the plant Notchless homolog, a WD repeat protein involved in seed development. Plant Molecular Biology, in press, DOI 10.1007/s11103-006-9064-4.

Clarke AE (1940) Fertilization and early embryo development in the potato. Am. Potato J. 17: 20-25.

de la Cruz J, Sanz-Martinez E, Remacha M (2005) The essential WD-repeat protein Rsa4p is required for rRNA processing and intra-nuclear transport of 60S ribosomal subunits. Nucleic Acids Res 33: 5728-39.

De Veylder L, Beeckman T, Beemster GT, Krols L, Terras F, Landrieu I, van der Schueren E, Maes S, Naudts M, Inze D (2001) Functional analysis of cyclin-dependent kinase inhibitors of Arabidopsis. Plant Cell 13: 1653-68.

Esau K (1977) Anatomy of Seed Plants. New York.

Galani K, Nissan TA, Petfalski E, Tollervey D, Hurt E (2004) Rea1, a dynein-related nuclear AAA-ATPase, is involved in late rRNA processing and nuclear export of 60 S subunits. J Biol Chem 279: 55411-8.

Garbarino JE, Gibbons IR (2002) Expression and genomic analysis of midasin, a novel and highly conserved AAA protein distantly related to dynein. BMC Genomics 3: 18.

Gavin AC, Bosche M, Krause R, Grandi P, Marzioch M, Bauer A, Schultz J, Rick JM, Michon AM, Cruciat CM, Remor M, Hofert C, Schelder M, Brajenovic M, Ruffner H, Merino A, Klein K, Hudak M, Dickson D, Rudi T, Gnau V, Bauch A, Bastuck S, Huhse B, Leutwein C, Heurtier MA, Copley RR, Edelmann A, Querfurth E, Rybin V, Drewes G, Raida M, Bouwmeester T, Bork P, Seraphin B, Kuster B, Neubauer G, Superti-Furga G (2002) Functional organization of the yeast proteome by systematic analysis of protein complexes. Nature 415: 141-7.

Geisler M, Nadeau J, Sack FD (2000) Oriented asymmetric divisions that generate the stomatal spacing pattern in arabidopsis are disrupted by the too many mouths mutation. Plant Cell 12: 2075-86.

Giaever G, Chu AM, Ni L, Connelly C, Riles L, Veronneau S, Dow S, Lucau-Danila A, Anderson K, Andre B, Arkin AP, Astromoff A, El-Bakkoury M, Bangham R, Benito R, Brachat S, Campanaro S, Curtiss M, Davis K, Deutschbauer A, Entian KD, Flaherty P, Foury F, Garfinkel DJ, Gerstein M, Gotte D, Guldener U, Hegemann JH, Hempel S, Herman Z, Jaramillo DF, Kelly DE, Kelly SL, Kotter P, LaBonte D, Lamb DC, Lan N, Liang H, Liao H, Liu L, Luo C, Lussier M, Mao R, Menard P, Ooi SL, Revuelta JL, Roberts CJ, Rose M, Ross-Macdonald P, Scherens B, Schimmack G, Shafer B, Shoemaker DD, Sookhai-Mahadeo S, Storms RK, Strathern JN, Valle G, Voet M, Volckaert G, Wang CY, Ward TR, Wilhelmy J, Winzeler EA, Yang Y, Yen G, Youngman E, Yu K, Bussey H, Boeke JD, Snyder M, Philippsen P, Davis RW, Johnston M (2002) Functional profiling of the Saccharomyces cerevisiae genome. Nature 418: 387-91.

Gietz RD, Woods RA (2002) Transformation of yeast by lithium acetate/single-stranded carrier DNA/polyethylene glycol method. Methods Enzymol 350: 87-96.

Hemerly A, Engler Jde A, Bergounioux C, Van Montagu M, Engler G, Inze D, Ferreira P (1995) Dominant negative mutants of the Cdc2 kinase uncouple cell division from iterative plant development. Embo J 14: 3925-36.

James P, Halladay J, Craig EA (1996) Genomic libraries and a host strain designed for highly efficient two-hybrid selection in yeast. Genetics 144: 1425-1436.

Kimble J, Simpson P (1997) The LIN-12/Notch signaling pathway and its regulation. Annu Rev Cell Dev Biol 13: 333-61.

Koop HU, Steinmuller K, Wagner H, Rossler C, Eibl C, Sacher L (1996) Integration of foreign sequences into the tobacco plastome via polyethylene glycol-mediated protoplast transformation. Planta 199: 193-201.

Lagace M, Chantha SC, Major G, Matton DP (2003) Fertilization induces strong accumulation of a histone deacetylase (HD2) and of other chromatin-remodeling proteins in restricted areas of the ovules. Plant Mol Biol 53: 759-69.

Lahmy S, Guilleminot J, Cheng CM, Bechtold N, Albert S, Pelletier G, Delseny M, Devic M (2004) DOMINO1, a member of a small plant-specific gene family, encodes a protein essential for nuclear and nucleolar functions. Plant J 39: 809-20.

Lantin S, O'Brien M, Matton DP (1999) Pollination, wounding and jasmonate treatments induce the expression of a developmentally regulated pistil dioxygenase at a distance, in the ovary, in the wild potato Solanum chacoense Bitt. Plant Mol Biol 41: 371-86.

Liu J, Jambunathan N, McNellis TW (2005) Transgenic expression of the von Willebrand A domain of the BONZAI 1/COPINE 1 protein triggers a lesion-mimic phenotype in Arabidopsis. Planta 221: 85-94.

Matton DP, Maes O, Laublin G, Xike Q, Bertrand C, Morse D, Cappadocia M (1997) Hypervariable Domains of Self-Incompatibility RNases Mediate Allele-Specific Pollen Recognition. Plant Cell 9: 1757-1766.

Mizukami Y (2001) A matter of size: developmental control of organ size in plants. Curr Opin Plant Biol 4: 533-9.

Mizukami Y, Fischer RL (2000) Plant organ size control: AINTEGUMENTA regulates growth and cell numbers during organogenesis. Proc Natl Acad Sci U S A 97: 942-7.

Neer EJ, Schmidt CJ, Nambudripad R, Smith TF (1994) The ancient regulatory-protein family of WD-repeat proteins. Nature 371: 297-300.

Nissan TA, Bassler J, Petfalski E, Tollervey D, Hurt E (2002) 60S pre-ribosome formation viewed from assembly in the nucleolus until export to the cytoplasm. Embo J 21: 5539-47.

Nissan TA, Galani K, Maco B, Tollervey D, Aebi U, Hurt E (2004) A pre-ribosome with a tadpole-like structure functions in ATP-dependent maturation of 60S subunits. Mol Cell 15: 295-301.

O'Brien M, Kapfer C, Major G, Laurin M, Bertrand C, Kondo K, Kowyama Y, Matton DP (2002) Molecular analysis of the stylar-expressed Solanum chacoense small asparagine-rich protein family related to the HT modifier of gametophytic self-incompatibility in Nicotiana. Plant J 32: 985-96.

Parchaliuk DL, Kirkpatrick RD, Agatep R, Simon SL, Gietz RD (1999) Yeast two-hybrid system screening. Technical Tips Online (http://tto.trends.com).

Popescu SC, Tumer NE (2004) Silencing of ribosomal protein L3 genes in N. tabacum reveals coordinate expression and significant alterations in plant growth, development and ribosome biogenesis. Plant J 39: 29-44.

Royet J, Bouwmeester T, Cohen SM (1998) Notchless encodes a novel WD40-repeat-containing protein that modulates Notch signaling activity. Embo J 17: 7351-60.

Scherl A, Coute Y, Deon C, Calle A, Kindbeiter K, Sanchez JC, Greco A, Hochstrasser D, Diaz JJ (2002) Functional proteomic analysis of human nucleolus. Mol Biol Cell 13: 4100-9.

Shi DQ, Liu J, Xiang YH, Ye D, Sundaresan V, Yang WC (2005) SLOW WALKER1, essential for gametogenesis in Arabidopsis, encodes a WD40 protein involved in 18S ribosomal RNA biogenesis. Plant Cell 17: 2340-54.

Smith TF, Gaitatzes C, Saxena K, Neer EJ (1999) The WD repeat: a common architecture for diverse functions. Trends Biochem Sci 24: 181-5.

Tschochner H, Hurt E (2003) Pre-ribosomes on the road from the nucleolus to the cytoplasm. Trends Cell Biol 13: 255-63.

Tsukaya H (2002) Interpretation of mutants in leaf morphology: genetic evidence for a compensatory system in leaf morphogenesis that provides a new link between cell and organismal theories. Int Rev Cytol 217: 1-39.

Ullah H, Chen JG, Young JC, Im KH, Sussman MR, Jones AM (2001) Modulation of cell proliferation by heterotrimeric G protein in Arabidopsis. Science 292: 2066-9.

van Nocker S, Ludwig P (2003) The WD-repeat protein superfamily in Arabidopsis: conservation and divergence in structure and function. BMC Genomics 4: 50.

Wang H, Zhou Y, Gilmer S, Whitwill S, Fowke LC (2000) Expression of the plant cyclin-dependent kinase inhibitor ICK1 affects cell division, plant growth and morphology. Plant J 24: 613-23.

Weijers D, Franke-van Dijk M, Vencken RJ, Quint A, Hooykaas P, Offringa R (2001) An Arabidopsis Minute-like phenotype caused by a semi-dominant mutation in a RIBOSOMAL PROTEIN S5 gene. Development 128: 4289-99.

Whittaker CA, Hynes RO (2002) Distribution and evolution of von Willebrand/integrin A domains: widely dispersed domains with roles in cell adhesion and elsewhere. Mol Biol Cell 13: 3369-87.

Wigge PA, Weigel D (2001) Arabidopsis genome: life without notch. Curr Biol 11: R112-4.

Williams EJ (1955) Seed failure in the Chippewa variety of *Solanum tuberosum*. Bot. Gaz. 10: 10-15.

CHAPITRE IV :

The *MIDASIN* and *NOTCHLESS* genes are essential for female gametophyte development in *Arabidopsis*

Manuscrit soumis pour publication.

Sier-Ching Chantha[1,2], Madoka Gray-Mitsumune[1,3], Josée Houde[1] and Daniel P. Matton[1]*.

[1]Institut de Recherche en Biologie Végétale (IRBV), Département de sciences biologiques, Université de Montréal, 4101 rue Sherbrooke est, Montréal, QC, Canada, H1X 2B2.

[2]College of Agriculture, University of Hawaii at Hilo, 200 W Kawili street, Hilo, Hawaii 96720, United States.

[3]Biology Department, Concordia University, 7141 rue Sherbrooke ouest, Montréal, QC, Canada, H4B 1R6

Keywords: female gametophyte, embryo sac, gametogenesis, midasin, notchless, ribosome

*Author for correspondance:

Tel: 1-514-872-3967

Fax: 1-514-872-9406

Email: dp.matton@umontreal.ca

COAUTHORSHIP DECLARATION FOR AN ARTICLE

1. Student identification and academic program

Sier-Ching Chantha

Ph. D. Biology

2. Article description

Sier-Ching Chantha, Madoka Gray-Mitsumune, Josée Houde and Daniel P. Matton.. The *MIDASIN* and *NOTCHLESS* genes are essential for female gametogenesis in ***Arabidopsis***. To be submitted.

3. Coauthors declaration other than the student

As a coauthor of the above mentionned article, I agree that Sier-Ching Chantha includes this article in her Ph. D. thesis entitled " Caractérisation fonctionnelle des gènes *NOTCHLESS* et *MIDASIN* lors du développement végétal".

Madoka Gray-Mitsumune	[redacted]	Oct 13, 2006
Coauthor	Signature	Date

DÉCLARATION DES COAUTEURS D'UN ARTICLE

1. Identification de l'étudiant et du programme

Sier-Ching Chantha

Ph. D. Sciences biologiques

2. Article description

Sier-Ching Chantha, Madoka Gray-Mitsumune, Josée Houde and Daniel P. Matton. The *MIDASIN* and *NOTCHLESS* genes are essential for female gametogenesis in *Arabidopsis*. À soumettre.

3. Coauthors declaration other than the student

À titre de coauteure de l'article identifié ci-dessus, je suis d'accord pour que Sier-Ching Chantha inclue cet article dans sa thèse de doctorat qui a pour titre "Caractérisation fonctionnelle des gènes *NOTCHLESS* et *MIDASIN* lors du développement végétal".

Josée Houde [redacted] 13/10/06

Coauteure Date

DÉCLARATION DES COAUTEURS D'UN ARTICLE

1. Identification de l'étudiant et du programme

Sier-Ching Chantha

Ph. D. Sciences biologiques

2. Description de l'article

Sier-Ching Chantha, Madoka Gray-Mitsumune, Josée Houde and Daniel P. Matton. The *MIDASIN* and *NOTCHLESS* genes are essential for female gametogenesis in *Arabidopsis*. À soumettre.

3. Déclaration des coauteurs autres que l'étudiante

À titre de coauteur de l'article identifié ci-dessus, je suis d'accord pour que Sier-Ching Chantha inclue cet article dans sa thèse de doctorat qui a pour titre "Caractérisation fonctionnelle des gènes *NOTCHLESS* et *MIDASIN* lors du développement végétal".

Daniel P. Matton [redacted] 19 oct 2006

Coauteur Date

4.1. ABSTRACT

Female gametophyte development in *Arabidopsis thaliana* follows a well-defined program that involves many fundamental cellular processes. In this study, we report the involvement of the *Arabidopsis thaliana MIDASIN1* (*AtMDN1*) gene during female gametogenesis through the phenotypic characterization of plants heterozygous for an insertional *mdn1* mutant allele. The *MDN1* yeast ortholog (also known as *REA1*) has previously been shown to encode a non-ribosomal protein involved in the maturation and assembly of the 60S ribosomal subunit. Heterozygous *MDN1/mdn1* plants were semisterile and *mdn1* allele transmission was mainly affected through the female gametophyte. Differential interference microscopy revealed that development of *mdn1* female gametophytes was considerably delayed compared to their wild-type siblings. However, delayed *mdn1* female gametophytes were able to reach maturity and a delayed pollination experiment showed that a small proportion of the ovules were functional. We also report that the *Arabidopsis NOTCHLESS* (*AtNLE*) gene is also required for female gametogenesis. In yeast, the NLE protein has been previously shown to interact with MDN1 and to be also involved in 60S subunit biogenesis. The introduction of an *AtNLE*-RNA interference construct in *Arabidopsis* led to semisterility defects in 75% of the primary transformants generated due to ovule abortion. Defective female gametophytes were mostly arrested at the one-nucleate developmental stage. Both *AtMDN1* and *AtNLE* are expressed in similar patterns in all the sporophytic organs. These data, taken together, suggest that the activity of both *AtMDN1* and *AtNLE* is essential for female gametogenesis progression as well as throughout the sporophytic phase of plant development, which is consistent with a function in a basic cellular function such as ribosome biogenesis.

4.2. INTRODUCTION

The reproductive phase of the angiosperm life cycle is characterized by a short-lived and reduced gametophytic generation (haploid), which contrasts with the dominant sporophytic generation (diploid), represented by the flowering plant. Moreover, development of the male and female gametophytes mostly depends on the parent sporophyte, taking place enclosed within the anther and the ovule, respectively. The sporophytic structures first produce sexually differentiated spores through meiosis of diploid spore mother cells. Whereas numerous microspores are produced in the anther, only one functional megaspore survives in the ovule. Gametogenesis then initiates from the resulting haploid spores to give rise to the mature gametophytes by only a few mitotic divisions (Drews and Yadegari 2002; Brukhin et al. 2005). The mature male gametophyte, represented by the pollen grain, consists of three cells: a vegetative cell harboring two sperm cells (McCormick 1993). The mature female gametophyte, represented by the embryo sac, is of the *Polygonum* type in about 70% of flowering plant species, including *Arabidopsis* (Willemse and van Went 1984; Huang and Russell 1992; Drews and Yadegari 2002). This type of embryo sac arrangement consists of seven cells: the egg cell flanked by two synergids at the micropylar pole, three antipodals at the opposite chalazal pole, and a diploid central cell. The sperm cells of the pollen grain are transported via a pollen tube into the embryo sac to fertilize the egg cell and the central cell, which initiates the formation of an diploid embryo and a triploid endosperm respectively.

The female gametophyte develops according to a well-defined program that involves many fundamental cellular processes (Schneitz et al. 1995; Christensen et al. 1997). In *Arabidopsis*, the functional megaspore undergoes three rounds of mitosis without cytokinesis, during which the nuclei migrate to specific positions to produce an eight-nucleate coenocytic embryo sac. Subsequent cellularization as well as fusion of the two polar nuclei of the future central cell give rise to a mature seven-celled embryo sac, as described earlier. The three antipodals finally degenerate around

flower anthesis resulting in a four-celled embryo sac. Mutations disrupting one of these cellular processes are likely to affect female gametogenesis and show reduced transmission through the female gametophyte to the next sporophytic generation (Feldmann et al. 1997; Drews et al. 1998; Grossniklaus and Schneitz 1998). Mutants showing defects during female gametogenesis progression have been mostly isolated through genetic screens in *Arabidopsis* and the identified genes disrupted in these mutants are involved in diverse cellular functions (Feldmann et al. 1997; Christensen et al. 1998; Howden et al. 1998; Christensen et al. 2002; Drews and Yadegari 2002; Brukhin et al. 2005; Pagnussat et al. 2005). For example, the underexpression of the *ARABINOGALACTAN PROTEIN 18* (*AGP18*) gene by RNA interference leads to a defect in the transition of the megaspore to a female gametophytic developmental program (Acosta-Garcia and Vielle-Calzada 2004). Insertional mutations in *NOMEGA* (Kwee and Sundaresan 2003) and *ANAPHASE PROMOTING-COMPLEX 2* (*APC2*) (Capron et al. 2003), encoding two different components of the E3 ligase anaphase promoting complex/cyclosome (APC/C) involved in cell cycle progression, result in the arrest of female gametogenesis after the first nuclear division. Disruption of *PROLIFERA* (*PRL*), encoding a Mcm7-like licensing factor essential for DNA replication (Springer et al. 1995), and targeted degradation of the *CHROMATIN-REMODELING PROTEIN 11* (*CHR11*) transcripts through RNA interference (Huanca-Mamani et al. 2005) also cause a premature arrest in nuclear division. In the *slow walker 1* (*swa1*) mutant, which is disrupted in a gene encoding a component of the large nucleolar U3 complex required for 18S ribosomal RNA biogenesis, nuclear proliferation in the embryo sac is delayed and asynchronized (Shi et al. 2005). Mutant alleles of the plant retinoblastoma homologue *RBR1*, a negative regulator of cell division, lead to excessive nuclear proliferation in the female gametophyte (Ebel et al. 2004).

In the present study, we report that disrupting the expression of the *Arabidopsis MIDASIN1* (*AtMDN1*) gene, encoding an AAA ATPase and MIDAS domains containing protein, causes semisterility by causing a delay in female

gametophyte development. In *Saccharomyces cerevisiae*, MDN1/REA1 was identified with NLE/RSA4 in the same protein complexes as non-ribosomal factors participating in 60S ribosomal subunit maturation (Bassler et al. 2001; Gavin et al. 2002; Nissan et al. 2002). The wild potato *Solanum chacoense* ScMDN1 ortholog was recently shown to interact with ScNLE in yeast two-hybrid assays (Chantha et al. 2006). Consistent with an involvement in a common cellular process, the introduction of an *AtNLE*-RNA interference construct in *Arabidopsis* also leads to a semisterility defects caused by defects in female gametophyte development. The female gametogenesis defects caused by the *mdn1* mutation and the *AtNLE-RNAi* construct are consistent with a function in a basic cellular function such as ribosome biogenesis.

4.3. MATERIALS AND METHODS

4.3.1. Plant material and growth conditions

Plants were grown in a growth chamber at 20-22 °C under a 16 h light/8 h dark cycle. Columbia (Col) and Wassilewskija (Ws) ecotypes of *Arabidopsis thaliana* were used for *AtMDN1* and *AtNLE* characterization, respectively. Seeds collected from agro-infiltrated plants were surface sterilized in 70% ethanol and 0.05% Tween-20 for 5 min, followed by 3 washes in 95% ethanol, and allowed to dry completely under a sterile flow hood. Seeds were plated on MS medium (1/2X MS medium, 0.1% sucrose, 0.6% agar, pH 5.7) without antibiotic or supplemented with 25 μg/ml kanamycin and 100 μg/ml carbenicilline and stratified in darkness at 4 °C for 2 days. Seedlings were transferred to soil and grown in growth chambers in the same conditions as stated above.

4.3.2. Cloning of *AtNLE*

Total RNA (1 μg) extracted from flowers at anthesis from *Arabidopsis* WS ecotype was reverse-transcribed by using the First strand cDNA synthesis kit for RT-PCR (AMV) (Roche Diagnostics, Laval, Qc) with oligo-p$(dT)_{15}$ primer, according to the manufacturer's instructions.The *AtNLE* cDNA sequence was PCR-amplified with primers NleWS-1 (5'-ATTCACACAGGTCGTCTTTGCGAAGCTC-3') and NleWS-2 (5'- TCCACCGCAAAAACCTATCCACAACAATA-3'), designed based on the *AtNLE* Columbia sequence available in GenBank. PCR products corresponding to *AtNLE* expected size was extracted from agarose gel and cloned into the pCR®4-TOPO vector using the TOPO TA cloning kit (Invitrogen Canada, Burlington, ON).

4.3.3. Generation of *AtNLE-RNAi* lines

A 766 bp fragment of *AtNLE* from *Arabidopsis* WS ecotype was PCR amplified from cloned cDNA with the NLEWS3 primer (5'-GAGA**CTCGAGGGATCC**CAGGCGGAAGCTGTTCTTTG-3'), containing the XhoI and BamHI restriction sites, and the NLEWS4 primer (5'-GAGA**GGCGCGCCGGTACC**TACAAGCTGTTGATGACCGG-3'), containing the AscI and KpnI restriction sites. The PCR fragment was first cloned in the sense orientation using the BamHI and KpnI sites of the silencing pDarth vector (O'Brien et al. 2002). The resulting plasmid was then used for a second cloning of the same PCR fragment in the antisense orientation using the AscI and XhoI sites. The plasmid was introduced into *Agrobacterium tumefasciens* stain LBA4404 by electroporation. *Arabidopsis* plants (WS ecotype) were transformed using the vacuum infiltration method described in (Clough and Bent 1998) with slight modifications. One third of a 3 ml overnight pre-culture of *Agrobacterium* carrying the silencing plasmid was used to inoculate 200 ml YEP (1% yeast extract, 1% peptone, 0.5% NaCl, pH 7.0) supplemented with 50 μg/ml kanamycin at 28 °C until $OD_{600} > 1.2$. Cells were harvested by centrifugation at 5 500 rpm for 10 min and resuspended in 10 ml infiltration medium (1/2X MS medium, 5% sucrose, 44 nM benzylaminopurine, 0.02% Silwet L-77, pH 5.7) and volume was completed to 600 ml. A beaker containing the inoculum was placed in a vacuum chamber. Plants were inverted and immersed into the bacteria suspension such that the inflorescences were completely submerged. Vacuum was applied for about 5 min such that bubbles were drawn from plant tissues. Infiltrated plants were grown in a growth chamber at 22 °C under 16 h light and 8 h dark. Seeds were collected and selected for kanamycin resistance, as described above. Transformation with the *AtNLE-RNAi* construct was confirmed by PCR amplification using the primers described above.

4.3.4. Isolation and gel blot analysis of RNA

Total RNA extraction and RNA gel blot analysis procedures are described in (Lantin et al. 1999; Lagace et al. 2003). RNA for RT-PCR analysis of *AtNLE* RNAi lines was isolated using the RNeasy® plant mini kit (Qiagen, Mississauga, ON). For RNA gel blot analysis, 10 µg of total RNA for each tissue samples were separated on gel. Probes were derived from partial *ScMDN1* cDNA or full length *AtNLE* cDNA labelled with α-[^{32}P]-dATP (ICN Biochemicals, Irvine, CA) using the High Prime DNA Labeling kit (Roche Diagnostics, Laval, QC). A ^{32}P-labelled *18S* probe was used as a control. Membranes were exposed at –85°C with intensifying screens on Kodak Biomax MR film (Interscience, Markham, ON).

4.3.5. Segregation Analysis

Seeds collected from heterozygous *mdn1* self cross and reciprocal crosses between heterozygous *mdn1* mutant and wild type plants were germinated on MS medium as described above. Genomic DNA from seedlings were extracted and PCR amplified for genotyping using the REDExtract-N-Amp™ Plant PCR Kit (Sigma-Aldrich). Presence of the WT *AtMDN1* allele was determined by amplification with the primers Midas1 (5'-AACTTACAACCTGCCTGTTC-3') and Midas2 (5'-AGAATTCCATCAGACCAAGC-3'). Presence of the *mdn1* mutant allele containing the T-DNA insertion was determined by amplification with the primers LBb1 (5'-GCGTGGACCGCTTGCTGCAACT-3') and Midas2. PCR reactions were performed under the following conditions: 1 cycle of 94 °C / 4 min; 35 cycles of 94 °C / 30 sec, 54 °C / 30 sec, 72 °C / 1 min; 1 cycle of 72 °C / 4 min.

4.3.6. Histological analysis

Arabidopsis floral organs were cleared with methyl salicylate as described in (Estrada-Luna et al. 2004). Siliques were dissected longitudinally with hypodermic needles (1 ml insulin syringes). Cleared ovules were observed on a Zeiss Axioimager M1 microscope (Carl Zeiss Canada, Toronto, ON) under Normaski optics and images were acquired with a Zeiss AxioCam MR digital camera. All images were processed for publication using Adobe Photoshop CS (Adobe Systems, San Jose, USA).

4.3.7. DNA sequencing and sequence analysis

Approximately 200 ng (5 µl) of plasmid DNA and 15 µl of reaction mixture containing 8.5 µl of water, 3.5 µl 5X sequencing buffer, 2 µl primer at 0.8 µM, and 1 µl Big Dye Terminator Ready Reaction Mix (PE Applied Biosystems) was used for the sequencing reaction. Sequencing reactions were preformed on a GeneAmp PCR System 9700 (PE Applied Biosystems), and the cycling conditions were: 96 °C, 10 sec; 50 °C, 5 sec, 60 °C, 4 min for 25 cycles. DNA sequencing was performed on an Applied Biosystem ABI 310 automated sequencer. Sequence alignments were performed with the ClustalW module of the MacVector 7.2.3 software (Accelrys Inc., San Diego, CA). Database searches were conducted with the BLAST program on the National Center for Biotechnology Information web service (http://www.ncbi.nih.nlm.gov).

The GenBank accession number for the *AtMDN1* Columbia ecotype cDNA sequence is NM_105382. The *AtMDN1* gene corresponds to locus At1g67120 and the *AtNLE* gene to locus At5g52820.

4.4 RESULTS

4.4.1. AtMIDASIN1 sequence analysis

Arabidopsis thaliana MIDASIN1 (*AtMDN1*) is a single-copy gene and is located on chromosome 1 (locus At1g67120). Based on computer-predicted exon-intron boundaries, the *AtMDN1* coding region is comprised within 73 exons and consists of 16 011 bp (accession number NM_105382) (Figure 4-1A). Although ESTs covering small portions of this sequence have been found, the expression of the predicted complete sequence has not been confirmed experimentally. The *AtMDN1* gene is predicted to encode a huge protein of 5 337 amino acids and a calculated molecular weight of 584.7 kDa, which makes its yeast ortholog the largest protein in the yeast proteome (Garbarino and Gibbons 2002).

A BLAST search of publicly available protein databases revealed that AtMDN1 showed significant overall sequence similarities with sequences from *Saccharomyces cerevisiae* (also known as YLR106p or REA1) (25% identity, 39% similarity, accession no. NP_013207) and *Homo sapiens* (25% identity, 41% similarity, accession no. AAM77722). Although the complete sequence of other MDN1 plant orthologs were not available, comparison with the 816 aa C-terminal sequence of *Solanum chacoense* ScMDN1 (Chantha et al. 2006) revealed about 45% identity and 59% similarity with the corresponding C-terminal part (covering 832 aa) of the *Arabidopsis* AtMDN1 sequence. The MDN1 protein comprises two highly conserved domains: an AAA ATPase domain in its N-terminal region and a MIDAS domain at its C-terminus (Figure 4-1B) (Garbarino and Gibbons 2002). Degrees of sequence identities and similarities for these domains between *Arabidopsis* MDN1 and some orthologs are shown in figure 4-1B. Proteins containing AAA ATPase and MIDAS domains are involved in diverse cellular processes and frequently function in multiprotein complexes (Whittaker and Hynes 2002; Iyer et al. 2004). The AAA

domain of MDN1 consists of six tandem ATPase domains, referred as AAA protomers, each characterized by several conserved motifs important for ATP sensing, binding, and hydrolysis (Figure 4-1C) (Garbarino and Gibbons 2002; Iyer et al. 2004). The AAA protomers are thought to fold altogether into a hexameric ring that changes in conformation upon ATP binding and hydrolysis (Garbarino and Gibbons 2002; Iyer et al. 2004). The MIDAS domain binds metal ions via a set of conserved sequence motifs that form a metal ion-dependent adhesion site (MIDAS) and is thought to mediate protein-protein interactions (Figure 4-1D) (Whittaker and Hynes 2002).

MDN1 was shown to be localized in the nucleus of yeast cells (Garbarino and Gibbons 2002). Analysis of the AtMDN1 amino acid sequence with the PredictNLS server [http://cubic.bioc.columbia.edu] revealed one potential nuclear localization signal, which is represented by a cluster of basic residues RKRKK (residues 791-795) located in the AAA domain. AtMDN1, like its yeast ortholog, is most probably localized to the nucleus.

4.4.2. The *mdn1* insertional mutant allele caused female semisterility

In order to define the function of *AtMDN1* during plant development, we analyzed the phenotypes associated with a T-DNA insertion mutant in the Columbia ecotype (Salk_057010) obtained from the Arabidopsis Biological Resource Center (ABRC) (Alonso et al. 2003). The T-DNA insertion site was estimated to be located within exon 27 of *AtMDN1* in the SIGnal database (http://signal.salk.edu/cgi-bin/tdnaexpress). This location was confirmed by PCR amplification using gene specific primers in combination with a T-DNA left border primer (data not shown). The T-DNA is predicted to disrupt the AAA-domain of AtMDN1 (Figure 4-1A, B), which is essential for the catalytic activity of the protein (Iyer et al. 2004), therefore rendering the AtMDN1 protein non-functional. The T-DNA insertional *AtMDN1*

mutant allele is referred to as *mdn1* and was used here for further analysis. Plants were individually genotyped by PCR amplification since the kanamycin resistance marker comprised in the T-DNA was suppressed, an effect that can be obtained after several generations of growth (http://signal.salk.edu).

None of the parental plants was homozygous for *mdn1*, suggesting that the mutant allele could not be fully transmitted through the gamethophytes and/or caused seed lethality. Heterozygous *MDN1/mdn1* plants showed no visible abnormalities in vegetative growth or development when compared to WT plants, which is expected for diploid lines carrying a recessive mutation. However, siliques produced by *MDN1/mdn1* plants were somehow shorter than the WT because of reduced seed set (Figure 4-2A, B). Quantitative determination of seed production showed that WT siliques were associated with nearly full seed set (5.1% ovule abortion) while *MDN1/mdn1* siliques produced normal seeds as well as small and whitish ovules, representing signs of ovule abortion, in about equal proportions (Figure 4-2B, D). Crosses between *MDN1/mdn1* pistils and pollen from WT anthers produced siliques bearing about 50% aborted ovules while crosses between WT pistils and pollen from *MDN1/mdnl* anthers led to almost full seed set (Figure 4-2D). These results confirm that the semisterility phenotype observed in *MDN1/mdnl* plants is attributable to the female reproductive organs.

4.4.3. The *mdn1* mutation affects predominantly the female gametophyte

Semisterility originating from ovule abortion in a heterozygous mutant is often indicative of a gametophytic mutation affecting the development or a reproductive function of the female gametophyte (Feldmann et al. 1997; Drews et al. 1998; Grossniklaus and Schneitz 1998). In the case of a fully penetrant female-specific gametophytic mutation, the expected segregation ratio of presence to absence of the *mdn1* allele in the progeny is 1:1, as the pollen grains of a heterozygous plant

carry either the *mdn1* or the *MDN1* allele and both types should fertilize in equal proportions WT female gametophytes exclusively, the *mdn1* female gametophytes being nonfunctional. Several female gametophytic mutations are, however, not specific and affect both female and male gametophytes, and as a consequence, show a segregation ratio lower than 1:1 (Drews and Yadegari 2002). We determined that the segregation ratio of the *mdn1* allele in the F1 progeny of selfed *MDN1/mdn1* plants was 1:2.4 (*MDN1/mdn1:MDN1/MDN1*) (n = 136) (Table 4-1). This distorted segregation ratio significantly lower than 1:1 suggests that *mdn1* is a general gametophytic mutation that affects the development and/or the reproductive function of both female and male gametophytes.

To determine to which extent the respective gametophytes were affected by *mdn1* in their ability to transmit their genes to the next generation, we analyzed the transmission efficiency of the *mdn1* allele through either sex in the progeny of reciprocal crosses between *MDN1/mdn1* and WT plants. Transmission efficiency (TE) of the *mdn1* allele was significantly reduced through the male gametophyte (TE_{male}=66.7%, n=94) but was more strongly reduced through the female gametophyte (TE_{female}=10.4%, n=170) (Table 4-1). These data indicate that the *mdn1* allele affects more severely the female gametophyte than the male gametophyte and that the *mdn1* allele is mainly transmitted to the progeny by the male gametophyte. Despite a significant transmission of the *mdn1* allele through both gametophytes, homozygous plants were not recovered from the progeny of selfed *MDN1/mdn1* plants, suggesting that the *mdn1* mutation may also cause embryonic lethality.

4.4.4. Female gametophyte development is impaired by the *mdn1* mutation

To investigate which aspect of female gametophyte development or reproductive function is compromised in *MDN1/mdn1* plants, we first analyzed by differential interference contrast (DIC) microscopy the phenotype of female

gametophytes in cleared ovules at flower anthesis. Female gametophyte developmental stages (FG) are defined according to Christensen et al. (1997) and flower development stages are defined according to Smyth et al. (1990). Developmental studies in *Arabidopsis* have shown that female gametogenesis in ovules comprised within one individual pistil is fairly synchronous and this synchrony allows the use of the WT female gametophytes of a pistil to predict the developmental stage of the mutant gametophytes within the same pistil (Christensen et al. 1997; Shi et al. 2005).

Among the female gametophytes examined from *MDN1/mdn1* pistils at flower anthesis (stage 13), about half were at the seven-celled (FG6) or four-celled (FG7) stages (Figure 4-3A and B; Table 4-2) while the other half covered a variety of earlier developmental stages, mostly including two-nucleate stage (FG3), four-nucleate stage (FG4), and eight-nucleate stages (FG5) (Figure 4-3C-E; Table 4-2). Because about half of the ovules were aborted in *MDN1/mdn1* siliques, it is likely that female gametophytes at the seven-celled (FG6) and four-celled (FG7) stages were WT whereas female gametophytes at earlier developmental stages bear the *mdn1* allele. Therefore, the *mdn1* mutation would affect female gametophyte development by retarding or arresting its development rather than affecting one of its reproductive function.

Despite the reduced transmission of the *mdn1* allele through the male gametophyte, although not as severely as through the female gametophyte, no obvious defects in pollen grain morphology could be detected in *MDN1/mdn1* anthers by DIC microscopy when compared to the WT (Figure 4-3F).

4.4.5. *mdn1* female gametophyte development is delayed and can progress to maturity

To determine whether the *mdn1* female gametophytes were arrested during the nuclear division stages or were delayed during their development and could further progress to the mature stage (FG7), we analyzed ovules from pistils at a later flower developmental stage. *MDN1/mdn1* pistils at about 30 hours after flowering (HAF) contained young developing seeds and small ovules in about equal proportions (Figure 4-2A). The developing seeds examined mostly contained octant stage embryos and some quadrant embryos (Figure 4-4E; Table 4-2), while undeveloped ovules from the same pistils contained female gametophytes at different developmental stages (Figure 4-4A-D; Table 4-2). These comprised two-nucleate stage (FG3), four-nucleate stage (FG4), eight-nucleate stage (FG5), seven-celled stage (FG6), and four-celled stage (FG7). About half of these delayed female gametophytes were at the four-celled stage (FG7) (Table 4-2) and showed a normal cellular constitution, with two synergids, one egg-cell, and a central cell (Figure 4-4D). Therefore, the *mdn1* mutation would primarily cause a delay rather than an arrest in female gametophyte development since a fraction of them can progress to maturity.

4.4.6. Delayed pollination of *MDN1/mdn1* pistils increased seed set

As a consequence of a slower development, the *mdn1* female gametophytes would not be mature when fertilization normally takes place in WT ovule siblings and hence remained unfertilized and eventually aborted. As shown above, several delayed *mdn1* female gametophytes can reach maturity and are likely to be functional. Also, as mentioned above, a small proportion of the female gametophytes can transmit the *mdn1* allele to their progeny (Table 4-1) and could possibly represent *mdn1* female gametophytes that reached maturity after a short delay and got fertilized. If this is the case, we could expect that the *mdn1* allele would be transmitted to the progeny in higher proportions when pollination time is delayed. To test this hypothesis, a delayed pollination experiment was performed with a strict

control on emasculation and pollination time. *MDN1/mdn1* flowers at stage 12b (Christensen et al. 1997) were emasculated and pistils were pollinated with pollen from WT anthers 24h (stage 13) and 48h (stage 14-15) after emasculation (Smyth et al. 1990). Seeds obtained from at least three independent plants for each pollination time were collected and scored for the presence of the *mdn1* allele. We determined that while 5% (10:190, *n*=200) of the progeny from the 24h group segregated the *mdn1* allele, 15.5% (31:169, *n*=200) of the progeny from the 48h group segregated the *mdn1* allele. These results suggest that *mdn1* female gametophytes are not defective in their ability of being fertilized but are rather impaired in their developmental progression, which is delayed compared to their WT siblings.

4.4.7. Expression of an *AtNLE* interference construct in transgenic plants caused female semisterility

Previous yeast two-hybrid screens have shown that the *Solanum chacoense* MDN1 (ScMDN1) ortholog interacts with the WD-repeat NOTCHLESS (ScNLE) protein (Chantha et al. 2006) and tandem affinity purification assays in yeast have isolated both proteins as components of the same pre-60S ribosomal protein complexes (Bassler et al. 2001; Gavin et al. 2002; Nissan et al. 2002). We therefore wanted to determine if the *AtNLE* gene acts in the same developmental pathway as the *AtMDN1* gene in *Arabidopsis*. Because no insertional mutation in the *AtNLE* gene could be identified, an *AtNLE* RNA interference (RNAi) construct was generated and used to transform WT *Arabidopsis* Wassilewskija (WS) ecotype to generate silencing of endogenous gene activity (Figure 4-5A). From the 21 primary transformants obtained, none showed any visible vegetative growth or developmental defects. However, several independant *AtNLE-RNAi* lines produced shorter siliques than the WT due to high levels of ovule abortion. Quantitative analysis revealed that 16 of the primary lines showed ovule abortion levels ranging on average from about 15% to almost 100% (Figure 4-5B) while WT plants showed about 9%. This semisterility

phenotype was maintained in the next generation for all the lines analysed. Crosses between *AtNLE-RNAi* pistils and pollen from WT anthers produced similar ovule abortion levels as in *AtNLE-RNAi* self crosses, while crosses between WT pistils and pollen from *AtNLE-RNAi* anthers led to almost full seed set (data not shown). These results therefore suggest that the semisterility phenotype observed in *AtNLE-RNAi* plants is attributable to the female reproductive organs.

4.4.8. Female gametophyte development is impaired in *AtNLE* RNAi lines

To investigate the nature of the developmental defect associated with the expression of the *AtNLE-RNAi* construct, we analyzed cleared ovules isolated from pistils of two transformed lines, *AtNLEi-3* and *AtNLEi-26*, that showed respectively an average of about 45% and 85% ovule abortion levels. We noticed in all the *AtNLE-RNAi* lines analyzed that the semisterility phenotype decreased in severity over time, as plants were getting older. For example, the first siliques produced by the *AtNLEi-26* line showed 100% aborted ovules while siliques produced later during inflorescence development contained a few seeds. Since the semisterility phenotype was maintained over the following generation for all the lines tested (data not shown), the transgene could in all cases be sexually transmitted to the descendants. The partial recovery from the semisterility phenotype could be attributable to progressive transcriptional silencing of the *AtNLE-RNAi* transgene itself, hence reducing RNA interference effectiveness over time (Kerschen et al. 2004). We first analyzed ovules from flowers at anthesis (stage 13) and defined the trend in female gametophyte developmental stages in data presented in Table 4-3. In WT siliques, the majority (~ 95 %) of ovules carried female gametophytes at the four-nucleate (FG4) stage or later, with the eight-nucleate (FG5) stage being predominant. In ovules of *AtNLEi*-3 siliques, less than 30% of the female gametophytes were at the four-nucleate (FG4) stage or later while the remaining ones were at earlier developmental stages. Among these delayed female gametophytes, the one-nucleate (FG1) was predominant (Figure

4-5C). As for *AtNLEi-26* siliques, the proportion of ovules bearing female gametophytes at the four-nucleate (FG4) stage or later was even lower (~ 16%) than in the *AtNLEi-3* line. Delayed female gametophytes in the *AtNLEi-26* line were mostly at the one-nucleate (FG1) stage and, in addition, some were at the megaspore forming stage (FG0) (Figure 4-5D) or degenerated (Figure 4-5E). In both *AtNLEi-3* and *AtNLEi-26* lines, some female gametophytes could reach the mature stage (FG7) and had a normal embryo sac morphology. These results suggest that the *AtNLE-RNAi* construct caused a delay or an arrest in female gametophyte development.

To better understand the female gametophyte developmental defect in *AtNLE-RNAi* lines, we also analyzed cleared ovules from siliques at later developmental stages, after pollination occurred and presented the scores of female gametophyte developmental stages in Table 4-3. In WT ovules, the majority (more than 95%) of the female gametophytes had reached the eight-nucleate (FG5) stage or later, with the seven-celled (FG7) stage being predominant. In ovules of *AtNLEi-3* siliques, about half of the female gametophytes were at the eight-nucleate (FG5) stage or later. The remaining half were at earlier developmental stages, being predominantly at around the one-nuclear (FG1) stage or degenerated. As for *AtNLEi-26* siliques, only about 25% of the female gametophytes reached the eight-nucleate (FG5) or later stages. As in the *AtNLEi-3* line, delayed female gametophytes of the *AtNLEi-26* line were mostly at the one-nucleate stage (FG1) and a considerable proportion was degenerated. Both *AtNLEi-3* and *AtNLEi-26* siliques also comprised some ovules bearing fertilized embryo sacs. Also for these lines, the proportion of delayed female gametophyte observed is consistent with the frequency of ovule abortion reported above. Taken altogether, these results suggest that the *AtNLE-RNAi* construct caused a developmental arrest early during female gametophyte formation, mostly at the one-nuclear (FG1) stage, and a higher proportion of degenerated embryo sacs.

4.4.9. *AtMDN1* and *AtNLE* are expressed throughout the plant

If MDN1 and NLE interact with each other *in planta*, we would expect their expression domains in plant organs to overlap. Gene expression patterns obtained from publicly accessible databases (Zimmermann et al. 2004) showed that both *AtMDN1* and *AtNLE* are ubiquitously expressed and show very similar expression profiles (Figure 4-6). *AtNLE* is however consistently expressed at higher levels than *AtMDN1*, being at least three times more abundant in all plant organs, except in the ovary where they are expressed at similar levels. Highest expression levels for both genes were found in tissues containing actively dividing cells, such as callus, shoot apex, radicle and hypocotyl. In flower organs more specifically, both *AtMDN1* and *AtNLE* were more highly expressed in the carpel. The constitutive and overlapping expression patterns of *AtMDN1* and *AtNLE* was confirmed by gel blot analysis performed on total RNAs isolated from various plant tissues (data not shown).

4.5. DISCUSSION

In *Saccharomyces cerevisiae*, MDN1 (also known as REA1) and NLE (known as RSA4) were identified as non-ribosomal factors in the same pre-60S ribosomal complexes (Bassler et al. 2001; Gavin et al. 2002; Nissan et al. 2002). Biogenesis of the 60S subunit is a highly coordinated process that progress from the nucleolus to the cytoplasm and that involves the participation of more than 70 trans-acting factors for the maturation of ribosomal RNAs and their assembly with ribosomal proteins (Fatica and Tollervey 2002; Fromont-Racine et al. 2003; Tschochner and Hurt 2003). Ribosome biogenesis was mostly characterized in yeast but most of the trans-acting factors identified, including MDN1/REA1 and NLE/RSA4 (Chantha et al. 2006), are well conserved in higher eukaryotes and ribosome biogenesis pathway is therefore expected to be similar in plants, animals and fungi (Fatica and Tollervey 2002; Fromont-Racine et al. 2003; Tschochner and Hurt 2003). The *Solanum chacoense* orthologs ScMDN1 and ScNLE were recently shown to interact together in two-hybrid assays, which brings support to the conservation of 60S subunit biogenesis process in plants (Chantha et al. 2006). In this study, we report the functional characterization of the *AtMDN1* and *AtNLE* genes in *Arabidopsis* and show their involvement in female gametogenesis.

The *MDN1* gene encodes a huge protein comprising a AAA ATPase domain in the N-terminal region and a MIDAS domain involved in protein interactions at its C-terminus (Garbarino and Gibbons 2002; Whittaker and Hynes 2002). Plant heterozygous for the *mdn1* insertional mutation showed a semisterility phenotype due to ovule abortion. The *mdn1* allele mainly impaired female gametogenesis. Analysis of cleared ovules at different floral developmental stages revealed that the development of *mdn1* female gametophytes was delayed compared to their WT siblings but could still progress to maturity. Moreover, our delayed pollination experiment showed that a small fraction of the *mdn1* female gametophytes could become functional and get fertilized. Interestingly, plants heterozygous for an

insertional mutation in the *SLOW WALKER1* (*SWA1*) gene, which encodes a trans-acting factor involved in 40S ribosomal subunit biogenesis, caused a similar delay in female gametogenesis in *Arabidopsis*, with some delayed *swa1* female gametophytes becoming mature and functional (Shi et al. 2005). These data altogether suggest that the *AtMDN1* gene is required for normal progression of female gametogenesis.

Additional observations revealed that the *AtMDN1* gene is involved in other aspects of plant development. Reciprocal crosses showed that *AtMDN1* activity is also required for male gametogenesis, although at a lesser extent than for female gametogenesis. The milder effect of *mdn1* on the male gametophyte could be explained by functional redundancy of the *AtMDN1* gene in the male gametophyte. This could also be explained by the lower number of cell cycles involved in male gametophyte development, being two compared to three for female gametogenesis, if residual *AtMDN1* activity meiotically is inherited from the diploid spore mother cell. Evidences for the requirement of *AtMDN1* function is during plant sporophytic development were also provided. No homozygous *mdn1* plant was recovered from self crosses although the *mdn1* allele could be partially transmitted through both male and female gametophytes. Furthermore, *AtMDN1* was constitutively expressed throughout the plant, with higher expression levels in young tissues.

The identification of both NLE/Rsa4p and MDN1/REA1 in 60S ribosomal subunit biogenesis in yeast (Nissan et al. 2002; Galani et al. 2004) and their interaction in plants (Chantha et al. 2006), suggested their involvement in similar aspect of female gametophyte development. Since no insertional line could be identified for the *AtNLE* gene, we analyzed *Arabidopsis* plants transformed with an *AtNLE-RNAi* construct. Variable expression levels of endogenous *AtNLE* transcript were observed, although none of the lines showed an important change in *AtNLE* transcript accumulation. However, the majority (~ 75%) of the primary transformed lines shared a semisterility phenotype with each line showing specific ovule abortion levels. This phenotype is also consistent with the semisterility phenotype reported

previously in transgenic *Solanum chacoense* plants underexpressing the *ScNLE* gene (Chantha et al. 2006). Moreover, the semisterility phenotype was maintained in the following generation. Previous studies reported that RNA interference is not always associated to detectable reduction in targeted gene transcript levels (Kerschen et al. 2004) and that levels of residual targeted gene transcript are not necessarily correlated to the degree of phenotype severity (Acosta-Garcia and Vielle-Calzada 2004; Chantha et al. 2006). In cleared ovules of the *AtNLE-RNAi* lines analyzed, female gametophytes in proportions corresponding to levels of aborted ovules were either degenerated or arrested at early developmental stages, including as early as during the megaspore forming stage (FG0) and with a predominance at the one-nucleate (FG1) stage. Therefore, *AtNLE* function is required from megaspore forming stages during the process of the female gametophyte formation.

Several lines of evidence suggest that the *AtNLE-RNAi* construct affected female gametophyte development from the sporophytic level. As shown for *AtMDN1*, *AtNLE* was constitutively expressed throughout the plant with highest expression levels in tissues containing actively dividing cells. Moreover, several of the generated *AtNLE-RNAi* lines produced siliques with 100% ovule abortion levels, indicating that the semisterility defect could not solely be caused by *AtNLE-RNAi* expression in the female gametophyte. Since no morphological defects were observed in the sporophytic structures of the ovules, the sporophytic effect of the *AtNLE-RNAi* is likely here not physical. One possible explanation for the sporophytic contribution to the female gametogenesis defect induced by *AtNLE-RNAi* is that normal *AtNLE* activity in ovule sporophytic tissues, such as in the megaspore mother cell, could be required for female gametophyte development. Another possibility would be that products generated by RNA interference from double-stranded *AtNLE* transcript accumulation in the sporophytic cells could cause post-transcriptional gene silencing in the megaspore and the developing female gametophyte, as was suggested previously (Acosta-Garcia and Vielle-Calzada 2004). RNA interference products could either be transmitted during meiosis of the megaspore mother cell or be

transported through plasmodesmata to the functional megaspore. The presence of plasmodesmata connecting the functional megaspore and the adjacent sporophytic nucellar cells creates an active communication bridge between these structures (Bajon et al. 1999). Variability in ovule abortion levels associated to the different defective *AtNLE-RNAi* lines could be caused by variability in the penetrance of RNA interference in each line. Deciphering more precisely the functional contribution of gametophytic versus sporophytic *AtNLE* activity in female gametogenesis will required the use of specific promoters to drive the expression of the *AtNLE-RNAi* line in the female gametophyte.

As mentioned above, the defects in female gametogenesis produced in heterozygous *mdn1* and *AtNLE-RNAi* lines were different, being somehow more severe in *AtNLE-RNAi* lines than in the *mdn1* mutant. This phenotypic difference can be explained in several ways. Although NLE/Rsa4p and MDN1/REA1 were involved in the same cellular process in yeast, they do not accomplish the same function during 60S subunit biogenesis and their respective function may not be equally essential. In yeast, while NLE/RSA4 represents one of the few trans-acting factors involved in all the maturation steps of the 60S ribosomal subunit, from early on in the nucleolus to the final maturation steps in the cytoplasm (Nissan et al. 2002), MDN1/REA1 is only involved in late nucleoplasmic pre-60S complexes that are close to their export to the cytoplasm (Galani et al. 2004). Another explanation could be that the function of NLE/Rsa4p and/or MDN1/REA1 may not be restricted to 60S subunit biogenesis, as was determined for other 60S trans-acting factors (Tschochner and Hurt 2003). In animals, the *NLE* gene was shown to be involved in the regulation of the Notch receptor activity (Royet et al. 1998; Cormier et al. 2006). The phenotypic difference could also be attributable to the different nature of the transformed lines studied. The developmental function of *AtMDN1* was analyzed through an heterozygous mutant line in which the WT allele could compensate for the non-functional mutant allele in sporophytic diploid cells. Residual *AtMDN1* activity provided by heterozygous diploid megaspore mother cell could therefore contribute to female gametophyte

development. The function of *AtNLE* was on the other hand analyzed through transformation with a *AtNLE* RNA interference and, as discussed above, activity of *AtNLE-RNAi* in sporophytic cells affected female gametophyte development.

The requirement of *MDN1* and *NLE* for normal female gametogenesis progression is consistent with data obtained from yeast and plant. In yeast, both MDN1/REA1 and NLE/RSA4 are essential since mutations in these genes lead to cell lethality while depletion of both proteins causes a significant slow growth phenotype (Galani et al. 2004; de la Cruz et al. 2005). Underexpression of *ScNLE* in *Solanum chacoense* by RNA interference was previously shown to cause a pleiotropic phenotype during plant sporophytic development, the major defect being the production of smaller organs due to reduced cell proliferation and cell enlargement (Chantha et al. 2006). However, unlike the sporophytic phenotype generated in *S. chacoense ScNLE*-RNA interference lines, no sporophytic defect was observed in *Arabidopsis AtNLE-RNAi* lines. This discrepancy could be explained by RNA interference showing different levels of effectiveness on the *NLE* gene in the sporophytic tissues of these two plant species. While clear reduction in *ScNLE* transcript levels were detected in *S. chacoense* transformants (Chantha et al. 2006), this was not the case for *AtNLE* transcripts in *Arabidopsis* transformants. Another explanation could be that *Arabidopsis* sporophytic development is more sensitive to changes in *AtNLE* expression levels and could not survive to an important reduction in transcript levels. These sporophytic developmental defects altogether with female gametogenesis defects suggest an essential function of both *MDN1* and *NLE* for normal cellular progression.

To date, very few ribosomal trans-acting factors have been characterized for their function during plant growth and development. Available genetic studies on a few ribosomal trans-acting factors in plants however point to their importance in diverse aspect of female gametophyte development. For example, an insertional mutation in the *Arabidopsis* ortholog of yeast Nop10, a trans-acting factor involved in

ribosomal RNA modifications during ribosomal biogenesis (Henras et al. 1998), causes the production of female gametophyte with unfused polar nuclei (Pagnussat et al. 2005). An insertional mutation in *SWA1*, encoding a trans-acting factor involved 40S ribosomal subunit biogenesis, causes a delay of female gametogenesis (Shi et al. 2005). Our data indicate that *AtMDN1* and *AtNLE*, encoding orthologs of yeast 60S ribosomal subunit trans-acting factors, are also essential for the normal progression of female gametogenesis in *Arabidopsis*.

4.6. ACKNOWLEDGEMENTS

We thank Dr. Michael Shintaku for generously providing lab space and equipment for carrying experiments from which some data published in this paper were obtained. This work was supported by the Natural Sciences and Engineering Research Council of Canada (NSERC) and from the Canada Research Chair program. S. C. Chantha is a recipient of Ph. D. fellowships from NSERC and from Le Fonds Québécois de la Recherche sur la Nature et les Technologies (FQRNT, Québec). D. P. Matton holds a Canada Research Chair in Functional Genomics and Plant Signal Transduction.

Table 4-1. Transmission efficiency (TE) of the *mdn1* allele

Parental genotypes female x male	Genotype of F_1 plants			TE*
	MDN1/mdn1	*MDN1/MDN1*	*mdn1/mdn1*	
MDN1/mdn1 X *MDN1/mdn1*	40	96	0	-
MDN1/mdn1 X *MDN1/MDN1*	16	154	-	10.4 %
MDN1/MDN1 X *MDN1/mdn1*	38	57	-	66.7 %

Seeds from each cross were collected and germinated. These F1 plants were then tested for *mdn1* allele transmission by PCR using a combination of gene-specific and T-DNA left border specific primers as described in methods.
*TE = (Number of mutant plants/number of wild-type plants) x 100%, through female or male gametes.

Table 4-2. Stages of female gametophyte or embryo development in *MDN1/mdn1* pistils

Floral stage	Pistil no.	Female gametophyte stages							Embryo stages		Total no.
		FG1	FG2	FG3	FG4	FG5	FG6	FG7	4-cell	8-cell	
Anthesis (stage 13)	A1				2	3	2	4			11
	A2			3	6	1	4	5			19
	A3			3	6	4	5	7			25
	A4		1	4	5	5	7	6			28
30 HAF	P1						3	2	1	5	11
	P2			1		1	3	4	1	11	20
	P3			1		1	3	5	3	8	21
	P4			1	1	1	4	7	4	9	27

Pistils from four different *MDN1/mdn1* plants were collected at the specified developmental stages and cleared. Ovules were dissected and analyzed by DIC for female gametophyte developemental stage determination.

Table 4-3. Stages of female gametophyte development in *AtNLE-RNAi* pistils at flower anthesis (A) and after pollination (P)

Line	Pistil no.*	Deg.	Female gametophyte stages									Total
			FG0	FG1	FG2	FG3	FG4	FG5	FG6	FG7	FG8	
WT	A1						2	9	4		3	18
	A2				1	1	3	14	2	1		22
iNle 3	A1			13	9	3	5	3				33
	A2	1		16	2			14		1		34
iNle 26	A1			11	1	3	4	1		4	2	26
	A2	2	5	17	7	2	3					36
	A3	2		21	2	5	1					31
WT	P1						1	7	5	23	10	46
	P2					1				12	6	19
	P3						1	5	5	24	8	43
iNle 3	P1	2		6	1	2		1		6	5	23
	P2		3		3						11	17
	P3	8		11	1			1			18	39
iNle 26	P1	7		8			1	1		3	1	21
	P2	5		19	3	3	2	9				41
	P3	4	4	11	2	2	2			6	2	33

Pistils were collected at the specified developmental stages and cleared.
Ovules were dissected and analyzed by DIC for female gametophyte developemental stage determination.
*A, refers to pistils collected at flower anthesis and; P, refers to the second pollinated pistil produced before the flower at anthesis stage.

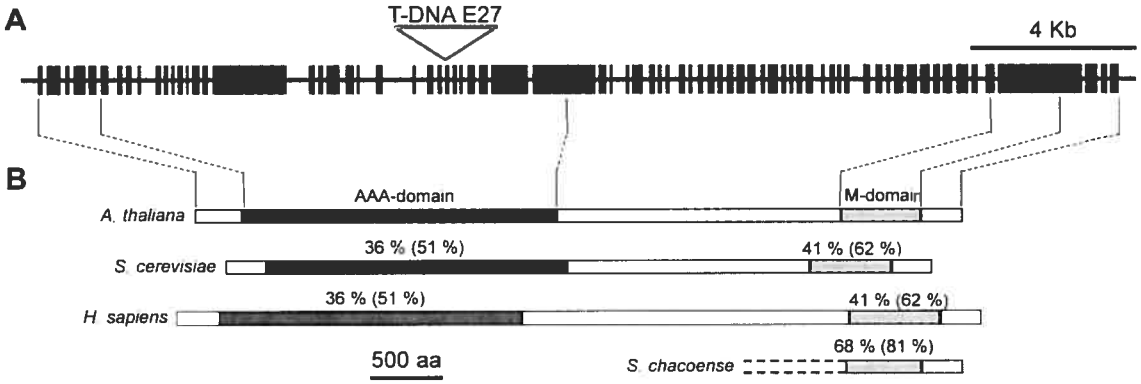
A
T-DNA E27
4 Kb
B
AAA-domain
M-domain
A. thaliana
36 % (51 %)
41 % (62 %)
S. cerevisiae
36 % (51 %)
41 % (62 %)
H. sapiens
500 aa
68 % (81 %)
S. chacoense

C

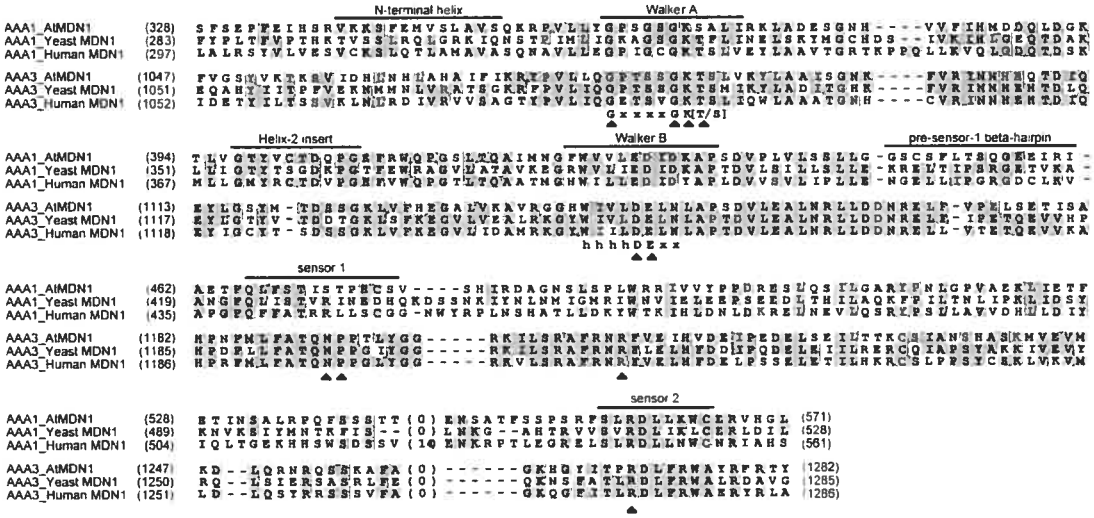
N-terminal helix
Walker A
Helix-2 insert
Walker B
pre-sensor-1 beta-hairpin
sensor 1
sensor 2
AAA1_AtMDN1
AAA1_Yeast MDN1
AAA1_Human MDN1
AAA3_AtMDN1
AAA3_Yeast MDN1
AAA3_Human MDN1

D

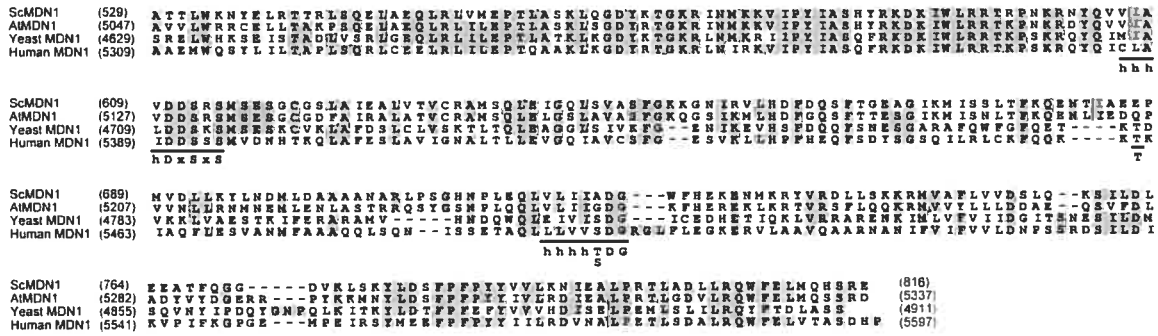
ScMDN1
AtMDN1
Yeast MDN1
Human MDN1

Figure 4-1. Genomic structure of AtMDN1, protein organization and sequence alignment of MDN1 orthologs. (A) Genomic organization of the *AtMDN1* gene and position of the T-DNA insertion. Exons are shown as black boxes and introns are represented by gray lines. The T-DNA is inserted in exon 27, resulting in the interruption of the AAA-domain. (B) Schematic diagrams of MDN1 protein orthologs. The AAA-domain and the MIDAS-domain are represented by dark gray and light gray boxes respectively. Sequence identities and similarities (brackets) between the AAA-domain and the MIDAS-domain of Arabidopsis MDN1 and orthologs (*Saccharomyces cerevisiae*, *Homo sapiens*, *Solanum chacoense*) are indicated above the corresponding boxes. (C) Amino acid sequence alignment of selected AAA1 and AAA3 promoters of the AAA-domain of MDN1 orthologs. Conserved motifs that characterize members of AAA ATPase family are shown above the alignement. Consensus sequences are indicated under the alignment. Critical residues involved in ATP sensing, binding and hydrolysis are identified by arrowheads. Colors indicating level of consensus apply to sequence conservation for a single AAA promoter and not to comparison between different AAA promoters. (D) Amino acid sequence alignment of the MIDAS-domain of MDN1 orthologs. Sequence motifs are underlined and consensus sequences are indicated under the alignment. In (C) and (D), sequence identity is highlighted in dark gray and similarity in light gray, dashes indicate gaps introduced to maximize homology, h indicates hydrophobic residues, x represents any residues.

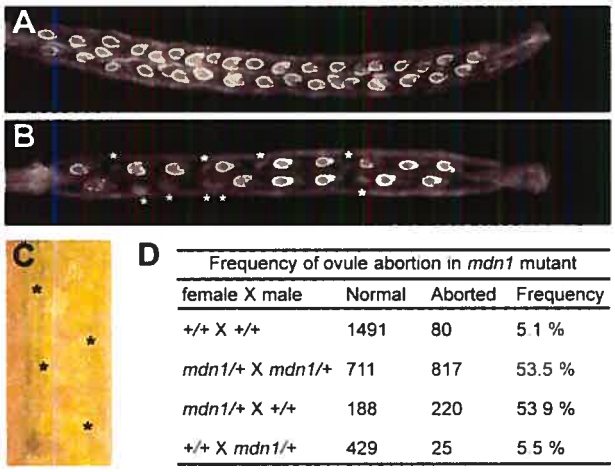

D

Frequency of ovule abortion in *mdn1* mutant			
female X male	Normal	Aborted	Frequency
+/+ X +/+	1491	80	5.1 %
mdn1/+ X *mdn1*/+	711	817	53.5 %
mdn1/+ X +/+	188	220	53.9 %
+/+ X *mdn1*/+	429	25	5.5 %

Figure 4-2. Semisterility in *MDN1/mdn1* mutant. (A, B) Cleared pollinated pistils around 30 hours after flowering. (A) WT pistil showing full seed set. (B) *MDN1/mdn1* pistil. The asterisks indicate the aborted ovules. About half of the siblings develop into seeds. (C) Mature *MDN1/mdn1* silique. The asterisks show small and white aborted ovules. (D) Frequency of ovule abortion in *MDN1/mdn1* mutant. Mature siliques obtained from crosses were opened and scored for the ovule abortion phenotype and mature seed production.

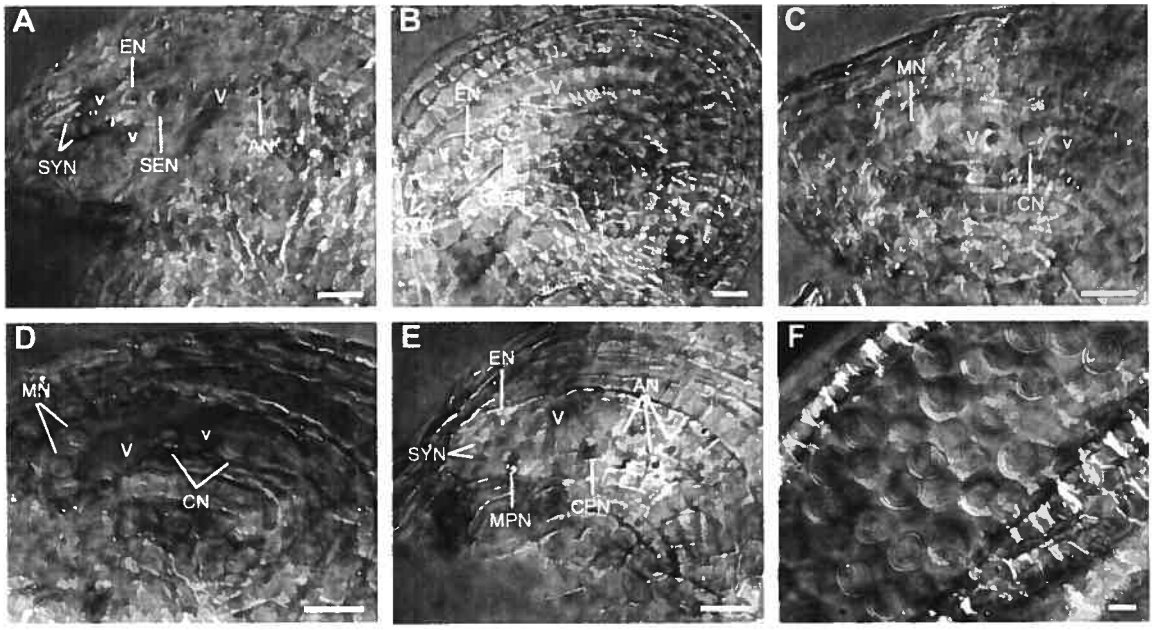

Figure 4-3. Female gametophyte and pollen grain development in *MDN1/mdn1* flowers at anthesis revealed by differential interference contrast (DIC) microscopy on cleared whole-mount preparations. (A) A female gametophyte at seven-celled stage FG6. Two synergid nuclei (SYN), an egg cell nucleus (EN), a prominent secondary endosperm nucleus (SEN), and three antipodal nuclei (AN) represent the seven cells forming the embryo sac at this stage. The central vacuole (V) and the smaller vacuoles (v) of the synergids are visible. (B) A female gametophyte at four-celled stage FG7. The antipodal cells have degenerated compared to stage FG6 (A). (C) A female gametophyte at stage FG3. A chalazal nucleus (CN) and micropylar nucleus (MN) are separated by a large central vacuole (V). A smaller vacuole (v) is present at the chalazal pole. (D) A female gametophyte at late stage FG4. Two chalazal nuclei (CN) and two micropylar nuclei (MN) are separated by a large central vacuole (V). A smaller vacuole (v) separates the two chalazal nuclei. (E) A female gametophyte at stage FG5. Three antipodal nuclei (AN) are at the chalazal pole while two synergid nuclei (SYN) and an egg cell nucleus are at the micropylar pole. The chalazal polar nucleus (CPN) and the micropylar polar nucleus (MPN) are migrating toward each other. (F) Pollen grains of a *MDN1/mdn1* anther. In all panels, female gametophytes are orientated with the micropylar pole left and the chalazal pole right. Bars = 10 μm.

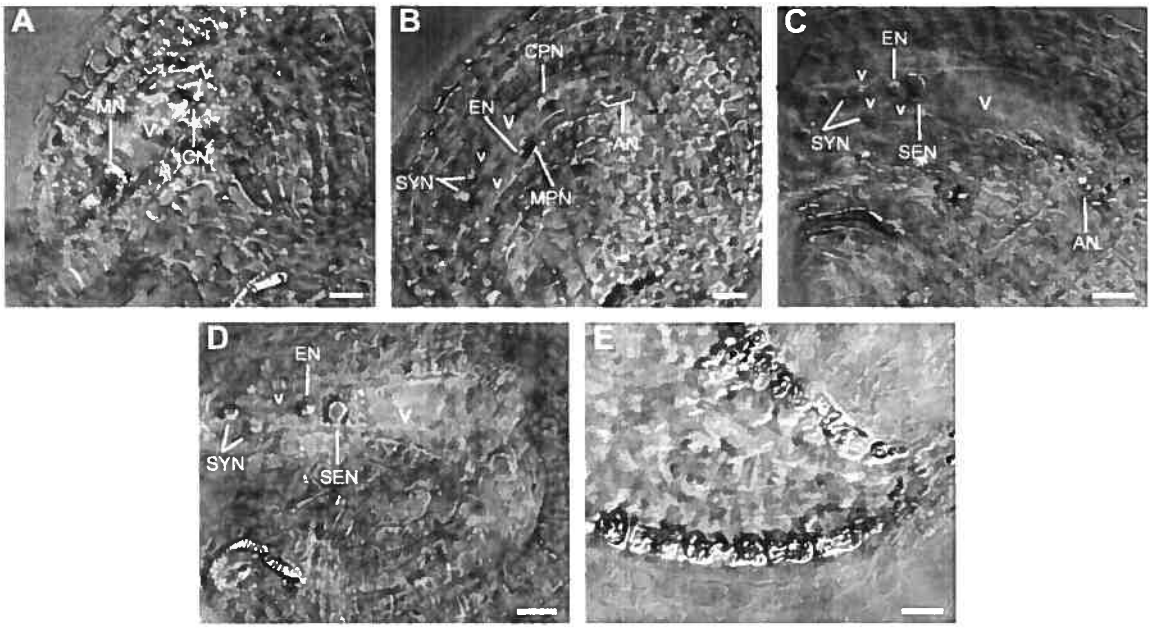

Figure 4-4. Female gametophyte development *MDN1/mdn1* pistils 30 hours after flowering revealed by differential interference contrast (DIC) microscopy of cleared whole-mount preparations. (A) A female gametophyte at stage FG3. A chalazal nucleus (CN) and micropylar nucleus (MN) are separated by a large central vacuole (V). A smaller vacuole (v) is present at the chalazal pole. (B) A female gametophyte at early stage FG5. Three antipodal nuclei (AN) are at the chalazal pole while two synergid nuclei (SYN) and an egg cell nucleus (EN) are at the micropylar pole. The chalazal polar nucleus (CPN) and the micropylar polar nucleus (MPN) are migrating toward each other. (C) A female gametophyte at early seven-celled stage FG6. Recent fusion of the polar nuclei gives the secondary endosperm nucleus (SEN) an elongated shape. (D) A female gametophyte at four-celled stage FG7. (E) WT seed containing an embryo at octant stage. In all panels, female gametophytes are orientated with the micropylar pole on the left and the chalazal pole on the right. Bars = 10 μm.

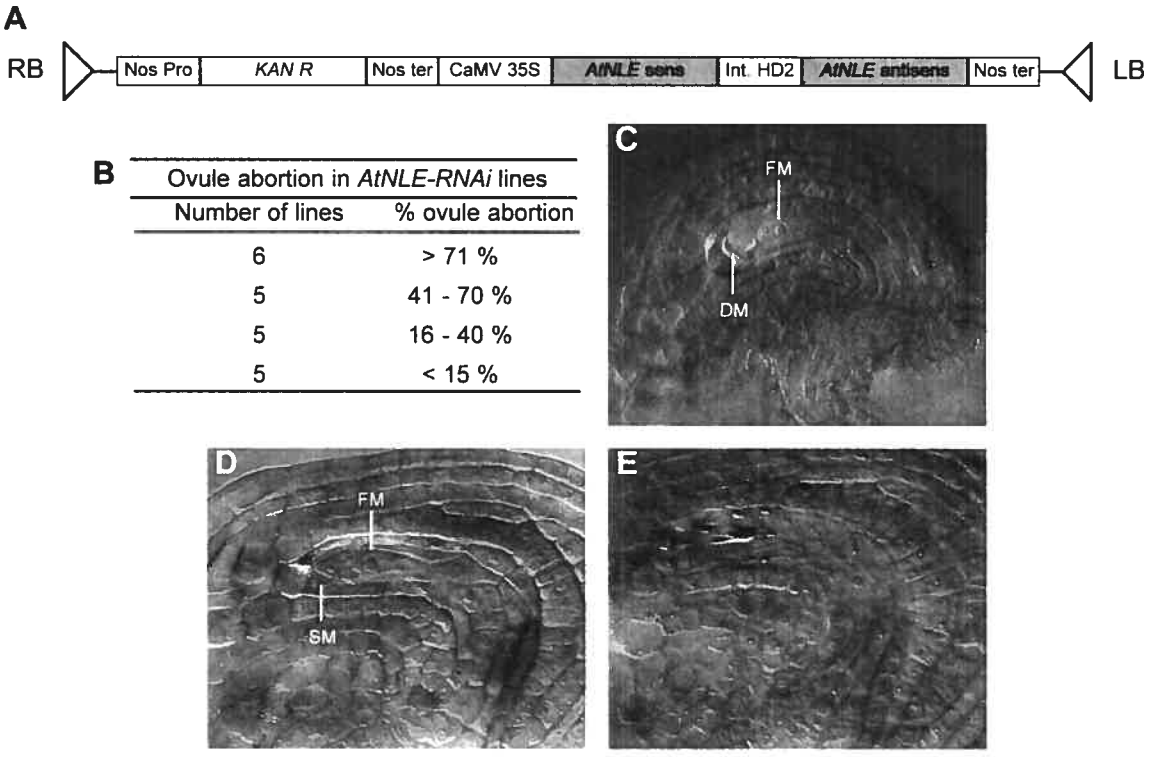

Figure 4-5. *AtNLE-RNAi* construct and ovule abortion levels and female gametophyte developmental defects in *AtNLE-RNAi* pistils at anthesis. (A) Schematic diagram of the *AtNLE* RNA interference construct used to generate post-transcritional gene silencing in transformed Arabidopsis lines. (B) Levels of ovule abortion observed in *AtNLE-RNAi* primary transformant lines. (C) Female gametophyte at stage FG1 from a *AtNLEi-3* pistil. FM, functional megaspore; DM, degenerated megaspores. (D) Female gametophyte at stage FG0 from a *AtNLEi-26* pistil. FM, functional megaspore; SM, sister megaspore during degeneration process. (E) Degenerated embryo sac from a *AtNLEi-26* pistil.

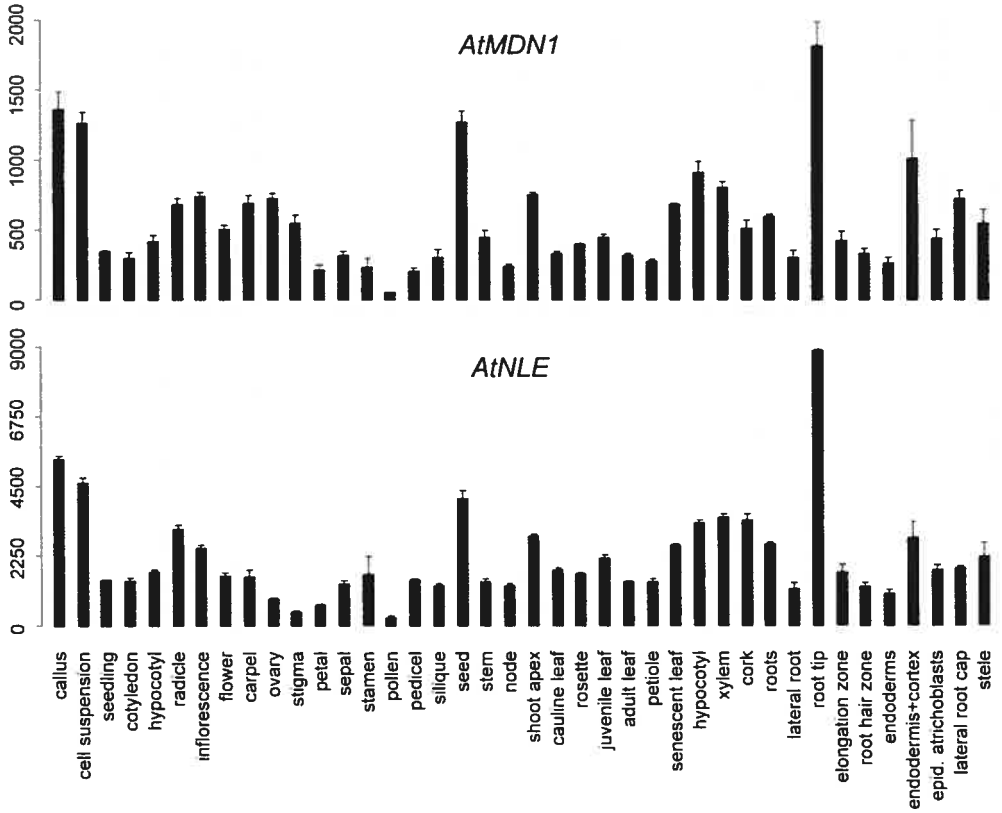

Figure 4-6. *AtMDN1* and *AtNLE* expression profiles in different plant organs and tissues as generated by the GeneAtlas tool of the GENEVESTIGATOR *Arabidopsis* microarray database. Signal intensity values are indicated on the left.

4.7. REFERENCES

Acosta-Garcia, G. and Vielle-Calzada, J.P. 2004. A classical arabinogalactan protein is essential for the initiation of female gametogenesis in Arabidopsis. *Plant Cell* **16**(10): 2614-2628.

Alonso, J.M., Stepanova, A.N., Leisse, T.J., Kim, C.J., Chen, H., Shinn, P., Stevenson, D.K., Zimmerman, J., Barajas, P., Cheuk, R., Gadrinab, C., Heller, C., Jeske, A., Koesema, E., Meyers, C.C., Parker, H., Prednis, L., Ansari, Y., Choy, N., Deen, H., Geralt, M., Hazari, N., Hom, E., Karnes, M., Mulholland, C., Ndubaku, R., Schmidt, I., Guzman, P., Aguilar-Henonin, L., Schmid, M., Weigel, D., Carter, D.E., Marchand, T., Risseeuw, E., Brogden, D., Zeko, A., Crosby, W.L., Berry, C.C., and Ecker, J.R. 2003. Genome-wide insertional mutagenesis of *Arabidopsis thaliana*. *Science* **301**(5633): 653-657.

Bajon, C., Horlow, C., Motamayor, J.C., Sauvanet, A., and Robert, D. 1999. Megasporogenesis in *Arabidopsis thaliana* L.: An ultrastructural study. *Sexual Plant Reproduction* **12**: 99-109

Bassler, J., Grandi, P., Gadal, O., Lessmann, T., Petfalski, E., Tollervey, D., Lechner, J., and Hurt, E. 2001. Identification of a 60S preribosomal particle that is closely linked to nuclear export. *Mol Cell* **8**(3): 517-529.

Brukhin, V., Curtis, M.D., and Grossniklaus, U. 2005. The angiosperm female gametophyte: no longer the forgotten generation. *Current Science* **89**(11): 1844-1852.

Capron, A., Serralbo, O., Fulop, K., Frugier, F., Parmentier, Y., Dong, A., Lecureuil, A., Guerche, P., Kondorosi, E., Scheres, B., and Genschik, P. 2003. The Arabidopsis anaphase-promoting complex or cyclosome: molecular and genetic characterization of the APC2 subunit. *Plant Cell* **15**(10): 2370-2382.

Chantha, S., Emerald, B., and Matton, D. 2006. Characterization of the plant Notchless homolog, a WD repeat protein involved in seed development. *Plant Molecular Biology* **in press**.

Christensen, C.A., Gorsich, S.W., Brown, R.H., Jones, L.G., Brown, J., Shaw, J.M., and Drews, G.N. 2002. Mitochondrial GFA2 is required for synergid cell death in Arabidopsis. *Plant Cell* **14**(9): 2215-2232.

Christensen, C.A., King, E.J., Jordan, J.R., and Drews, G.N. 1997. Megagametogenesis in Arabidopsis wild-type and *Gf* mutant. *Sexual Plant Reproduction* **10**: 49-64.

Christensen, C.A., Subramanian, S., and Drews, G.N. 1998. Identification of gametophytic mutations affecting female gametophyte development in Arabidopsis. *Dev Biol* **202**(1): 136-151.

Clough, S.J. and Bent, A.F. 1998. Floral dip: a simplified method for Agrobacterium-mediated transformation of Arabidopsis thaliana. *Plant J* **16**(6): 735-743.

Cormier, S., Le Bras, S., Souilhol, C., Vandormael-Pournin, S., Durand, B., Babinet, C., Baldacci, P., and Cohen-Tannoudji, M. 2006. The murine ortholog of notchless, a direct regulator of the notch pathway in Drosophila melanogaster, is essential for survival of inner cell mass cells. *Mol Cell Biol* **26**(9): 3541-3549.

de la Cruz, J., Sanz-Martinez, E., and Remacha, M. 2005. The essential WD-repeat protein Rsa4p is required for rRNA processing and intra-nuclear transport of 60S ribosomal subunits. *Nucleic Acids Res* **33**(18): 5728-5739.

Drews, G.N., Lee, D., and Christensen, C.A. 1998. Genetic analysis of female gametophyte development and function. *Plant Cell* **10**(1): 5-17.

Drews, G.N. and Yadegari, R. 2002. Development and function of the angiosperm female gametophyte. *Annu Rev Genet* **36**: 99-124.

Ebel, C., Mariconti, L., and Gruissem, W. 2004. Plant retinoblastoma homologues control nuclear proliferation in the female gametophyte. *Nature* **429**(6993): 776-780.

Estrada-Luna, A.A., Garcia-Aguilar, M., and Vielle-Calzada, J.-P. 2004. Female reproductive development and pollen tube growth in diploid genotypes of *Solanum cardiophyllum* Lindl. *Sexual Plant Reproduction* **17**(3): 117-124.

Fatica, A. and Tollervey, D. 2002. Making ribosomes. *Curr Opin Cell Biol* **14**(3): 313-318.

Feldmann, K.A., Coury, D.A., and Christianson, M.L. 1997. Exceptional segregation of a selectable marker (KanR) in Arabidopsis identifies genes important for gametophytic growth and development. *Genetics* **147**(3): 1411-1422.

Fromont-Racine, M., Senger, B., Saveanu, C., and Fasiolo, F. 2003. Ribosome assembly in eukaryotes. *Gene* **313**: 17-42.

Galani, K., Nissan, T.A., Petfalski, E., Tollervey, D., and Hurt, E. 2004. Real, a dynein-related nuclear AAA-ATPase, is involved in late rRNA processing and nuclear export of 60 S subunits. *J Biol Chem* **279**(53): 55411-55418.

Garbarino, J.E. and Gibbons, I.R. 2002. Expression and genomic analysis of midasin, a novel and highly conserved AAA protein distantly related to dynein. *BMC Genomics* **3**(1): 18.

Gavin, A.C., Bosche, M., Krause, R., Grandi, P., Marzioch, M., Bauer, A., Schultz, J., Rick, J.M., Michon, A.M., Cruciat, C.M., Remor, M., Hofert, C., Schelder, M., Brajenovic, M., Ruffner, H., Merino, A., Klein, K., Hudak, M., Dickson, D., Rudi, T., Gnau, V., Bauch, A., Bastuck, S., Huhse, B., Leutwein, C., Heurtier, M.A., Copley, R.R., Edelmann, A., Querfurth, E., Rybin, V., Drewes, G., Raida, M., Bouwmeester, T., Bork, P., Seraphin, B., Kuster, B., Neubauer, G., and Superti-Furga, G. 2002. Functional organization of the yeast proteome by systematic analysis of protein complexes. *Nature* **415**(6868): 141-147.

Grossniklaus, U. and Schneitz, K. 1998. The molecular and genetic basis of ovule and megagametophyte development. *Semin Cell Dev Biol* **9**(2): 227-238.

Henras, A., Henry, Y., Bousquet-Antonelli, C., Noaillac-Depeyre, J., Gelugne, J.P., and Caizergues-Ferrer, M. 1998. Nhp2p and Nop10p are essential for the function of H/ACA snoRNPs. *Embo J* **17**(23): 7078-7090.

Howden, R., Park, S.K., Moore, J.M., Orme, J., Grossniklaus, U., and Twell, D. 1998. Selection of T-DNA-tagged male and female gametophytic mutants by segregation distortion in Arabidopsis. *Genetics* **149**(2): 621-631.

Huanca-Mamani, W., Garcia-Aguilar, M., Leon-Martinez, G., Grossniklaus, U., and Vielle-Calzada, J.P. 2005. CHR11, a chromatin-remodeling factor essential for nuclear proliferation during female gametogenesis in Arabidopsis thaliana. *Proc Natl Acad Sci U S A* **102**(47): 17231-17236.

Huang, B.-Q. and Russell, S.D. 1992. Female germ unit: organization, isolation, and fonction. *Int Rev Cytol* **140**: 233-292.

Iyer, L.M., Leipe, D.D., Koonin, E.V., and Aravind, L. 2004. Evolutionary history and higher order classification of AAA+ ATPases. *J Struct Biol* **146**(1-2): 11-31.

Kerschen, A., Napoli, C.A., Jorgensen, R.A., and Muller, A.E. 2004. Effectiveness of RNA interference in transgenic plants. *FEBS Lett* **566**(1-3): 223-228.

Kwee, H.S. and Sundaresan, V. 2003. The *NOMEGA* gene required for female gametophyte development encodes the putative APC6/CDC16 component of the Anaphase Promoting Complex in Arabidopsis. *Plant J* **36**(6): 853-866.

Lagace, M., Chantha, S.C., Major, G., and Matton, D.P. 2003. Fertilization induces strong accumulation of a histone deacetylase (HD2) and of other chromatin-remodeling proteins in restricted areas of the ovules. *Plant Mol Biol* **53**(6): 759-769.

Lantin, S., O'Brien, M., and Matton, D.P. 1999. Pollination, wounding and jasmonate treatments induce the expression of a developmentally regulated pistil dioxygenase at a distance, in the ovary, in the wild potato Solanum chacoense Bitt. *Plant Mol Biol* **41**(3): 371-386.

McCormick, S. 1993. Male Gametophyte Development. *Plant Cell* **5**(10): 1265-1275.

Nissan, T.A., Bassler, J., Petfalski, E., Tollervey, D., and Hurt, E. 2002. 60S pre-ribosome formation viewed from assembly in the nucleolus until export to the cytoplasm. *Embo J* **21**(20): 5539-5547.

O'Brien, M., Kapfer, C., Major, G., Laurin, M., Bertrand, C., Kondo, K., Kowyama, Y., and Matton, D.P. 2002. Molecular analysis of the stylar-expressed *Solanum chacoense* small asparagine-rich protein family related to the HT

modifier of gametophytic self-incompatibility in Nicotiana. *Plant J* **32**(6): 985-996.

Pagnussat, G.C., Yu, H.J., Ngo, Q.A., Rajani, S., Mayalagu, S., Johnson, C.S., Capron, A., Xie, L.F., Ye, D., and Sundaresan, V. 2005. Genetic and molecular identification of genes required for female gametophyte development and function in Arabidopsis. *Development* **132**(3): 603-614.

Royet, J., Bouwmeester, T., and Cohen, S.M. 1998. Notchless encodes a novel WD40-repeat-containing protein that modulates Notch signaling activity. *Embo J* **17**(24): 7351-7360.

Schneitz, K., Hülskamp, M., and Pruitt, R.E. 1995. Wild-type ovule development in *Arabidopsis thaliana*: a light microscope study of cleared whole-mount tissue. *Plant Journal* **7**(5): 731-749.

Shi, D.Q., Liu, J., Xiang, Y.H., Ye, D., Sundaresan, V., and Yang, W.C. 2005. *SLOW WALKER1*, essential for gametogenesis in Arabidopsis, encodes a WD40 protein involved in 18S ribosomal RNA biogenesis. *Plant Cell* **17**(8): 2340-2354.

Smyth, D.R., Bowman, J.L., and Meyerowitz, E.M. 1990. Early flower development in Arabidopsis. *Plant Cell* **2**(8): 755-767.

Springer, P.S., McCombie, W.R., Sundaresan, V., and Martienssen, R.A. 1995. Gene trap tagging of PROLIFERA, an essential MCM2-3-5-like gene in Arabidopsis. *Science* **268**(5212): 877-880.

Tschochner, H. and Hurt, E. 2003. Pre-ribosomes on the road from the nucleolus to the cytoplasm. *Trends Cell Biol* **13**(5): 255-263.

Whittaker, C.A. and Hynes, R.O. 2002. Distribution and evolution of von Willebrand/integrin A domains: widely dispersed domains with roles in cell adhesion and elsewhere. *Mol Biol Cell* **13**(10): 3369-3387.

Willemse, M.T.M. and van Went, J.L. 1984. The female gametophyte. in *Embryology of Angiosperms* (ed. B.M. Johri, ed.), pp. 159-196. Springer-Verlag, Berlin.

Zimmermann, P., Hirsch-Hoffmann, M., Hennig, L., and Gruissem, W. 2004. GENEVESTIGATOR. Arabidopsis microarray database and analysis toolbox. *Plant Physiol* **136**(1): 2621-2632.

CHAPITRE V :
DISCUSSION GÉNÉRALE

5.1. Le gène *NOTCHLESS* code pour une protéine à WD-repeat évolutivement conservée chez les eucaryotes

Les protéines à WD-repeat (WDR) forment une grande famille de protéines presqu'exclusivement eucaryotiques (Neer et al. 1994; Smith et al. 1999). Dans le génome d'*Arabidopsis*, 237 protéines à WDR ont été répertoriées et classées par analyse de séquence en 143 sous-familles, desquelles une majorité présente une homologie évidente avec des protéines de la levure, de la drosophile et/ou de l'humain (van Nocker and Ludwig 2003). Cette conservation évolutive à travers les eucaryotes suggère que plusieurs protéines à WDR sont des composantes de la machinerie cellulaire commune aux champignons, aux animaux et aux végétaux (Smith et al. 1999; van Nocker and Ludwig 2003). Des protéines à WDR ont été identifiées dans une gamme étendue de processus cellulaires, comprenant entre autres exemples la transduction de signal, la dégradation des protéines, la modification de la chromatine, la transcription des gènes et la modification des ARN ribosomaux et messagers (Smith et al. 1999; van Nocker and Ludwig 2003).

En contraste à cette grande diversité fonctionnelle, les protéines à WDR sont unifiées par un module commun qui est le motif WD-repeat (WDR), aussi connu sous les noms de β-transducin repeat, WD-40 repeat et GH-WD repeat (Neer et al. 1994). Le motif WDR se défini comme étant une séquence de 44 à 66 acides aminés (aa) caractérisée par la présence habituelle d'un dipeptide GH (glycine-histidine) à environ 20 aa de l'extrémité N-terminale et d'un dipeptide WD (tryptophane-aspartate) à l'extrémité C-terminale. Cette unité WDR est répétée en tandem de

quatre (4) à seize (16) fois à l'intérieur d'une protéine et l'ensemble des unités WDR (le domaine WDR) adopte une structure en forme d'hélice, dans laquelle le nombre de pales reflète le nombre d'unités WDR (Wall et al. 1995; Lambright et al. 1996; Sondek et al. 1996). Cette structure servirait de plateforme rigide pour la formation de complexes protéiques, soit pour la coordination d'interactions réversibles avec plusieurs ensembles de protéines ou en tant que composante intégrale de complexes protéiques plus stables (Smith et al. 1999; van Nocker and Ludwig 2003). Bien que certaines protéines à WDR sont constituées exclusivement d'unités WDR, la majorité possèdent cependant des extensions N-terminale et/ou C-terminale rattachées au domaine WDR et/ou une insertion dans la domaine WDR, conférant une spécificité fonctionnelle à la protéine (Neer et al. 1994; Smith et al. 1999).

Chez les végétaux, les protéines à WDR jusqu'à présent caractérisées ont été impliquées dans plusieurs aspects du cycle de développement de la plante. Ces processus de développement inclus par exemple la photomorphogénèse (*COP1*, (Osterlund et al. 1999)), la régulation de la voie de l'auxine (*AGB1*, (Ullah et al. 2003)), le développement floral (*LUG*, (Conner and Liu 2000)), le développement des gamétophytes (*SWA1*, (Shi et al. 2005), et l'initiation du développement de l'albumen de la graine (*FIE*, *MSI1* (Chaudhury et al. 1997; Ohad et al. 1999; Kohler et al. 2003a)). Cependant, les fonctions de la majorité des membres de la famille des protéines à WDR sont encore inconnues. NOTCHLESS (NLE) représente un exemple d'une protéine à WDR dont la fonction cellulaire était jusqu'à présent mal comprise et dont le rôle lors du développement de la plante était inconnu. Il a été déterminé dans cette présente étude que le gène *NLE* existe en une seule copie dans les génomes de *Solanum chacoense* (fig. 2-1B, p.60), et d'*Arabidopsis thaliana*. La protéine NLE représente de plus le seul membre de sa sous-famille (van Nocker and Ludwig 2003), étant composée d'un domaine WDR à huit unités WDR et d'une extension N-terminale, nommée domaine Notchless (Nle) et de fonction inconnue (fig. 2-1A, p.60) (Royet et al. 1998). Les séquences en acide aminé des homologues de NLE identifiés chez diverses espèces tant fongiques qu'animales et végétales sont hautement

conservées (fig. 2-1A, p.60) (Royet et al. 1998). Il a été de plus démontré dans cette étude qu'une surexpression du gène *NLE* de *Solanum chacoense* (*ScNLE*) ou de *Drosophila melanogaster* (*DmNLE*) dans la drosophile affectent de façon similaire la formation des poils sensoriels sur le thorax (fig. 2-1C, p.60), indiquant que les protéines ScNLE et DmNLE fonctionnent de façon similaire. Ainsi, la conservation évolutive de NLE chez plusieurs espèces eucaryotes de plus qu'un fonctionnement analogue des protéines ScNLE et DmNLE suggèrent une conservation de la fonction moléculaire de la protéine NLE chez les eucaryotes.

5.2. NOTCHLESS et la biogenèse de la sous-unité ribosomale 60S

L'homologue de NLE chez la levure, connu sous les noms de YCR072cp et RSA4cp, a été identifiée récemment comme étant une protéine non-ribosomale impliquée dans la biogenèse de la sous-unité 60S du ribosome (Bassler et al. 2001; Nissan et al. 2002; Saveanu et al. 2003; Nissan et al. 2004; de la Cruz et al. 2005). Le ribosome, qui représente la machinerie de traduction des ARNm en protéines, est assemblé à partir des sous-unités ribosomales 40S et 60S lors de l'initiation de la traduction et est composé au total de plus de 70 protéines ribosomales et de quatre différents types d'ARN ribosomaux (ARNr) (Fatica and Tollervey 2002; Fromont-Racine et al. 2003; Tschochner and Hurt 2003). La biogenèse des sous-unités ribosomales a été en majeure partie caractérisée chez la levure *Saccharomyces cerevisiae* et est un processus hautement coordonné qui débute dans le nucléole, évolue à travers le nucléoplasme et les pores de l'enveloppe nucléaire pour finalement se terminer dans le cytoplasme. Tout au long de cette progression, une multitude de complexes riboprotéiques intermédiaires, dont la composition en protéines ribosomales et en espèces d'ARNr évolue, sont successivement générés. Pour la biogenèse de la sous-unité ribosomale 60S particulièrement, plus de 70 protéines non-ribosomales sont requises pour orchestrer la maturation des ARNr à partir de leurs précurseurs, leur assemblage aux protéines ribosomales ainsi que le transport intracellulaire des complexes pré-60S. Certains de ces facteurs possèdent une activité

enzymatique connue, tel que des endonucléases et exoribonucléases, des ARN hélicases et des méthylases, mais la fonction précise de la plupart des protéines non-ribosomales dans de ce processus cellulaire est toujours indéterminée (Fromont-Racine et al. 2003). La purification biochimique de quelques complexes pré-60S a cependant permis d'établir l'ordre d'association des protéines non-ribosomales aux complexes pré-60S ainsi que l'aspect souvent transitoire de leur association (Bassler et al. 2001; Harnpicharnchai et al. 2001; Saveanu et al. 2001; Fatica et al. 2002; Nissan et al. 2002; Saveanu et al. 2003).

Dans cette présente étude, l'utilisation de deux systèmes de double-hybride de la levure (*yeast two-hybrid system*), le système nucléaire GAL4 et le système cytoplasmique *Sos Recruitment*, a permis d'associer NLE à la biogenèse de la sous-unité 60S du ribosome chez les végétaux également. Les recherches de candidats effectués avec le domaine Nle ou le domaine WDR séparément, ou encore la protéine ScNLE entière, ont mené à l'isolement d'homologues des protéines MIDASIN1 (MDN1, REA1 ou YLR106p) et Nop Seven Associated 2 (NSA2 ou YER126p) de la levure (fig. 3-5, p.107). Tout comme NLE/RSA4p, MDN1 (Bassler et al. 2001; Nissan et al. 2002; Nissan et al. 2004) et NSA2 (Harnpicharnchai et al. 2001; Fatica et al. 2002) sont des protéines non-ribosomales qui participent à la biogenèse de la sous-unité ribosomale 60S chez la levure et concordent ainsi vers une fonction cellulaire commune. La pertinence des interactions entre ces protéines est de plus supportée par le fait que NLE/RSA4p ait été identifiée à plusieurs reprises dans les mêmes complexes protéiques que NSA2 (Nissan et al. 2002; Saveanu et al. 2003) et/ou MDN1/REA1p (Bassler et al. 2001; Nissan et al. 2002; Nissan et al. 2004) par purification d'affinité en tandem (*tandem affinity purification*) chez la levure. La conservation de la majorité des composantes de la voie de synthèse des ribosomes, incluant NLE/RSA4p (fig. 2-1A, p.60), MDN1 (fig. 4-1B, C, p.146) et NSA2, chez les eucaryotes indique par ailleurs que le mécanisme d'assemblage du ribosome soit évolutivement conservé chez les animaux, les végétaux et la levure (Fatica and Tollervey 2002; Tschochner and Hurt 2003). Les gènes *NLE* et *MDN1* montrent de

plus des profils d'expression très similaires dans les organes de *S. chacoense* (fig. 2-2, p.62; 3-6, p.108) et d'*Arabidopsis* (fig. 4-6, p.152).

La purification par affinité utilisée chez la levure afin d'isoler des complexes pré-60S a permis de définir leur composition sans toutefois établir des interactions directes entre chacune de ses composantes. Une interaction possiblement directe entre ScNLE et ScMDN1 a été définie dans cette étude, notamment par l'utilisation d'un système de double-hybride cytoplasmique (*Sos Recruitment*). Dans ce système, les interactions protéiques se produisent à l'extérieur du noyau et donc à l'écart de la majorité des protéines non-ribosomales endogènes de la levure, limitant ainsi leur intervention possible dans l'interaction ScNLE-ScMDN1. Cette interaction impliquerait le domaine Nle de ScNLE (fig. 3-5B, p.107), alors que le domaine WDR de ScNLE semble pour sa part interagir avec ScNSA2. Puisque ScMDN1 représente la principale protéine à avoir été isolée dans les deux systèmes de double-hybride utilisés, celle-ci a fait l'objet d'une caractérisation plus approfondie dans cette étude. D'une longueur de 4910 aa et avec un poids moléculaire de 560 kDa, MDN1 représente la plus grosse protéine du génome de la levure (Garbarino and Gibbons 2002). MDN1 comprend principalement un domaine ATPase dans sa région N-terminale, qui est lié par un long domaine intermédiaire au domaine MIDAS (domaine-M) en C-terminal (fig. 4-1, p.146). Le domaine-M contient un motif de liaison à un ion métallique nommé MIDAS (metal ion-dependent adhesion site), essentiel à l'établissement d'une interaction protéine-protéine (Whittaker and Hynes 2002). Le domaine MIDAS de ScMDN1 serait par ailleurs impliqué dans l'interaction avec le domaine Nle de ScNLE (fig. 3-5C, p.107). Malgré la présence de domaines de type MIDAS dans plusieurs protéines végétales (Liu et al. 2005), ScMDN1 représente le seul candidat possédant un tel motif à avoir été isolé par double-hybride, supportant une fois de plus la pertinence de l'interaction ScNLE-ScMDN1.

Chez la levure, MDN1 a été identifié principalement dans les complexes pré-60S nucléoplasmiques tardifs et pourrait jouer un rôle dans leur exportation à travers

les pores de l'enveloppe nucléaire (Bassler et al. 2001; Nissan et al. 2002; Galani et al. 2004; Nissan et al. 2004). NLE/RSA4p a pour sa part été identifié dans tous les complexes pré-60S nucléolaires, nucléoplasmiques et cytoplasmiques purifiés chez la levure (Bassler et al. 2001; Nissan et al. 2002; Saveanu et al. 2003). En accord avec de tels résultats, la protéine chimérique ScNLE-GFP montre une localisation nucléaire et cytoplasmique dans les cellules végétales (fig. 3-7, p.109). De part la nature structurale de NLE en tant que protéine à WDR, il a été proposé que NLE/RSA4p servirait de plateforme stable pour l'interaction d'autres protéines non-ribosomales impliquées dans la maturation et l'assemblage de la sous-unité 60S, à partir des étapes précoces dans le nucléole jusqu'à sa dissociation finale dans le cytoplasme (de la Cruz et al. 2005). Basé sur les résultats obtenus ici par double-hybride et considérant la conservation évolutive du processus de biogenèse des ribosomes, NSA2 et MDN1 pourraient représenter de telles protéines non-ribosomales se liant de façon transitoire aux complexes pré-60S par l'intermédiaire de NLE/RSA4p afin d'accomplir leur fonction spécifique.

5.3. Fonction du gène *NOTCHLESS* lors du développement gamétophytique et sporophytique

Afin d'étudier les fonctions du gène *NLE* lors du développement végétal, des lignées transformées ont été générées avec des constructions permettant l'expression constitutive soit de *ScNLE* dans l'orientation antisens soit d'un fragment de *ScNLE* ou *AtNLE* (fig. 4-5A, p.151) dans les orientations sens et antisens. Les mécanismes d'interférence d'ARN induits par la présence de molécules d'ARN double-brin issues de l'expression de telles constructions provoquent un silençage post-transcriptionnel de l'activité du gène ciblé chez les lignées transformées (Waterhouse et al. 1998; Chuang and Meyerowitz 2000; Smith et al. 2000). Ces lignées ont été générées avec *Solanum chacoense* ainsi qu'avec la plante modèle *Arabidopsis thaliana*, chez qui les stades du développement reproductif ont été bien caractérisés et pour qui plusieurs outils et données sur des lignées mutantes sont disponibles, facilitant ainsi l'analyse et

la comparaison des phénotypes obtenus. Des analyses combinées des profils d'expression et des phénotypes générés par interférence d'ARN dans les lignées transformées ont mis en évidence l'importance du gène *NLE* dans les stades de développement gamétophytique et sporophytique de la plante. Les sections suivantes discutent des principales facettes du développement touchées par l'induction de l'interférence d'ARN ciblant l'activité du gène *NLE* chez *S. chacoense* et *Arabidopsis* et soulevées dans de cette étude.

5.3.1. Rôle du gène *NLE* lors du développement sporophytique

Une sous-expression de *ScNLE* dans les lignées transformées de *S. chacoense* résulte en la production d'une multitude d'effets lors de la phase de développement sprorophytique, le plus remarquable étant une réduction dans la taille des organes aériens (fig. 3-2, p.104). Chez les végétaux, la taille finale d'un organe est déterminée par sa composition en nombre de cellules (prolifération cellulaire) et en taille de ces cellules (expansion cellulaire) (Mizukami 2001). Des mesures effectuées sur les cellules épidermales de la face adaxiale des feuilles ont ici révélé que la réduction en taille des organes des lignées sous-exprimant *ScNLE* est une conséquence de la réduction en nombre et en taille des cellules (fig. 3-3, p.105). La réduction en nombre de cellules semble apparaître à des stades très précoces du développement des feuilles, possiblement au stade de recrutement des cellules du méristème apical de la tige aux primordia d'organes, puisque les lignées sous-exprimant *ScNLE* produisent des méristèmes apicaux de plus petite taille mais contenant des cellules de taille équivalente au type sauvage (fig. 3-2F, p.104). Également, les réductions en nombre de cellules sont détectées à des jeunes stades du développement des feuilles, alors que les tailles des cellules épidermales des lignées sous-exprimant *ScNLE* sont similaires à celles du type sauvage (fig. 3-3, p.105). En somme, ces observations suggèrent que *ScNLE* joue un rôle important pour la croissance et la division cellulaires.

Des phénotypes sporophytiques additionnels découlant possiblement de défectuosités dans la croissance cellulaire ont de plus été observés dans les lignées sous-exprimant *ScNLE*. Par exemple, des réductions du nombre de structures composants certains organes, tels que le nombre de folioles formés par feuille et le nombre de pétales par fleur, ainsi qu'une perte de tissu dans certains organes, tels que les pétales et la tige (fig. 3-2C-E, p.104), pourraient être causées par un nombre réduit de cellules dans les primordia d'organes. Une augmentation de l'index stomatal, c'est-à-dire du nombre de stomates formés par nombre total de cellules épidermales, observée à la surface adaxiale des feuilles des lignées sous-exprimant *ScNLE* (fig. 3-4, p.106), pourrait être due à une réduction du nombre de cellules épidermales produites par les méristémoïdes.

Un rôle de *NLE* dans la croissance cellulaire est appuyé par le profil d'expression de *ScNLE*. L'expression de *ScNLE* a été localisée dans des tissus de l'apex de la tige contenant des cellules en division active, tels que les méristèmes apicaux et axillaires, les méristèmes floraux, les primordia d'organes ainsi que le procambium (fig. 2-2C, p.62; 3-1, p.103). L'activité de *ScNLE* a de plus été associée aux stades de la fécondation et d'initiation du développement de la graine chez *S. chacoense*, ses niveaux d'expression augmentant considérablement dans les ovules et les ovaires autour de 36 à 42 heures après une pollinisation compatible (fig. 2-2A, B, p.62). Cette augmentation n'est cependant que transitoire, les niveaux d'expression de *ScNLE* redescendant à des niveaux plus faibles quelques heures suivant l'augmentation initiale (fig. 2-2A, B, p.62). Dans les ovaires 48 heures suivant une pollinisation compatible, qui correspond à l'expression maximale du gène, *ScNLE* a été principalement localisée dans le placenta, les tissus vasculaires, l'endothelium de l'ovule ainsi que dans le zygote (fig. 2-3, p.63). Il est intéressant de noter que, de façon similaire à *ScNLE*, plusieurs gènes pour qui l'expression a été rapportée dans divers tissus de l'ovule et de l'ovaire sont également exprimés dans le méristème apical de la tige (Bowman et al. 1991; Lu et al. 1996; Porat et al. 1998), illustrant le caractère en quelque sorte méristématique des cellules de l'ovaire.

L'expression de *ScNLE* induite par la fécondation s'accorde également avec un rôle dans la croissance cellulaire, puisqu'une période de division cellulaire intensive caractérise le premier stade de développement du fruit suite à la fécondation (Gillaspy et al. 1993; Tanksley 2004). Les taux élevés d'avortement de graines observés dans les lignées sous-exprimants *ScNLE* (fig. 2-7E-G, p.67) pourrait résulter d'une mauvaise coordination de la croissance des différents tissus - albumen triploïde, embryon diploïde, tégument de l'ovule - qui sont de constitution génétique différente et pourraient présenter des niveaux différents de pénétrance du mécanisme d'interférence d'ARN.

Finalement, chez la levure, NLE/RSA4p et MDN1 sont essentielles à la survie et à la croissance des cellules puisque des mutations dans les gènes correspondant sont létales (Gavin et al. 2002) et leur déplétion entraîne un ralentissement significatif de la croissance cellulaire (Galani et al. 2004; de la Cruz et al. 2005). Considérant que la synthèse des ribosomes est rapidement induite et est très élevée dans les cellules en division (Stefanovsky et al. 2001; Tschochner and Hurt 2003), l'expression de *ScNLE* dans les cellules en division concorde avec une implication de *ScNLE* dans la biogenèse de la sous-unité ribosomale 60S.

Contrairement aux lignées de *S. chacoense* sous-exprimants *ScNLE*, aucune des lignées transformées *AtNLE-RNAi* d'*Arabidopsis* générées ne montre de défectuosités reliés au développement sporophytique. Cette absence de phénotype est surprenante puisque que *AtNLE* est exprimé de façon constitutive dans tous les organes de la plante (fig. 4-6, p.152). De plus, bien que constitutive, l'expression de *AtNLE* est plus abondante dans des tissus ou organes comprenant des populations de cellules en division. Cependant, alors que des diminutions significatives dans les niveaux de transcrits de *ScNLE* ont été détectées dans les lignées sous-exprimantes de *S. chacoense* (fig. 2-7B, p.67), aucune diminution évidente des niveaux de transcrits de *AtNLE* n'a été détectée dans les lignées *AtNLE-RNAi*. La divergence entre les

données obtenues chez *S. chacoense* et *Arabidopsis* pourrait ainsi être expliquée par des différences d'efficacité du mécanisme d'interférence d'ARN sur le gène *NLE* dans les tissus sporophytiques de ces deux espèces (Kerschen et al. 2004). Une explication alternative serait que le stade de développement sporophytique chez *Arabidopsis* est plus sensible aux variations des niveaux d'expression du gène *NLE* et pourrait ne pas survivre à une réduction perceptible des niveaux de transcrit de *AtNLE*, empêchant ainsi la génération de lignées transgéniques sous-exprimants *AtNLE*. Dans un tel cas, l'utilisation d'un promoteur inductible pour conduire l'expression de la construction d'interférence *AtNLE-RNAi* pourrait être utilisée pour afin de déterminer le rôle de *AtNLE* lors du stade de développement sporophytique chez *Arabidopsis*.

5.3.2. Rôle du gène *NLE* lors du développement gamétophytique

En plus de contribuer au développement sporophytique de la plante, il a été démontré dans cette étude que la fonction du gène *NLE* semble être sollicitée également lors du développement du gamétophyte femelle. L'interférence d'ARN ciblant l'activité du gène *NLE* chez *S. chacoense* et *Arabidopsis* résulte en la production d'un phénotype commun, soit la formation de fruits de plus petite taille montrant des taux considérables d'avortement d'ovules (fig. 2-7E-G, p.67; fig. 4-5, p.151). Les ovules avortés restent petits et blanchâtres comparativement aux plus grosses structures que forment les graines dans les fruits en développement. Chez *Arabidopsis*, 75 % des lignées transgéniques primaires *AtNLE-RNAi* montrent ce phénotype de semistérilité, avec des niveaux d'avortement d'ovules caractéristiques à chacune des lignées (fig. 4-5, p.151). Des croisements réciproques avec des plants de type sauvage ont révélé que cette défectuosité est reliée aux structures reproductives femelles. Dans les ovules des lignées *AtNLE-RNAi* analysées, des gamétophytes femelles en proportions équivalentes aux taux d'ovules avortés étaient soit dégénérés ou bien arrêtés à divers stades précoces de développement, incluant des stades aussi précoces que pendant la formation des mégaspores (FG0) et avec une prédominance

au stade de gamétogenèse à un noyau (FG1) (tableau 4-3, p.145; fig. 4-5C, p.151). Les sacs embryonnaires immatures ne pouvant être fécondés, ceux-ci dégénèrent éventuellement et entraînent l'avortement des ovules. Un arrêt du développement des gamétophytes femelles pourrait également être la cause de l'avortement des ovules observé dans les lignées sous-exprimantes de *S. chacoense*. Ainsi, une activité normale du gène *AtNLE* semble essentielle à la progression du développement du gamétophyte femelle à partir de stades aussi précoces que lors de la formation des mégaspores.

Plusieurs observations suggèrent que l'expression de *AtNLE-RNAi* affecte le développement du gamétophyte femelle au moins au niveau sporophytique. D'abord, tel que mentionné précédemment, *AtNLE* est exprimé de façon constitutive dans tous les organes de la plante, avec une plus grande abondance dans les tissus ou organes comprenant des populations de cellules en division (fig. 4-6, p.152). De plus, les siliques produites par quelques lignées *AtNLE-RNAi* montrent des niveaux d'avortement de 100%, indiquant que le phénotype de semistérilité ne peut être causé uniquement par une expression gamétophytique de *AtNLE-RNAi*. Puisqu'aucune défectuosité dans les structures sporophytiques de l'ovule n'a été observée, l'effet sporophytique de *AtNLE-RNAi* sur le développement des gamétophytes femelles ne semble pas être de nature physique. Une explication alternative de la contribution sporophytique de *AtNLE-RNAi* serait qu'une activité normale du gène *AtNLE* dans les tissus sporophytiques de l'ovule, tels que la cellule-mère des mégaspores ou les cellules du nucelle, pourrait être nécessaire au développement du gamétophyte femelle. Une autre possibilité serait que les produits d'interférence d'ARN provenant des transcrits d'ARN double-brin dans la cellule-mère diploïde des mégaspores et/ou les cellules sporophytiques adjacentes pourraient causer le silençage post-transcriptionnel de *AtNLE* dans le gamétophyte femelle en développement, tel que suggéré précédemment (Acosta-Garcia and Vielle-Calzada 2004). Les produits d'interférence d'ARN pourraient être transmis lors de la méiose de la cellule-mère des mégaspores ou bien être transportés dans la mégaspore fonctionnelle via les

plasmodesmes. La présence de plasmodesmes reliant la mégaspore fonctionnelle aux cellules sporophytiques adjacentes suggère une communication active entre ces structures (Bajon et al. 1999). La variabilité dans les niveaux d'avortement associée aux différentes lignées *AtNLE-RNAi* pourrait être causée par de la variabilité dans la pénétrance du mécanisme d'interférence d'ARN dans chacune des lignées.

Les défectuosités reliées à la mégagamétogénèse dans les lignées *AtNLE-RNAi* suggèrent fortement que le gène *AtNLE* soit exprimé dans le gamétophyte femelle. La présence de *AtNLE* dans cette structure en développement serait en accord avec un rôle dans la croissance cellulaire. Une analyse spatiale et temporelle plus détaillée du gène *AtNLE* pendant les divers stades de développement de l'ovule permettra d'éclaircir ce point. De plus, la contribution respective de l'activité de *AtNLE-RNAi* des tissus sporophytiques versus gamétophytiques dans le développement du gamétophyte femelle pourrait être définie par l'utilisation d'un promoteur permettant de diriger spécifiquement l'expression de la construction d'interférence d'ARN dans le gamétophyte femelle en développement.

5.4. Caracterisation fonctionnelle de *AtMDN1* chez *Arabidopsis*

5.4.1. Rôle du gène *AtMDN1* dans le développement de la plante

L'interaction identifiée entre ScNLE et ScMDN1 par double-hybride (fig. 3-5B, p.107) ainsi que l'isolement des deux homologues de la levure dans les mêmes complexes ribosomaux pré-60S (Nissan et al. 2002; Galani et al. 2004) suggèrent que MDN1 et NLE participent au même processus de développement chez les végétaux. La caractérisation d'une lignée hétérozygote pour une mutation insertionnelle dans le gène *AtMDN1*, nommée *mdn1*, a permis de démontrer son implication dans le développement du gamétophyte femelle chez *Arabidopsis*.

Les plantes hétérozygotes pour la mutation *mdn1* sont semistériles due à l'avortement d'ovules (fig. 4-2A, p.148). Lors de croisements réciproques avec des plants de type sauvage, il a été démontré que la transmission de l'allèle *mdn1* par l'entremise du gamétophyte femelle est principalement affectée (tableau 4-1, p.144). Les gamétophytes femelles portant la mutation *mdn1* présentent un développement retardé comparativement à ceux portant l'allèle de type sauvage (fig. 4-3, p.149; tableau 4-2, p.144). Cependant, plusieurs des gamétophytes femelles *mdn1* peuvent se développer en sac embryonnaire mature (fig. 4-4, p.150; tableau 4-2, p.144). Une expérience de pollinisation retardée a également révélé qu'une proportion significative de sacs embryonnaires *mdn1* sont fonctionnelles et peuvent être fécondées, permettant ainsi la transmission de l'allèle *mdn1* à la génération suivante à travers les gamétophytes femelles (tableau 4-1, p.144). En somme, ces résultats montrent que le gène *AtMDN1* est requis pour la progression normale du développement du gamétophyte femelle, et non pour ses fonctions reproductives.

Plusieurs observations indiquent de plus que le gène *AtMDN1* participe à d'autres aspects du développement de la plante. Les résultats des croissements réciproques ont révélé que le développement du gamétophyte mâle est aussi affecté par la mutation *mdn1*, bien qu'à un degré moindre que le gamétophyte femelle (tableau 4-1, p.144). Cet effet moins prononcé sur le gamétophyte mâle pourrait être expliqué par une redondance fonctionnelle du gène ou pourrait refléter le plus petit nombre de divisions cellulaires impliqué dans le développement du gamétophyte mâle, de sorte que la mutation serait en partie récupérée par l'activité résiduelle de AtMDN1 transmise par la cellule mère des microspore lors de la méiose. *AtMDN1* serait également essentiel au développement sporophytique de la plante, puisqu'aucune plante homozygote pour *mdn1* n'a pu être récupérée des auto-croisements, malgré que l'allèle *mdn1* puisse être transmis partiellement par les gamétophytes femelles et mâles. De plus, de façon similaire à *AtNLE*, le gène *AtMDN1* est exprimé de façon constitutive dans tous les organes de la plantes, avec

une plus grande abondance dans les tissus ou organes contenant des cellules en division (fig. 4-6, p.152).

5.4.2. Comparaison des phénotypes avec les lignées *AtNLE-RNAi*

Bien que, par homologie fonctionnelle, AtNLE et AtMDN1 interagiraient ensemble et participeraient au même processus cellulaire, le développement des gamétophytes femelles semble plus sévèrement touché dans les lignées *AtNLE-RNAi* que par la présence de la mutation *mdn1*. Plusieurs hypothèses peuvent être évoquées pour expliquer ces différences phénotypiques. Considérant que AtMDN1 et AtNLE soient tous deux impliqués dans la biogenèse des ribosomes, ces protéines n'accomplissent pas exactement les mêmes fonctions lors de ce processus et pourraient ne pas être également essentielles. En effet, chez la levure, alors que NLE/RSA4p est requis dans toutes les étapes de la biogenèse de la sous-unité 60S (Nissan et al. 2002), MDN1 est quant à lui requis tout juste avant l'exportation des complexes pré-60S du noyau vers le cytoplasme (Galani et al. 2004). Une autre possibilité serait que la fonction de AtNLE et/ou de AtMDN1 ne soit pas restreinte à la même et seule fonction cellulaire, tel qu'il a été déterminé pour quelques autres protéines non-ribosomales de la levure (Tschochner and Hurt 2003). Par exemple, les orthologues de NLE chez les animaux ont été impliqués dans la régulation de la voie de signalisation Notch (Royet et al. 1998; Cormier et al. 2006). Finalement, les différences phénotypiques pourraient être attribuables à la nature même des lignées mutantes comparées. D'une part, la fonction de *AtMDN1* a été définie à travers une lignée hétérozygote pour la mutation *mdn1*, dans laquelle la fonction d'un allèle de type sauvage peut compenser pour l'allèle non-fonctionnel *mdn1* dans les tissus diploïdes sporophytiques. Une activité résiduelle de AtMDN1 provenant de la cellule-mère des mégaspores pourrait également influencer le développement du gamétophyte femelle. D'autre part, la fonction de *AtNLE* a été analysée à travers le mécanisme d'interférence et, tel que mentionné précédemment, l'activité de *AtNLE-*

RNAi reliée aux cellules sporophytiques semble influencer le développement des gamétophytes femelles. En somme, malgré les différences entre les phénotypes causés par *mdn1* et *AtNLE-RNAi*, il est possible de conclure que l'activité de ces deux gènes est essentielle à la progression du développement du gamétophyte femelle.

Il a été déterminé chez la levure que plus de 170 protéines non-ribosomales participent à l'élaboration des petites et grosses sous-unités ribosomales (Fromont-Racine et al. 2003). Or, très peu d'homologues de ces protéines non-ribosomales ont été caractérisées pour leur fonction dans le développement et la croissance des végétaux. Les quelques données génétiques disponibles mettent cependant en évidence leur importance dans divers aspect du développement du gamétophyte femelle. Il est par exemple intéressant de soulever que le phénotype de retard dans le développement du gamétophyte femelle causé par la mutation *mdn1* est similaire à celui obtenu avec une mutation insertionnelle dans le gène *SLOW WALKER 1* (*SWA1*) d'*Arabidopsis*, qui code pour une protéine à WDR impliqué dans la maturation des ARN ribosomaux (Shi et al. 2005). De plus, une mutation insertionnelle dans l'homologue de *NOP10* de la levure, codant aussi pour un facteur impliqué dans la modification des ARNr ribosomaux (Henras et al. 1998), mène à la formation de sac embryonnaire dont les noyaux polaires sont non-fusionnés (Pagnussat et al. 2005).

CHAPITRE VI :

CONCLUSION

Cette étude visant à définir la fonction cellulaire de ScNLE a permis d'identifier ScMDN1 comme partenaire d'interaction et, par homologie fonctionnelle à la levure, d'associer ainsi NLE et MDN1 à la biogenèse de la sous-unité ribosomale 60S chez les végétaux. Les défectuosités dans la croissance cellulaire, observées par interférence d'ARN ciblant *NLE* ou par la mutation *mdn1* chez *S. chacoense* et/ou *Arabidopsis*, concordent avec les données obtenues chez la levure. Un ralentissement de la croissance cellulaire suite à une déplétion des protéines NLE/RSA4p et MDN1 chez la levure provient de défectuosités dans la maturation des précurseurs des ARN ribosomaux et d'une réduction des niveaux de sous-unités 60S matures (Galani et al. 2004; de la Cruz et al. 2005). Ainsi, l'attribution d'un rôle définitif de NLE et MDN1 dans la biogenèse des ribosomes chez les végétaux pourrait être obtenue par l'analyse des espèces d'ARN ribosomaux et des niveaux de sous-unités 60S générés suite au déclenchement d'un système d'expression inductible des mécanismes d'interférence d'ARN visant *NLE* ou *MDN1*.

Il a de plus été déterminé dans cette étude que les gènes *NLE* et *MDN1* semblent essentiels à la progression du développement du gamétophyte femelle et également à plusieurs aspects du développement sporophytique. La contribution fonctionnelle des gènes *NLE* et *MDN1* respectivement à chacun de ces aspects du développement pourrait cependant être éclaircie de plusieurs façons. D'abord une analyse spatiale et temporelle plus détaillée de l'expression de ces gènes pendant les divers stades de développement de l'ovule permettrait de préciser leur rôle dans le développement du gamétophyte femelle. De plus, dans les cas de *NLE*, l'utilisation d'un promoteur spécifique ciblant l'expression des constructions d'interférence d'ARN dans la mégaspore fonctionnelle et dans le gamétophyte femelle permettrait de définir

la contribution de l'activité gamétophytique du gène dans le développement du gamétophyte femelle. Des analyses préliminaires sur une portion du promoteur de *ScNLE* ont par ailleurs permis de définir une région régulatrice qui répond au signal de la fécondation dans les ovaires de *S. chacoense* (fig. 2-4, p.64; 2-6, p.66). Une telle région régulatrice pourrait être utilisée pour limiter l'expression des constructions d'interférence d'ARN ciblant *ScNLE* et d'en étudier spécifiquement les effets suite à la fécondation. L'identification plus précise des élements régulateurs impliqués dans cette réponse pourrait aussi éventuellement mener à une meilleure compréhension des évènements moléculaires et cellulaires déclenchés lors de la fécondation et de l'initiation du développement de la graine.

BIBLIOGRAPHIE

Acosta-Garcia, G. and Vielle-Calzada, J.P. 2004. A classical arabinogalactan protein is essential for the initiation of female gametogenesis in Arabidopsis. *Plant Cell* **16**(10): 2614-2628.

Artavanis-Tsakonas, S., Rand, M.D., and Lake, R.J. 1999. Notch signaling: cell fate control and signal integration in development. *Science* **284**(5415): 770-776.

Bajon, C., Horlow, C., Motamayor, J.C., Sauvanet, A., and Robert, D. 1999. Megasporogenesis in Arabidopsis thaliana L.: an ultrastructural study. *Sexual Plant Reproduction* **12**: 99-109.

Bassler, J., Grandi, P., Gadal, O., Lessmann, T., Petfalski, E., Tollervey, D., Lechner, J., and Hurt, E. 2001. Identification of a 60S preribosomal particle that is closely linked to nuclear export. *Mol Cell* **8**(3): 517-529.

Bowman, J.L., Drews, G.N., and Meyerowitz, E.M. 1991. Expression of the Arabidopsis floral homeotic gene AGAMOUS is restricted to specific cell types late in flower development. *Plant Cell* **3**(8): 749-758.

Brukhin, V., Curtis, M.D., and Grossniklaus, U. 2005. The angiosperm female gametophyte: no longer the forgotten generation. *Current Science* **89**(11): 1844-1852.

Capron, A., Serralbo, O., Fulop, K., Frugier, F., Parmentier, Y., Dong, A., Lecureuil, A., Guerche, P., Kondorosi, E., Scheres, B., and Genschik, P. 2003. The Arabidopsis anaphase-promoting complex or cyclosome: molecular and genetic characterization of the APC2 subunit. *Plant Cell* **15**(10): 2370-2382.

Chaudhury, A.M. and Berger, F. 2001. Maternal control of seed development. *Semin Cell Dev Biol* **12**(5): 381-386.

Chaudhury, A.M., Ming, L., Miller, C., Craig, S., Dennis, E.S., and Peacock, W.J. 1997. Fertilization-independent seed development in Arabidopsis thaliana. *Proc Natl Acad Sci U S A* **94**(8): 4223-4228.

Choi, Y., Gehring, M., Johnson, L., Hannon, M., Harada, J.J., Goldberg, R.B., Jacobsen, S.E., and Fischer, R.L. 2002. DEMETER, a DNA glycosylase domain protein, is required for endosperm gene imprinting and seed viability in arabidopsis. *Cell* **110**(1): 33-42.

Christensen, C.A., Gorsich, S.W., Brown, R.H., Jones, L.G., Brown, J., Shaw, J.M., and Drews, G.N. 2002. Mitochondrial GFA2 is required for synergid cell death in Arabidopsis. *Plant Cell* **14**(9): 2215-2232.

Christensen, C.A., King, E.J., Jordan, J.R., and Drews, G.N. 1997. Megagametogenesis in Arabidopsis wild-type and *Gf* mutant. *Sexual Plant Reproduction* **10**: 49-64.

Christensen, C.A., Subramanian, S., and Drews, G.N. 1998. Identification of gametophytic mutations affecting female gametophyte development in Arabidopsis. *Dev Biol* **202**(1): 136-151.

Chuang, C.F. and Meyerowitz, E.M. 2000. Specific and heritable genetic interference by double-stranded RNA in Arabidopsis thaliana. *Proc Natl Acad Sci U S A* **97**(9): 4985-4990.

Clarke, A.E. 1940. Fertilization and early embryo development in the potato. *Am Potato J* **17**: 20-25.

Colombo, L., Franken, J., Van der Krol, A.R., Wittich, P.E., Dons, H.J., and Angenent, G.C. 1997. Downregulation of ovule-specific MADS box genes from petunia results in maternally controlled defects in seed development. *Plant Cell* **9**(5): 703-715.

Conner, J. and Liu, Z. 2000. LEUNIG, a putative transcriptional corepressor that regulates AGAMOUS expression during flower development. *Proc Natl Acad Sci U S A* **97**(23): 12902-12907.

Cormier, S., Le Bras, S., Souilhol, C., Vandormael-Pournin, S., Durand, B., Babinet, C., Baldacci, P., and Cohen-Tannoudji, M. 2006. The murine ortholog of notchless, a direct regulator of the notch pathway in Drosophila melanogaster, is essential for survival of inner cell mass cells. *Mol Cell Biol* **26**(9): 3541-3549.

de la Cruz, J., Sanz-Martinez, E., and Remacha, M. 2005. The essential WD-repeat protein Rsa4p is required for rRNA processing and intra-nuclear transport of 60S ribosomal subunits. *Nucleic Acids Res* **33**(18): 5728-5739.

Dnyansagar, V.R. and Cooper, D.C. 1960. Development of the seed of *Solanum phureja*. *American Journal of Botany* **47**: 176-186.

Dresselhaus, T. 2006. Cell-cell communication during double fertilization. *Curr Opin Plant Biol* **9**(1): 41-47.

Dresselhaus, T., Lorz, H., and Kranz, E. 1994. Representative cDNA libraries from few plant cells. *Plant J* **5**(4): 605-610.

Drews, G.N., Lee, D., and Christensen, C.A. 1998. Genetic analysis of female gametophyte development and function. *Plant Cell* **10**(1): 5-17.

Drews, G.N. and Yadegari, R. 2002. Development and function of the angiosperm female gametophyte. *Annu Rev Genet* **36**: 99-124.

Ebel, C., Mariconti, L., and Gruissem, W. 2004. Plant retinoblastoma homologues control nuclear proliferation in the female gametophyte. *Nature* **429**(6993): 776-780.

Estrada-Luna, A.A., Garcia-Aguilar, M., and Vielle-Calzada, J.P. 2004. Female reproductive development and pollen tube growth in diploid genotypes of *Solanum cardiophyllum* Lindl. *Sexual Plant Reproduction* **17**: 117-124.

Evans, M.M. and Kermicle, J.L. 2001. Interaction between maternal effect and zygotic effect mutations during maize seed development. *Genetics* **159**(1): 303-315.

Fatica, A., Cronshaw, A.D., Dlakic, M., and Tollervey, D. 2002. Ssf1p prevents premature processing of an early pre-60S ribosomal particle. *Mol Cell* **9**(2): 341-351.

Fatica, A. and Tollervey, D. 2002. Making ribosomes. *Curr Opin Cell Biol* **14**(3): 313-318.

Feldmann, K.A., Coury, D.A., and Christianson, M.L. 1997. Exceptional segregation of a selectable marker (KanR) in Arabidopsis identifies genes important for gametophytic growth and development. *Genetics* **147**(3): 1411-1422.

Fromont-Racine, M., Senger, B., Saveanu, C., and Fasiolo, F. 2003. Ribosome assembly in eukaryotes. *Gene* **313**: 17-42.

Galani, K., Nissan, T.A., Petfalski, E., Tollervey, D., and Hurt, E. 2004. Rea1, a dynein-related nuclear AAA-ATPase, is involved in late rRNA processing and nuclear export of 60 S subunits. *J Biol Chem* **279**(53): 55411-55418.

Garbarino, J.E. and Gibbons, I.R. 2002. Expression and genomic analysis of midasin, a novel and highly conserved AAA protein distantly related to dynein. *BMC Genomics* **3**(1): 18.

Gavin, A.C., Bosche, M., Krause, R., Grandi, P., Marzioch, M., Bauer, A., Schultz, J., Rick, J.M., Michon, A.M., Cruciat, C.M., Remor, M., Hofert, C., Schelder, M., Brajenovic, M., Ruffner, H., Merino, A., Klein, K., Hudak, M., Dickson, D., Rudi, T., Gnau, V., Bauch, A., Bastuck, S., Huhse, B., Leutwein, C., Heurtier, M.A., Copley, R.R., Edelmann, A., Querfurth, E., Rybin, V., Drewes, G., Raida, M., Bouwmeester, T., Bork, P., Seraphin, B., Kuster, B., Neubauer, G., and Superti-Furga, G. 2002. Functional organization of the yeast proteome by systematic analysis of protein complexes. *Nature* **415**(6868): 141-147.

Germain, H., Rudd, S., Zotti, C., Caron, S., O'Brien, M., Chantha, S.C., Lagace, M., Major, F., and Matton, D.P. 2005. A 6374 unigene set corresponding to low abundance transcripts expressed following fertilization in Solanum chacoense Bitt, and characterization of 30 receptor-like kinases. *Plant Mol Biol* **59**(3): 515-532.

Gillaspy, G., Ben-David, H., and Gruissem, W. 1993. Fruits: A Developmental Perspective. *Plant Cell* **5**(10): 1439-1451.

Grini, P.E., Jurgens, G., and Hülskamp, M. 2002. Embryo and endosperm development is disrupted in the female gametophytic capulet mutants of Arabidopsis. *Genetics* **162**(4): 1911-1925.

Grossniklaus, U. and Schneitz, K. 1998. The molecular and genetic basis of ovule and megagametophyte development. *Semin Cell Dev Biol* **9**(2): 227-238.

Grossniklaus, U., Vielle-Calzada, J.P., Hoeppner, M.A., and Gagliano, W.B. 1998. Maternal control of embryogenesis by MEDEA, a polycomb group gene in Arabidopsis. *Science* **280**(5362): 446-450.

Guitton, A.E. and Berger, F. 2005. Loss of function of MULTICOPY SUPPRESSOR OF IRA 1 produces nonviable parthenogenetic embryos in Arabidopsis. *Curr Biol* **15**(8): 750-754.

Harnpicharnchai, P., Jakovljevic, J., Horsey, E., Miles, T., Roman, J., Rout, M., Meagher, D., Imai, B., Guo, Y., Brame, C.J., Shabanowitz, J., Hunt, D.F., and Woolford, J.L., Jr. 2001. Composition and functional characterization of yeast 66S ribosome assembly intermediates. *Mol Cell* **8**(3): 505-515.

Hejatko, J., Pernisova, M., Eneva, T., Palme, K., and Brzobohaty, B. 2003. The putative sensor histidine kinase CKI1 is involved in female gametophyte development in Arabidopsis. *Mol Genet Genomics* **269**(4): 443-453.

Hennig, L., Gruissem, W., Grossniklaus, U., and Kohler, C. 2004. Transcriptional programs of early reproductive stages in Arabidopsis. *Plant Physiol* **135**(3): 1765-1775.

Henras, A., Henry, Y., Bousquet-Antonelli, C., Noaillac-Depeyre, J., Gelugne, J.P., and Caizergues-Ferrer, M. 1998. Nhp2p and Nop10p are essential for the function of H/ACA snoRNPs. *Embo J* **17**(23): 7078-7090.

Higashiyama, T. 2002. The synergid cell: attractor and acceptor of the pollen tube for double fertilization. *J Plant Res* **115**(1118): 149-160.

Higashiyama, T., Kuroiwa, H., Kawano, S., and Kuroiwa, T. 1998. Guidance in vitro of the pollen tube to the naked embryo sac of torenia fournieri. *Plant Cell* **10**(12): 2019-2032.

Higashiyama, T., Kuroiwa, H., and Kuroiwa, T. 2003. Pollen-tube guidance: beacons from the female gametophyte. *Curr Opin Plant Biol* **6**(1): 36-41.

Holding, D.R. and Springer, P.S. 2002. The Arabidopsis gene PROLIFERA is required for proper cytokinesis during seed development. *Planta* **214**(3): 373-382.

Howden, R., Park, S.K., Moore, J.M., Orme, J., Grossniklaus, U., and Twell, D. 1998. Selection of T-DNA-tagged male and female gametophytic mutants by segregation distortion in Arabidopsis. *Genetics* **149**(2): 621-631.

Hu, W., Wang, Y., Bowers, C., and Ma, H. 2003. Isolation, sequence analysis, and expression studies of florally expressed cDNAs in Arabidopsis. *Plant Mol Biol* **53**(4): 545-563.

Huang, B.-Q. and Russell, S.D. 1992. Female germ unit: organization, isolation, and fonction. *Int Rev Cytol* **140**: 233-292.

Huang, B.Q. and Sheridan, W.F. 1996. Embryo Sac Development in the Maize indeterminate gametophyte1 Mutant: Abnormal Nuclear Behavior and Defective Microtubule Organization. *Plant Cell* **8**(8): 1391-1407.

Huck, N., Moore, J.M., Federer, M., and Grossniklaus, U. 2003. The Arabidopsis mutant *feronia* disrupts the female gametophytic control of pollen tube reception. *Development* **130**(10): 2149-2159.

Hülskamp, M., Schneitz, K., and Pruitt, R.E. 1995. Genetic Evidence for a Long-Range Activity That Directs Pollen Tube Guidance in Arabidopsis. *Plant Cell* **7**(1): 57-64.

Kasahara, R.D., Portereiko, M.F., Sandaklie-Nikolova, L., Rabiger, D.S., and Drews, G.N. 2005. MYB98 is required for pollen tube guidance and synergid cell differentiation in Arabidopsis. *Plant Cell* **17**(11): 2981-2992.

Kerschen, A., Napoli, C.A., Jorgensen, R.A., and Muller, A.E. 2004. Effectiveness of RNA interference in transgenic plants. *FEBS Lett* **566**(1-3): 223-228.

Kim, H.U., Li, Y., and Huang, A.H. 2005. Ubiquitous and endoplasmic reticulum-located lysophosphatidyl acyltransferase, LPAT2, is essential for female but not male gametophyte development in Arabidopsis. *Plant Cell* **17**(4): 1073-1089.

Kimble, J. and Simpson, P. 1997. The LIN-12/Notch signaling pathway and its regulation. *Annu Rev Cell Dev Biol* **13**: 333-361.

Klucher, K.M., Chow, H., Reiser, L., and Fischer, R.L. 1996. The AINTEGUMENTA gene of Arabidopsis required for ovule and female

gametophyte development is related to the floral homeotic gene APETALA2. *Plant Cell* **8**(2): 137-153.

Kohler, C., Hennig, L., Bouveret, R., Gheyselinck, J., Grossniklaus, U., and Gruissem, W. 2003a. Arabidopsis MSI1 is a component of the MEA/FIE Polycomb group complex and required for seed development. *Embo J* **22**(18): 4804-4814.

Kohler, C., Hennig, L., Spillane, C., Pien, S., Gruissem, W., and Grossniklaus, U. 2003b. The Polycomb-group protein MEDEA regulates seed development by controlling expression of the MADS-box gene PHERES1. *Genes Dev* **17**(12): 1540-1553.

Kranz, E., Bautor, J., and Lörz, H. 1991. *In vitro* fertlisation of single, isolated gametes of maize (*Zea mays* L.). *Sexual Plant Reproduction* **4**: 12-16.

Kumlehn, J., Kirik, V., Czihal, A., Altschmied, L., Matzk, F., and al., e. 2001. Parthenogenetic egg cells of wheat: cellular and molecular studies. *Sexual Plant Reproduction* **14**: 239-243.

Kwee, H.S. and Sundaresan, V. 2003. The *NOMEGA* gene required for female gametophyte development encodes the putative APC6/CDC16 component of the Anaphase Promoting Complex in Arabidopsis. *Plant J* **36**(6): 853-866.

Lambright, D.G., Sondek, J., Bohm, A., Skiba, N.P., Hamm, H.E., and Sigler, P.B. 1996. The 2.0 A crystal structure of a heterotrimeric G protein. *Nature* **379**(6563): 311-319.

Le, Q., Gutierrez-Marcos, J.F., Costa, L.M., Meyer, S., Dickinson, H.G., Lorz, H., Kranz, E., and Scholten, S. 2005. Construction and screening of subtracted cDNA libraries from limited populations of plant cells: a comparative analysis of gene expression between maize egg cells and central cells. *Plant J* **44**(1): 167-178.

Li, Z. and Thomas, T.L. 1998. PEI1, an embryo-specific zinc finger protein gene required for heart-stage embryo formation in Arabidopsis. *Plant Cell* **10**(3): 383-398.

Liu, J., Jambunathan, N., and McNellis, T.W. 2005. Transgenic expression of the von Willebrand A domain of the BONZAI 1/COPINE 1 protein triggers a lesion-mimic phenotype in Arabidopsis. *Planta* **221**(1): 85-94.

Lu, P., Porat, R., Nadeau, J.A., and O'Neill, S.D. 1996. Identification of a meristem L1 layer-specific gene in Arabidopsis that is expressed during embryonic pattern formation and defines a new class of homeobox genes. *Plant Cell* **8**(12): 2155-2168.

Luo, M., Bilodeau, P., Dennis, E.S., Peacock, W.J., and Chaudhury, A. 2000. Expression and parent-of-origin effects for FIS2, MEA, and FIE in the endosperm and embryo of developing Arabidopsis seeds. *Proc Natl Acad Sci U S A* **97**(19): 10637-10642.

Luo, M., Bilodeau, P., Koltunow, A., Dennis, E.S., Peacock, W.J., and Chaudhury, A.M. 1999. Genes controlling fertilization-independent seed development in Arabidopsis thaliana. *Proc Natl Acad Sci U S A* **96**(1): 296-301.

Maheshwari, P. 1950. *An Introduction to the Embryology of Angiosperms*. McGraw-Hill, New York.

Mansfield, S.G., Briarty, L.G., and Erni, S. 1991. Early embryogenesis in *Arabidopsis thaliana*. I. The mature embryo sac. *Canadian Journal of Botany* **69**: 447-460.

Marton, M.L., Cordts, S., Broadhvest, J., and Dresselhaus, T. 2005. Micropylar pollen tube guidance by egg apparatus 1 of maize. *Science* **307**(5709): 573-576.

McCormick, S. 2004. Control of male gametophyte development. *Plant Cell* **16 Suppl**: S142-153.

Mizukami, Y. 2001. A matter of size: developmental control of organ size in plants. *Curr Opin Plant Biol* **4**(6): 533-539.

Moore, J.M., Calzada, J.P., Gagliano, W., and Grossniklaus, U. 1997. Genetic characterization of hadad, a mutant disrupting female gametogenesis in Arabidopsis thaliana. *Cold Spring Harb Symp Quant Biol* **62**: 35-47.

Murgia, M., Huang, B.-Q., Tucker, S.C., and Musgrave, M.E. 1993. Embryo sac lacking antipodal cells in *Arabidopsis thaliana* (Brassicaceae). *American Journal of Botany* **80**: 824-838.

Neer, E.J., Schmidt, C.J., Nambudripad, R., and Smith, T.F. 1994. The ancient regulatory-protein family of WD-repeat proteins. *Nature* **371**(6495): 297-300.

Nissan, T.A., Bassler, J., Petfalski, E., Tollervey, D., and Hurt, E. 2002. 60S pre-ribosome formation viewed from assembly in the nucleolus until export to the cytoplasm. *Embo J* **21**(20): 5539-5547.

Nissan, T.A., Galani, K., Maco, B., Tollervey, D., Aebi, U., and Hurt, E. 2004. A pre-ribosome with a tadpole-like structure functions in ATP-dependent maturation of 60S subunits. *Mol Cell* **15**(2): 295-301.

Ohad, N., Margossian, L., Hsu, Y.C., Williams, C., Repetti, P., and Fischer, R.L. 1996. A mutation that allows endosperm development without fertilization. *Proc Natl Acad Sci U S A* **93**(11): 5319-5324.

Ohad, N., Yadegari, R., Margossian, L., Hannon, M., Michaeli, D., Harada, J.J., Goldberg, R.B., and Fischer, R.L. 1999. Mutations in FIE, a WD polycomb group gene, allow endosperm development without fertilization. *Plant Cell* **11**(3): 407-416.

Okamoto, T., Scholten, S., Lorz, H., and Kranz, E. 2005. Identification of genes that are up- or down-regulated in the apical or basal cell of maize two-celled embryos and monitoring their expression during zygote development by a cell manipulation- and PCR-based approach. *Plant Cell Physiol* **46**(2): 332-338.

Osterlund, M.T., Ang, L.H., and Deng, X.W. 1999. The role of COP1 in repression of Arabidopsis photomorphogenic development. *Trends Cell Biol* **9**(3): 113-118.

Pagnussat, G.C., Yu, H.J., Ngo, Q.A., Rajani, S., Mayalagu, S., Johnson, C.S., Capron, A., Xie, L.F., Ye, D., and Sundaresan, V. 2005. Genetic and molecular identification of genes required for female gametophyte development and function in Arabidopsis. *Development* **132**(3): 603-614.

Palanivelu, R., Brass, L., Edlund, A.F., and Preuss, D. 2003. Pollen tube growth and guidance is regulated by POP2, an Arabidopsis gene that controls GABA levels. *Cell* **114**(1): 47-59.

Pischke, M.S., Jones, L.G., Otsuga, D., Fernandez, D.E., Drews, G.N., and Sussman, M.R. 2002. An Arabidopsis histidine kinase is essential for megagametogenesis. *Proc Natl Acad Sci U S A* **99**(24): 15800-15805.

Porat, R., Lu, P., and O'Neill, S.D. 1998. Arabidopsis SKP1, a homologue of a cell cycle regulator gene, is predominantly expressed in meristematic cells. *Planta* **204**(3): 345-351.

Raghavan, V. 2003. Some reflections on double-fertilization, from its discovery to the present. *New Phytologist* **159**: 565-583.

Ray, S., Golden, T., and Ray, A. 1996. Maternal effects of the short integument mutation on embryo development in Arabidopsis. *Dev Biol* **180**(1): 365-369.

Ray, S.M., Park, S.S., and Ray, A. 1997. Pollen tube guidance by the female gametophyte. *Development* **124**(12): 2489-2498.

Reiser, L., Modrusan, Z., Margossian, L., Samach, A., Ohad, N., Haughn, G.W., and Fischer, R.L. 1995. The BELL1 gene encodes a homeodomain protein involved in pattern formation in the Arabidopsis ovule primordium. *Cell* **83**(5): 735-742.

Rotman, N., Rozier, F., Boavida, L., Dumas, C., Berger, F., and Faure, J.E. 2003. Female control of male gamete delivery during fertilization in *Arabidopsis thaliana*. *Curr Biol* **13**(5): 432-436.

Royet, J., Bouwmeester, T., and Cohen, S.M. 1998. Notchless encodes a novel WD40-repeat-containing protein that modulates Notch signaling activity. *Embo J* **17**(24): 7351-7360.

Russell, S.D. 1992. Double fertilization. *Int Rev Cytol* **140**: 357-388.

-. 1996. Attraction and transport of male gametes for fertilization. *Sexual Plant Reproduction* **9**: 337-342.

Saveanu, C., Bienvenu, D., Namane, A., Gleizes, P.E., Gas, N., Jacquier, A., and Fromont-Racine, M. 2001. Nog2p, a putative GTPase associated with pre-60S

subunits and required for late 60S maturation steps. *Embo J* **20**(22): 6475-6484.

Saveanu, C., Namane, A., Gleizes, P.E., Lebreton, A., Rousselle, J.C., Noaillac-Depeyre, J., Gas, N., Jacquier, A., and Fromont-Racine, M. 2003. Sequential protein association with nascent 60S ribosomal particles. *Mol Cell Biol* **23**(13): 4449-4460.

Schneitz, K. 1999. The molecular and genetic control of ovule development. *Curr Opin Plant Biol* **2**(1): 13-17.

Schneitz, K., Hülskamp, M., Kopczak, S.D., and Pruitt, R.E. 1997. Dissection of sexual organ ontogenesis: a genetic analysis of ovule development in Arabidopsis thaliana. *Development* **124**(7): 1367-1376.

Schneitz, K., Hülskamp, M., and Pruitt, R.E. 1995. Wild-type ovule development in *Arabidopsis thaliana*: a light microscope study of cleared whole-mount tissue. *Plant Journal* **7**(5): 731-749.

Shi, D.Q., Liu, J., Xiang, Y.H., Ye, D., Sundaresan, V., and Yang, W.C. 2005. *SLOW WALKER1*, essential for gametogenesis in Arabidopsis, encodes a WD40 protein involved in 18S ribosomal RNA biogenesis. *Plant Cell* **17**(8): 2340-2354.

Shimizu, K.K. and Okada, K. 2000. Attractive and repulsive interactions between female and male gametophytes in Arabidopsis pollen tube guidance. *Development* **127**(20): 4511-4518.

Smith, N.A., Singh, S.P., Wang, M.B., Stoutjesdijk, P.A., Green, A.G., and Waterhouse, P.M. 2000. Total silencing by intron-spliced hairpin RNAs. *Nature* **407**(6802): 319-320.

Smith, T.F., Gaitatzes, C., Saxena, K., and Neer, E.J. 1999. The WD repeat: a common architecture for diverse functions. *Trends Biochem Sci* **24**(5): 181-185.

Sondek, J., Bohm, A., Lambright, D.G., Hamm, H.E., and Sigler, P.B. 1996. Crystal structure of a G-protein beta gamma dimer at 2.1A resolution. *Nature* **379**(6563): 369-374.

Springer, P.S., Holding, D.R., Groover, A., Yordan, C., and Martienssen, R.A. 2000. The essential Mcm7 protein PROLIFERA is localized to the nucleus of dividing cells during the G(1) phase and is required maternally for early Arabidopsis development. *Development* **127**(9): 1815-1822.

Springer, P.S., McCombie, W.R., Sundaresan, V., and Martienssen, R.A. 1995. Gene trap tagging of PROLIFERA, an essential MCM2-3-5-like gene in Arabidopsis. *Science* **268**(5212): 877-880.

Sprunck, S., Baumann, U., Edwards, K., Langridge, P., and Dresselhaus, T. 2005. The transcript composition of egg cells changes significantly following fertilization in wheat (Triticum aestivum L.). *Plant J* **41**(5): 660-672.

Stefanovsky, V.Y., Pelletier, G., Hannan, R., Gagnon-Kugler, T., Rothblum, L.I., and Moss, T. 2001. An immediate response of ribosomal transcription to growth factor stimulation in mammals is mediated by ERK phosphorylation of UBF. *Mol Cell* **8**(5): 1063-1073.

Sundaresan, V., Springer, P., Volpe, T., Haward, S., Jones, J.D., Dean, C., Ma, H., and Martienssen, R. 1995. Patterns of gene action in plant development revealed by enhancer trap and gene trap transposable elements. *Genes Dev* **9**(14): 1797-1810.

Tanksley, S.D. 2004. The genetic, developmental, and molecular bases of fruit size and shape variation in tomato. *Plant Cell* **16 Suppl**: S181-189.

Tschochner, H. and Hurt, E. 2003. Pre-ribosomes on the road from the nucleolus to the cytoplasm. *Trends Cell Biol* **13**(5): 255-263.

Ullah, H., Chen, J.G., Temple, B., Boyes, D.C., Alonso, J.M., Davis, K.R., Ecker, J.R., and Jones, A.M. 2003. The beta-subunit of the Arabidopsis G protein negatively regulates auxin-induced cell division and affects multiple developmental processes. *Plant Cell* **15**(2): 393-409.

van Nocker, S. and Ludwig, P. 2003. The WD-repeat protein superfamily in Arabidopsis: conservation and divergence in structure and function. *BMC Genomics* **4**(1): 50.

Vielle-Calzada, J.P., Thomas, J., Spillane, C., Coluccio, A., Hoeppner, M.A., and Grossniklaus, U. 1999. Maintenance of genomic imprinting at the Arabidopsis medea locus requires zygotic DDM1 activity. *Genes Dev* **13**(22): 2971-2982.

Wall, M.A., Coleman, D.E., Lee, E., Iniguez-Lluhi, J.A., Posner, B.A., Gilman, A.G., and Sprang, S.R. 1995. The structure of the G protein heterotrimer Gi alpha 1 beta 1 gamma 2. *Cell* **83**(6): 1047-1058.

Waterhouse, P.M., Graham, M.W., and Wang, M.B. 1998. Virus resistance and gene silencing in plants can be induced by simultaneous expression of sense and antisense RNA. *Proc Natl Acad Sci U S A* **95**(23): 13959-13964.

Webb, M.C. and Gunning, B.E.S. 1990. Embryo sac development in *Arabidopsis thaliana*. I. Megasporogenesis, including the microtubular cytoskeleton. *Sexual Plant Reproduction* **3**: 244-256.

-. 1994. Embryo sac development in *Arabidopsis thaliana*. II. The cytoskeleton during megagametogenesis *Sexual Plant Reproduction* **7**: 153-163.

Weterings, K. and Russell, S.D. 2004. Experimental analysis of the fertilization process. *Plant Cell* **16 Suppl**: S107-118.

Whittaker, C.A. and Hynes, R.O. 2002. Distribution and evolution of von Willebrand/integrin A domains: widely dispersed domains with roles in cell adhesion and elsewhere. *Mol Biol Cell* **13**(10): 3369-3387.

Willemse, M.T.M. and van Went, J.L. 1984. The female gametophyte. in *Embryology of Angiosperms* (ed. B.M. Johri, ed.), pp. 159-196. Springer-Verlag, Berlin.

Yadegari, R. and Drews, G.N. 2004. Female gametophyte development. *Plant Cell* **16 Suppl**: S133-141.

Yadegari, R., Kinoshita, T., Lotan, O., Cohen, G., Katz, A., Choi, Y., Katz, A., Nakashima, K., Harada, J.J., Goldberg, R.B., Fischer, R.L., and Ohad, N. 2000. Mutations in the FIE and MEA genes that encode interacting polycomb proteins cause parent-of-origin effects on seed development by distinct mechanisms. *Plant Cell* **12**(12): 2367-2382.

Yang, H., Kaur, N., Kiriakopolos, S., and McCormick, S. 2006. EST generation and analyses towards identifying female gametophyte-specific genes in Zea mays L. *Planta*.

Yu, H.J., Hogan, P., and Sundaresan, V. 2005. Analysis of the female gametophyte transcriptome of Arabidopsis by comparative expression profiling. *Plant Physiol* **139**(4): 1853-1869.